UNIVERSITY OF ALBERTA

RELEASE FORM

NAME OF AUTHOR: DAVID ANDREW TORVI

TITLE OF THESIS: A FINITE ELEMENT MODEL OF HEAT TRANSFER IN SKIN SUBJECTED TO A FLASH FIRE

DEGREE: MASTER OF SCIENCE

YEAR THIS DEGREE GRANTED: SPRING 1992

Permission is hereby granted to THE UNIVERSITY OF ALBERTA LIBRARY to reproduce single copies of this thesis and to lend or sell such copies for private, scholarly or scientific research purposes only.

The author reserves all other publication and other rights in association with the copyright in the thesis, and except as hereinbefore provided neither the thesis nor any substantial portion thereof may be printed or otherwise reproduced in any material form whatever without the author's prior written permission.

_____

Permanent Address:

4724 Chapel Rd., N.W.

Calgary, Alberta

T2L 1A6

DATED: _____

UNIVERSITY OF ALBERTA

A FINITE ELEMENT MODEL OF HEAT TRANSFER IN SKIN SUBJECTED TO A FLASH FIRE

BY

DAVID ANDREW TORVI

A thesis submitted to the Faculty of Graduate Studies and Research in partial fulfillment of the requirements for the degree of MASTER OF SCIENCE.

DEPARTMENT OF MECHANICAL ENGINEERING

EDMONTON, ALBERTA

SPRING, 1992

UNIVERSITY OF ALBERTA

FACULTY OF GRADUATE STUDIES AND RESEARCH

The undersigned certify that they have read, and recommend to the Faculty of Graduate Studies and Research for acceptance, a thesis entitled A FINITE ELEMENT MODEL OF HEAT TRANSFER IN SKIN SUBJECTED TO A FLASH FIRE submitted by DAVID ANDREW TORVI in partial fulfillment of the requirements for the degree of MASTER OF SCIENCE.

_____

Dr. J.D. Dale (Supervisor)

_____

Dr. A. Craggs

_____

Dr. B.M. Crown

_____

Dr. R.E. Hayes

Date: _____

ABSTRACT

A variable property, multiple layer finite element model was developed to predict skin temperatures and times to second and third degree burns under simulated flash fire conditions. Hermitian temperature elements were used to model the heat transfer in the skin.

Thermal physical properties of the skin vary widely by person and body location. A sensitivity study of burn predictions to these variations was undertaken using the finite element model. It was found that the initial temperature gradient, and variations in thermal physical properties over the ranges used in multiple layer skin models had minimal effects on second degree burn predictions, but larger effects on third degree burn predictions. It was also found that the blood perfusion source term in Pennes' bioheat transfer equation could be neglected in predicting second degree burns due to flash fires.

The skin surface boundary condition after flash fire exposures is difficult to predict. A convection and radiation boundary condition after the exposure was found to have no effect on second degree burn predictions, as these burns occur before the exposure ends. This boundary condition may have an effect in predicting slower developing third degree burns.

The finite element model, which incorporates multiple skin layers and variable properties, was more suitable for making temperature and burn predictions for a step heat flux than a closed form solution based on a single skin layer with constant properties. However, if only second degree burn predictions are required from heat flux data for a large number of test sensors, the closed form solution was found to be preferable as its predictions were only slightly different from those of the finite element model, but required less computing time.

ACKNOWLEDGEMENTS

The author wishes to acknowledge the following for their help in the preparation of this thesis.

- Dr. J.D. Dale for his supervision of this research.
- Dr. A. Craggs for help with the derivation of the finite element matrix equation.
- Mr. E.Y. Leung, who performed a literature search on skin burns before writing the finite difference code for the University of Alberta mannequin. This literature search was used extensively by the author in the preparation of this thesis.
- The Province of Alberta, Department of Mechanical Engineering, and E.I. DU PONT DE NEMOURS AND COMPANY for funding during this research.
- My parents, for their inspiration throughout my entire education.
- My wife, Heather, for her love, support, and great patience during this research.

TABLE OF CONTENTS

CHAPTER 1 INTRODUCTION 1

1.1 Characteristics of Flash Fires 2

1.2 The Skin 4

1.2.1 Epidermis 4

1.2.2 Dermis 5

1.2.3 Subcutaneous Tissue 5

1.2.4 Other Features 5

1.3 Temperature Regulation Under Normal Circumstances 8

1.4 Microscopic and Macroscopic Responses of the Skin to Thermal Insult 9

1.4.1 First Degree Burns 9

1.4.2 Second Degree Burns 10

1.4.3 Third Degree Burns 11

1.4.4 Fourth Degree Burns 11

1.4.5 Systemic Effects of Heat Trauma 11

1.5 The Bioheat Transfer Equation 12

1.6 Skin Burn Research 14

1.6.1 Henriques and Moritz 14

1.6.2 Buettner 16

1.6.3 Stoll 17

1.6.4 Hardy 18

1.6.5 Mehta and Wong 19

1.6.6 Takata 20

1.7 Aerotherm's Critique of Skin Burn Models 21

1.8 Fabric and Clothing Tests 22

1.8.1 Skin Simulants 22

1.8.2 Thermal Protective Performance Test 23

1.8.3 Mannequin testing 25

1.8.3.1 Early Mannequin Research 25

1.8.3.2 Thermo-man® 25

1.8.3.3 Minnesota Woman 26

1.8.3.4 Mannequin Testing at the University of Alberta 26

1.9 Overview of this Study 27

CHAPTER 2 DEVELOPMENT OF THE FINITE ELEMENT MODEL 28

2.1 The Finite Element Method 29

2.2 Derivation of Finite Element Matrix Equation 30

2.3 Finite Element Computer Program 35

2.4 Comparison of Finite Element Solutions with Closed Form Solutions for Classical Boundary Condition Problems 40

2.4.1 Constant heat flux boundary condition 40

2.5 Testing of the Burn Integral Routine 47

2.6 Summary 51

CHAPTER 3 EFFECTS OF THERMAL PHYSICAL PROPERTIES AND SURFACE BOUNDARY CONDITION 52

3.1 Skin Thermal Physical Property Literature Search 53

3.2 Variable Property Finite Element Program 54

3.2.1 Time Steps and Number of Elements Required 54

3.3 Variable Property Sensitivity Study 59

3.3.1 Skin thickness 60

3.3.2 Temperature gradients in the skin 61

3.3.3 Thermal Properties 67

3.3.3.1 Volumetric Heat Capacity 67

3.3.3.2 Thermal Conductivity 70

3.3.4 Blood Perfusion 77

3.4 Sensitivity Study of Surface Boundary Condition After Exposure 79

3.5 Summary of the Effects of Variable Skin Properties and Boundary Condition 83

CHAPTER 4 COMPARISON OF SKIN BURN MODELS 85

4.1 Comparison of Temperature-Time Histories 86

4.2 Comparison of Burn Predictions 90

4.2.1 Second Degree Burns 90

4.2.2 Third Degree Burns 93

4.3 Pre-Exponential Factor and Activation Energy in Henriques' Burn Integral 96

4.3.1 Second Degree Burns 96

4.3.2 Third Degree Burns 98

4.4 Selection of Models for Flash Fire Burn Predictions 99

CHAPTER 5 CONCLUSIONS AND RECOMMENDATIONS 102

5.1 Conclusions 103

5.2 Recommendations 104

REFERENCES 106

APPENDICES 114

APPENDIX 1: DERIVATION OF FINITE ELEMENT MATRIX EQUATION 115

APPENDIX 2: SAMPLE DATAFILE 124

APPENDIX 3: CALCULATION OF RADIATION AND CONVECTION BOUNDARY CONDITIONS 125

A3.1 Natural Convection Heat Loss 125

A3.2 Radiation Heat Loss 127

A3.3 Total Heat Loss 127

LIST OF TABLES

2.1 Comparison of Times to First and Second Degree Burns Due to an Imposed Surface Temperature Determined Using the Burn Integral Computer Module with those of Henriques and Moritz [18] 48

2.2 Comparison of the Value of Henriques' Burn Integral Calculated from Henriques and Moritz's Measured Data with Their Criteria for First and Second Degree Burn for Various Surface Temperatures 50

3.1 Thermal Physical Properties Used in Testing the Variable Property, Multiple Layer Finite Element Skin Model 55

3.2 Comparison of Times to Second and Third Degree Burn Determined Using 5 and 10 Finite Element Models 58

3.3 Comparison of Temperatures and Dermal Damage Determined Using Two Time Step Schemes From 5-10 s After the Beginning of a 83.2 kW/m^2 Exposure 59

3.4 Times to Second and Third Degree Burn Predicted Using the Finite Element Model and Different Initial Nodal Heat Fluxes 62

3.5 Times to Second and Third Degree Burns Predicted Using Four Different Initial Temperature Gradients 66

3.6 Times to Second and Third Degree Burn Predicted Using the Lowest and Highest Published Values of Volumetric Heat Capacity of the Different Skin Layers 68

3.7 Times to Second and Third Degree Burn Predicted Using the Lowest and Highest Published Values of Specific Heat for Each Skin Layer 70

3.8 Times to Second and Third Degree Burn Predicted Using the Lowest and Highest Published Values of Thermal Conductivity for Each Skin Layer 72

3.9 Times to Second and Third Degree Burn Predicted Using the Lowest and Highest Common Values of In Vivo and In Vitro Thermal Conductivity 73

3.10 Maximum Basal Layer and Dermal Base Temperature Differences Over the Published Range of In Vitro Thermal Conductivities 74

3.11 Times to Second Degree Burn Predicted Using Different Thermal Conductivity Values With and Without Perfusion 75

3.12 Comparison of Times to Second Degree Burn Predicted Using the Single Layer, Constant Property Finite Element Model, and Thermal Properties from Perkins [54], Mitchell [63], and Stoll [64] 76

3.13 Times to Second and Third Degree Burns Predicted Using Various Blood Perfusion Rates and Heat Fluxes 78

3.14 Times for Second and Third Degree Burns Predicted When Convection Heat Loss Is or Is Not Included in the Skin Model 82

4.1 Times to Second Degree Burn Calculated by Finite Element and Closed Form Solution Models, and Observed by Stoll 91

4.2 Times to Third Degree Burn Calculated by the Finite Element Model and Closed Form Solutions 94

4.3 Comparison of Times to Second Degree Burn Predicted Using the Different Values of the Pre-Exponential Factor and Activation Energy Found in the Literature 97

4.4 Comparison of Times to Third Degree Burn Predicted Using the Different Values of the Pre-Exponential Factor and Activation Energy Found in the Literature 98

LIST OF FIGURES

1.1 Normal Cross-Sectional Anatomy of Skin 6

1.2 Cross-Sectional Anatomy of the Epidermis 7

2.1(a) Linear Temperature Element 33

2.1(b) Quadratic Temperature Element 33

2.1(c) Hermitian Temperature Element 33

2.2(a) Flow Diagram of Finite Element Computer Program - Initial Stages 36

2.2(b) Flow Diagram of Finite Element Computer Program - Skin Temperature Module 37

2.2(c) Flow Diagram of Finite Element Computer Program - Epidermal Burn Module 38

2.2(d) Flow Diagram of Finite Element Computer Program - Dermal Burn Module 39

2.3 Imposed Step Heat Flux Function 42

2.4 Comparison of Basal Layer Temperatures Determined Using Finite Element Model with Closed Form Solution 43

2.5 Comparison of Basal Layer Temperatures Predicted Using Closed Form Solution and Various Finite Element Schemes 45

2.6 Comparison of Dermal Base Temperatures Predicted Using Closed Form Solution and Various Finite Element Schemes 46

3.1 Comparison of Basal Layer Temperatures Determined Using the Variable Property Finite Element Program and Four Different Time Steps 56

3.2 Comparison of Basal Layer Temperatures Determined Using 5,7, and 10 Hermitian Elements 57

3.3 Comparison of Basal Layer Temperature-Time Histories Determined Using Three Different Initial Temperature Gradients 64

3.4 Comparison of Dermal Base Temperature-Time Histories Determined Using Three Different Initial Temperature Gradients 65

3.5 Comparison of Basal Layer Temperatures Determined Using Insulated, and Convection and Radiation Surface Boundary Conditions After Exposure 81

4.1 Basal Layer Temperature-Time Histories Determined Using Finite Element and Closed Form Solutions and Reported by Stoll [25] 88

4.2 Surface Temperature-Time Histories Determined Using Finite Element Solution and Measured by Stoll [25] 89

4.3 Times to Second Degree Burn as Predicted by Finite Element and Closed Form Solutions, and Observed by Stoll [26] 92

NOMENCLATURE

Notation

c	specific heat (J/kg · °C)
dt	time step (s)
G	blood perfusion rate ($m^3/s/m^3$ tissue)
g	gravitational acceleration (9.81 m/s^2)
Gr	Grashof number (dimensionless)
h	convection heat transfer coefficient ($W/m^2 \cdot °C$)
i	time step number (dimensionless)
k	thermal conductivity (W/m · °C)
L	total skin thickness, height of vertical cylinder (m)
l	thickness of one skin finite element (m)
P	pre-exponential factor (s^{-1})
Pr	Prandtl number (dimensionless)
q	heat flux (W/m^2, $cal/cm^2 \cdot s$)
R	ideal gas constant (8.314 J/kg · mol · °C, 1.986 kcal/kg · mol · °C)
r	Courant number (dimensionless)
Ra	Rayleigh number (dimensionless)
S(t)	step function
T	temperature (°C, K)
t	time (s)
x	depth (m)

Greek symbols

α	thermal diffusivity (m^2/s)
β	inverse of film temperature (K^{-1})
ΔE	activation energy (J/mol, cal/mol)
Δt	time step (s)
ϵ	emissivity (dimensionless)
ν	kinematic viscosity (m^2/s)

ρ	density (kg/m^3)
τ	dummy variable of integration (s)
σ	Stefan Boltzmann constant (5.669×10^{-8} $W/m^2 \cdot K^4$)
Ω	Henriques' burn integral value (dimensionless)

Subscripts

a	absorbed, node number
b	blood, node number
c	core, convection, calculated
D	dermis
d	node number
e	element
ex	exposure
f	film
h	Hermitian
i	initial
L	linear
m	measured
o	original
q	quadratic
r	radiation
s	surface
∞	ambient, surroundings
t	total

Superscripts

'	first derivative with respect to x
''	second derivative with respect to x
$\cdot$	first derivative with respect to time
(j)	time step (j)
(j+1)	time step (j+1)

CHAPTER 1
INTRODUCTION

A large number of people are injured every year as a result of burns, many of which are caused by industrial accidents. In order to minimize or prevent burns from possible accidents, workers wear protective clothing. To properly assess protective clothing alternatives, realistic tests must be performed to determine how much thermal protection candidate pieces of clothing can provide.

Beginning in the latter part of World War II, and continuing to the present, models have been developed to help make predictions of skin burns due to thermal trauma. These models have been used, along with tests developed over the same time period, in order to evaluate and develop protective clothing for military and industrial applications, and to assess treatments of skin burns.

In this study, a finite element model of the skin was constructed to predict burns resulting from a particular industrial accident, the flash fire. The thermal physical properties of skin reported in the literature vary widely, and the boundary condition on the skin surface after the flash fire ends is difficult to determine. This model was used to investigate the effects of variations in thermal physical properties and surface boundary condition on skin burn predictions for flash fires. The burn predictions made by this variable property, multiple layer finite element skin model were then compared to those made using a closed form solution based on a single skin layer with constant properties. The finite element model and this research are described in this report.

In this introductory chapter, background information pertinent to the study will be presented. This information includes descriptions of the characteristics of the industrial accident studied here, the anatomy and physiology of the skin and skin burns, important skin burn research, and protective fabric and clothing tests commonly used.

1.1 Characteristics of Flash Fires

There are many hazardous situations in industry where burns may occur.

According to Alberta Occupational Health and Safety [1]*, there were 14 people burned due to fires in upstream oil and gas industries in the province in 1990. This number is small, both in absolute terms and relative to the large numbers of workers employed in these areas. However in some industries, the number of burns were much higher than in others. From 1983 to 1990, persons representing about 0.35% of the total number of estimated person-years employed in well testing and battery tank operation were burned on average each year. In battery tank operation, close to 11% of all lost time claims during the same period were due to burns. Regardless of the number of burns, injuries suffered were often severe; over 50% of burn victims required hospital stays of 21 days or more.

The use of proper protective clothing may reduce or prevent injuries to an individual from an accident. The number of lost time claims in Alberta due to burns in the oil and gas industries decreased from a high of 58 (0.08% of estimated person-years employed) in 1985 to 14 (0.02%) in 1990. This decline has been partly attributed to the increased use of protective clothing in these industries.

One hazardous situation encountered in some of these industries is the flash fire. Flash fires can result from the release of combustible gas, such as a leak at a well head or a compressor station. They are of short duration, typically less than 5 s, and involve heat fluxes up to 2 $cal/cm^2 \cdot s$ (83.72 kW/m^2) [2]. Protective clothing for these high intensity, short duration exposures is different from that for longer exposures to different heat fluxes, such as firefighters' turnout coats.

Protective clothing can be evaluated under simulated accident situations using results from an instrumented mannequin to predict the burns a person wearing this protective clothing in an actual flash fire would receive. To make these predictions, a heat transfer model must be developed based on the structure of the skin.

---

* Numbers in square brackets denote references

1.2 The Skin

The skin is the largest organ in the body both in terms of surface area (1.6 to 1.9 m^2 for most adults) and weight (about 15% of total body weight). It serves many important functions. Besides covering the entire body, it protects the tissue beneath from physical, chemical, and thermal trauma. It forms an impermeable barrier preventing tissue fluids, electrolytes, and proteins from leaving, and environmental chemicals from entering. Through the skin come the sensations of touch, pain, and temperature changes. If there are temperature changes, the skin and its components serve as the temperature regulation centre for the body.

The skin consists of two layers, the epidermis and dermis (or corium), which are referred to as cutaneous tissue. Directly below the cutaneous tissue is the subcutaneous tissue. The general structure of the skin is shown in Figure 1.1, and is basically the same over the entire body, with anatomical and physiological differences in some regions. The main features of the skin are discussed below. For further information the reader is referred to [3], [4], and [5].

1.2.1 Epidermis

The epidermis is the very thin (0.06 to 0.8 mm thick, depending on location and person) outer layer of the skin. It contains no blood vessels or connective tissue, and receives nourishment from the dermis below. The epidermis consists of four layers. These are, from bottom to top, the stratum germinativum (basal layer), stratum spinosum (prickle cell layer), stratum granulosum, and the stratum corneum (horny layer). In the soles of the feet and the palms of the hand, there is an extra layer, the stratum lucidum, between the stratum granulosum and the stratum corneum. The structure of the epidermis is shown in more detail in Figure 1.2. Cells in the basal layer of the epidermis constantly divide to form new cells, which move upwards through the other layers. These cells eventually die and are converted to keratin, a water repellant protein, which makes up the horny layer.

The epidermis contacts the underlying dermis through a three dimensional series of irregular interpapillary folds, which increase the surface area of contact and hence increase shear resistance.

1.2.2 Dermis

The dermis is much thicker (20 to 30 times) than the epidermis. It provides the strength and elasticity for the skin, and contains the glands, hair follicles, lymphatic vessels, nerves, and blood vessels. It consists of two layers. The papillary (subepithelial) layer, lies adjacent to the epidermis. It contains small, vascularized, highly sensitive, rounded, conical structures (papillae) which interlock with corresponding depressions on the base of the epidermis. These form papillary ridges on the palms and soles which help in gripping. The patterns in the epidermis above these ridges are finger, palm, and sole prints. The epidermis gets nutrients and oxygen from diffusion through these papillae. The reticular layer, below the papillary layer, is a thick, robust layer made up of connective tissue formed into a closely meshed elastic fibre/collagen fibre network.

1.2.3 Subcutaneous Tissue

The subcutaneous tissue consists of connective tissue and specializes in the formation and storage of fat. In some parts of the body, such as the neck or the face, subcutaneous muscle exists under the fat layer.

1.2.4 Other Features

Other features of interest in the skin include the circulatory system, receptors, and melanocytes. Blood flows through a network of branching arteries and veins interconnected in a regular pattern called the circulatory system. This blood flow is responsible for nutritional and oxygen supply, cellular and humoral (fluid) defence, and

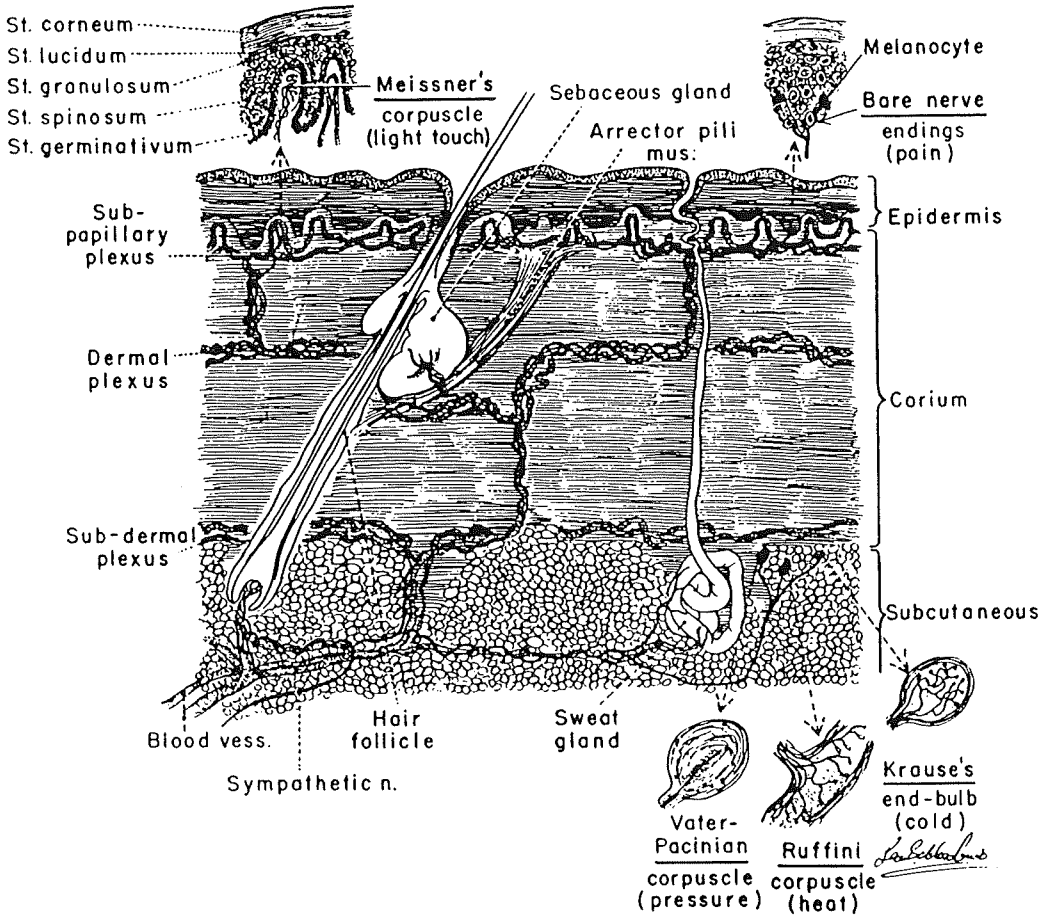

Figure 1.1 Normal Cross-Sectional Anatomy of the Skin. Reprinted from [6] With Permission.

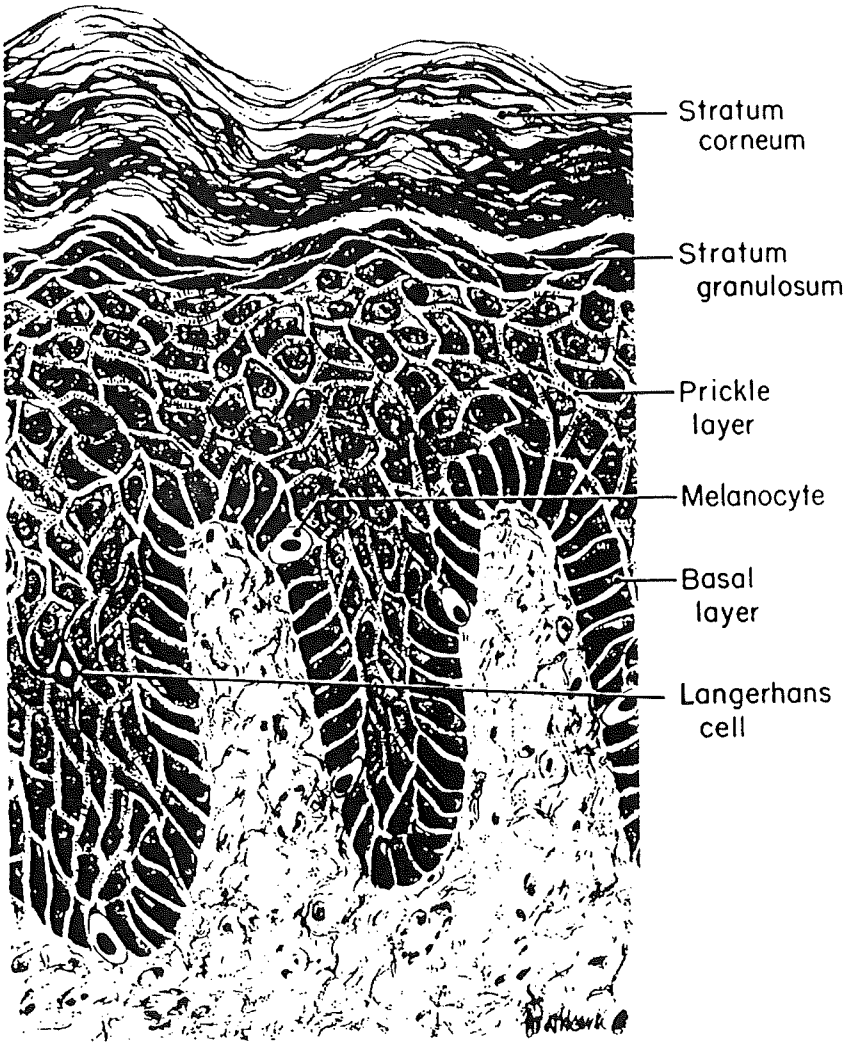

Figure 1.2 Cross-Sectional Anatomy of the Epidermis. Reprinted from [7] with permission.

thermal regulation. Receptors are the distal ends of dendrites of sensory neurons. Those found in the skin, when stimulated, initiate sensations of touch, pressure, warmth, cold, and pain. Melanocytes are cells that produce melanin, the main skin pigment. The quantity of melanin determines skin colour, and can change due to heredity, external factors (e.g. sunlight), or certain hormones.

1.3 Temperature Regulation Under Normal Circumstances

The body's core temperature remains fairly constant, ranging from 36.2°C in early morning to 37.6°C in late afternoon. As the biochemical reactions in the body must take place at certain rates, which are dependant on core temperature, it is critical that this temperature be maintained within a small range. This is done by balancing the energy gains from the catabolism of food by muscles and glands with energy losses, mostly by heat transfer through the skin.

Heat is dissipated to the environment through the skin in four ways: evaporation of sweat, and radiation, convection, and conduction from the skin surface. Evaporation of sweat accounts for the majority of heat transfer at higher ambient temperatures. Radiation from the skin dissipates most of the heat at lower ambient temperatures. The amount of heat lost through radiation can be increased or decreased through dilation or vasoconstriction of the surface blood vessels. Significant convection heat transfer only occurs if air flows across the skin at a high velocity. Losses through conduction only occur if the body is in contact with a cooler surface, such as clothing.

Temperature is controlled through a group of cells in the anterior portion of the hypothalamus (located on the top of the brain stem), referred to as the "human thermostat". These thermal receptor neurons are stimulated by very small changes (about 0.01°C) from the usual 37°C "setpoint temperature" of the blood that circulates to them. If the blood temperature is higher than this setpoint, signals are sent to the sweat glands to produce more sweat, and to the surface blood vessels to dilate. If the temperature is colder than the setpoint, two responses occur. Heat loss is decreased by reducing the amount of sweat produced, and the blood flow to surface vessels is reduced through

vasoconstriction. At the same time energy production is increased through increased catabolism by inducing shivering and voluntary muscle contractions. It is also thought that other hot and cold receptors in the skin send messages which result in voluntary actions by a person such as turning on a fan when it feels warm, or putting on a sweater when it feels cold.

Sometimes when conditions are very warm, the body cannot dissipate energy as fast as it is gained. This leads to heat stroke and its associated effects. Bacteria and viruses can bring pyrogens into the body which cause fevers by temporarily resetting the body's internal thermostat upwards.

1.4 Microscopic and Macroscopic Responses of the Skin to Thermal Insult

Burns are the one of the worst injuries possible to man. Many different local and systemic responses occur in the skin as a result of thermal insult. Burns take a great deal of time to heal and are sometimes difficult to treat clinically. The systemic effects provide further complications which must also be treated. Damage can become a serious social hindrance and a blow to self esteem if it occurs on visible portions of skin.

Burns are usually classified clinically as first, second, third, or fourth degree burns. As shall be discussed later, burns are temperature and time dependant. Therefore, two different exposures can result in the same degree of burn, but leave the skin with different appearances. Hence, making an exact clinical classification of actual burns is difficult, and in practice may take days. However, the following general comments, summarized from [3], are appropriate.

1.4.1 First Degree Burns

The only major response of the skin indicative of first degree burns is vasodilation of the subpapillary vessels, which results in redness of the burned region. Other local effects are minimal besides slight edema (puffy swelling caused by accumulation of serum - the watery portion of fluid left after coagulation) and irritation of nerve endings

in layers deeper than the stratum corneum. There are negligible systemic effects. Discomfort is temporary, and healing is normally quick with no permanent scarring or discolouration.

1.4.2 Second Degree Burns

Second degree (or partial thickness) burns are characterized by capillary damage which results in tissue edema and blisters. Cells can become swollen or lose their internal structure, and thus distorted may partially block blood vessels. There is a loss of fluids, leading to many systemic effects, and a loss of plasma volume, which is a major factor in causing shock in untreated burn patients. Second degree burns may be further classified as superficial or deep, depending on the penetration depth of the injured zone.

Superficial second degree burns are those in which a significant fraction of the cells at the base of the dermis are not destroyed. Therefore healing can occur in a normal pattern. There is an accumulation of edema fluid, and blistering occurs when the stratum corneum forces a waterproof covering over the wound to prevent an influx of bacteria. If this blister ruptures, the wound is more susceptible to infection, and there is an increased evaporative loss, requiring an increase in metabolism to maintain body temperature. Healing is normally prompt and without scarring since the majority of the cells at the dermal base are not injured.

Deep second degree burns result in much of the dermal base being lost. Certain elements such as hair follicles and glands may remain. There is widespread stasis (slowing or stoppage of circulation) and destruction of cells in the subpapillary plexus. Blistering is not widespread, but an eschar of plasma and dead cells forms over the wound. This eschar is water permeable, which leads to a very high evaporative loss, and a danger of infection. If the infection can be limited, there is potential for spontaneous regeneration of the skin. The wound would then be resurfaced from undamaged cells in hair follicles and the margins of the injured area. This new skin is thinner, lacks the secretions necessary to lubricate the surface, has decreased sensory capacity, and is

lighter in colour than the surrounding tissue due to the permanent loss of melanocytes. Interpapillary ridges do not redevelop and therefore the new skin is more susceptible to damage from tangential stress.

1.4.3 Third Degree Burns

Third degree (full thickness) burns occur when all epidermal elements and the supporting dermal structures are destroyed. There is no vascular response in the region of full thickness burn as all local blood vessels are destroyed, hence cellular and fluid responses of inflammation are confined to the periphery of this area. With no blood flow, the cells in this region of full thickness burn eventually die. Large volumes of extravascular fluid are lost due to injury to tissue beneath and surrounding the area of full thickness injury. These fluids collect beneath the wound even before swelling is visible on the surface after severe burns. The overlying eschar has no active nervous sensitivity and is highly permeable to water and bacteria. There is no possibility for spontaneous healing, and skin grafts are required for resurfacing from the margins of the wound.

1.4.4 Fourth Degree Burns

Fourth degree burns can occur with the incineration of tissue. Muscle, bone, and other structures below the subcutaneous tissue may be injured. Healing is not significantly different from that with third degree burns except for greater complications due to the injuries to underlying tissue.

1.4.5 Systemic Effects of Heat Trauma

There are also systemic effects of heat trauma, as a major burn will alter the functions of all organ systems to some extent. Some of these changes are a direct result of the thermal stress and the inflammatory mediators within the body which are released locally into the circulatory system. However most are due to the altered condition of the

skin. These systemic changes include the following.

- The shock resulting from fluid loss.
- A decrease in cardial output due to fluid losses and perhaps the release of myocardial depressant factors.
- Severe injuries to the respiratory system, which can occur through direct inhalation of combustion products and edema formation, even if the respiratory system has not been directly burned.
- An increase in the metabolic rate to compensate for the large heat losses from surface evaporation of water from the injured areas. Evaporative cooling also leads to shivering and increased metabolic rates.
- Other complications such as nutritional defects, and altered immune function.

1.5 The Bioheat Transfer Equation

The bioheat transfer equation, first proposed by Pennes [8] in 1948, is as follows.

$$\rho c \frac{\partial T}{\partial t} = k \nabla^2 T - G(\rho c)_b (T - T_c) \qquad (1.1)$$

This equation was derived based on a model where the skin lies above an isothermal core, the temperature of which is kept constant at the body's core temperature. Blood perfuses the dermis and subcutaneous tissues and transfers heat to or from the skin. Several assumptions were made in order to get the equation in the simplified form shown above [9,10,11].

- Heat conduction and storage within the tissues are both governed by the general linear theory of heat conduction.
- Tissue properties vary from layer to layer, but are constant over each layer.
- The blood enters the tissues at the body's core temperature which is assumed to remain constant.
- Heat transfer is assumed negligible between the large blood vessels (arteries and veins) and the tissue.

- The local blood flow rates are assumed constant, so there is no accumulations of blood with time in the blood vessels.

In deriving Equation 1.1, the skin was also assumed to be opaque. If the skin is diathermanous, rather than opaque, absorbed radiation must also be taken into account. The equation would then be

$$\rho c \frac{\partial T}{\partial t} = k \nabla^2 T - G(\rho c)_b (T - T_c) + q_a(t) \qquad (1.2)$$

where $q_a(t)$ is the net energy absorbed per unit volume of tissue.

The rate of metabolic energy production is sometimes included in these equations for low intensity, long duration exposures, or when studying temperatures in the skin under normal ambient conditions. As this rate is typically between 100 and 300 W/m^2 [12] it can be neglected relative to the large heat fluxes (e.g. 84 kW/m^2 [2]) from flash fires, and is therefore not included in either Equation (1.1) or (1.2).

These equations can be solved analytically or numerically for initially isothermal skin with constant properties, or numerically for skin with an initial temperature gradient and variable properties, subject to various boundary conditions. Normally if skin is modelled with variable properties, it is divided into the three layers, epidermis, dermis, and subcutaneous tissue, each of a different thickness with different thermal physical properties. One exception to this approach in the recent literature is Patterson (reported in [11]) who used a two region model consisting of an outer shell representing the passive epidermis, an inner shell representing the subcutaneous region, and a heat source at the boundary between these two regions representing the dermis and its blood flow. Recently a new bioheat transfer equation has been introduced by Weinbaum and Jiji [13]. This has led to some debate in the literature (e.g. [14]) over the use of the Pennes' bioheat transfer equation, and what the blood perfusion term included in it physically represents. However, for this work the traditional bioheat transfer equation will continue to be used.

1.6 Skin Burn Research

Much of the research which led to equations to predict skin burns was started during or immediately after World War II. During the war, large numbers of people sustained burns from fires which consumed entire city blocks during air raids, or from atomic bomb blasts. In order to protect people from similar and other thermal threats, it was first necessary to understand the effects of thermal trauma on the skin.

1.6.1 Henriques and Moritz

F.C. Henriques, Jr., and A.R. Moritz [15-19], working at the Harvard Medical School, were among the first to publish in this area. They maintained the surface of the skin at an elevated temperature by exposing it to hot water, and compared the severity of burns for different surface temperatures and times of exposure [16]. Pigs were used for most of the tests, as pig's skin is the closest anatomically to human skin, the only major difference being that pigs do not perspire. Some tests were also performed on human volunteers on the fronts of the thorax and forearms.

It was found [19] that skin damage could be represented as a chemical rate process, and that a first order Arrhenius rate equation could be used for the rate of tissue damage,

$$\frac{d\Omega}{dt} = P \exp\left(-\frac{\Delta E}{R\,T}\right) \tag{1.3}$$

Equation (1.3) can be integrated to produce

$$\Omega = \int_0^t P \exp\left(-\frac{\Delta E}{R\,T}\right) dt \tag{1.4}$$

This integration is performed over the time the basal layer temperature, T, is greater than or equal to 44°C during heating. As discussed below, 44°C is the threshold temperature for thermal damage.

It was found that for surface temperatures less than or equal to 50°C, the basal layer temperature was the same as the surface temperature during practically the entire exposure. Equation (1.4) was then integrated for this constant temperature over time. Arbitrarily setting $\Omega = 1.0$ for second degree burns, and substituting the measured surface temperatures and times to second degree burn, the constants P and ΔE were determined.

The activation energy, ΔE, was found to be 150 000 cal/mol (627 900 J/mol). This activation energy is very close to that of thermal denaturation (destruction through heating) of proteins (such as keratin in the epidermis). Therefore, the investigators postulated that this is the process by which skin tissue is destroyed. The value of the pre-exponential factor, P, was found to be 3.1×10^{98}. The basal layer temperature was found to be the key temperature in predicting epidermal skin damage, with 44°C the threshold temperature for damage. As Equations (1.3) and (1.4) suggest, damage is dependent on temperature and time. For example, at a basal layer temperature of 44°C, a six hour exposure was necessary for irreversible damage to begin, while at 70°C, less than an one second exposure was required. It was also found that first degree burns occurred when $\Omega = 0.53$.

Henriques and Moritz also experimentally determined the values of the thermal conductivity and specific heat for the various layers of pig's skin [15]. They also found that the blood flow in the dermis and subcutaneous regions did not have a significant effect on epidermal tissue damage [16]. As different temperature-time histories can produce the same severity of burn, the use of colour was found not to be a reliable criterion in judging burn severity [16]. As mentioned earlier, pigs do not sweat, whereas humans do. Below air temperatures of 120°C, man was said to resist heat better than pigs, but above 120°C perspiration would boil, and the advantage gained from sweating would be lost [18].

1.6.2 Buettner

Konrad Buettner [20-23] joined the United States Air Force School of Aviation Medicine after World War II. Buettner's work began in Germany in the latter part of World War II. This work was motivated by air raids, such as those on Hamburg in the summer of 1943, where over 40 000 people were killed in three nights [20]. He investigated the effects of heat on unprotected skin, and when covered by a proposed protective system consisting of an aluminum coated paper or cloth suit, boots of glass fibre, a mask made of chaff (aluminum strips used to jam radar), and eye protection.

In the United States, Buettner published papers [21-23] which further examined heat transfer in the skin. He assumed that the skin could be represented as an inert solid with a plane, infinite boundary with material constants independent of depth and temperature. Solutions to the differential equation representing the heat transfer in such a solid,

$$\rho c \frac{\partial T}{\partial t} = k \frac{\partial^2 T}{\partial x^2} \tag{1.5}$$

subject to different boundary conditions representing various heat exposures, were presented.

Buettner agreed with the use of the Henriques' burn integral. However much of his work involved determining the threshold of unbearable pain when non-penetrating infrared radiation was used to heat the skin of human volunteers [22]. The skin temperature at this threshold was found to be 44.8°C. He also estimated the depth of the pain receptors to be about 100 μm, found that precooling the skin tends to increase the time to pain, and found that the heat conduction in the upper part of the skin does not depend on blood flow. If high intensity radiation was used, peripheral blood flow and wetness of the skin did not influence the temperature at the pain threshold, nor did it influence the time to this threshold. Buettner also experimentally determined thermal conductivity and volumetric heat capacity values for the skin. He also performed numerical analysis and experiments to predict skin burns from penetrating flash radiation

exposures, such as those from atomic bomb blasts [23].

1.6.3 Stoll

Alice M. Stoll worked at the United States Naval Air Development Center and published extensively from the late 1950's to early 1970's [24-27]. In her early work with Leon C. Greene [24], sites on the volar surface of the forearm were blackened with India ink and irradiated with heat fluxes from 0.050 to 0.400 cal/cm^2·s (2.093 to 16.744 kW/m^2). From these tests, the temperature at the pain receptors for the least perceivable pain was found to be 43.2°C (note that this was the threshold for the least perceivable pain, rather than the threshold for unbearable pain, which Buettner found to be 44.8°C). The product of the skin's thermal conductivity, density, and specific heat ($k\rho c$), or thermal inertia, was measured, and found to increase with irradiance. It was thought that this increase was due to an increase in thermal conductivity with tissue temperature.

Exposure times to second degree burns observed for all exposures greater than 0.150 cal/cm^2·s (6.279 kW/m^2) were close to those predicted using Henriques' burn integral. However, the values of the burn integral itself were different from those predicted using Henriques' equation. Stoll noted that Henriques and Moritz had neglected damage which was done during cooling (which is almost one-third of the total damage at higher intensity exposures). She also believed that variations in thermal properties during cooling should be taken into account. (Later, Weaver and Stoll [25] developed a model which included these variations.) Stoll found that the results from her experiments could be predicted using Henriques' burn integral if the pre-exponential factor and activation energy values were changed to the following [25]:

- $P = 2.185 \times 10^{124}\ s^{-1}$ $\quad 44 \leq T < 50°C$

  $\Delta E/R = 93\ 534.9\ K$

- $P = 1.823 \times 10^{51}\ s^{-1}$ $\quad T \geq 50°C$

  $\Delta E/R = 39\ 109.8\ K$

Stoll also estimated the average depth of the pain receptors in the skin to be

240 μm (which would be about 140 μm into the dermis). This was said to explain the fact that high heat flux/short duration exposures can cause epidermal damage without pain.

Later Stoll began to look at the protection offered to the skin by fabrics [26,27]. One of her experiments was an early forerunner to the modern Thermal Protective Performance (TPP) test which will be discussed in Section 1.8.2. This test was used to determine the effect of increasing the spacing between layers of clothing. She also found that vapourization of moisture in fabrics and from perspiration was relatively unimportant in fabric/skin heat transfer. These fabric tests eventually led to instrumented mannequin tests, which will be discussed in Section 1.8.3.

1.6.4 Hardy

James D. Hardy and Martin Lipkin [28] used the following equation presented by Buettner [21] for non-penetrating radiation

$$T(x,t) - T_i = \frac{2\, q_o \sqrt{t}}{\sqrt{k\rho c\, \pi}} \tag{1.6}$$

in order to determine the thermal inertia of living skin, and excised bone, fat, muscle, and skin. They found that the thermal inertia of living skin increased with increased blood flow and moisture in the skin.

Hardy also examined [29,30] the relationship between stimulus and pain intensity. He found that pain was dependant only on temperature, whereas damage depended on temperature and time. At the pain threshold temperature of about 45°C, tissue damage, protein denaturation, and pain and reflex reactions all began, regardless of the type, intensity, and duration of the thermal stimulus and initial skin temperature. Pain was also explained in terms of just noticeable difference (j.n.d.) units. (According to Weber's Law, the j.n.d. of a stimulus at any intensity is a constant proportion of that intensity. The value of the constant of proportionality is different for each sensation.)

Hardy also found that it took at least 20 s for the body to respond to increased temperatures with increased blood flow.

1.6.5 Mehta and Wong

Arun K. Mehta and Franklin Wong [9,10], working at the Massachusetts Institute of Technology, tested fabrics over skin simulants. They made various comments on the research previously done, and presented results of their own research. Mehta and Wong stated that the mode of heat transfer was not important in predicting burns, just the size of the thermal dose to the skin. They agreed with the use of Henriques' burn integral for predicting the extent of skin burns. However, they believed that the equation as presented by Henriques and Moritz was only valid for superficial (i.e. epidermal) burns. In addition, they pointed out that the temperatures that the previous investigators measured and used to calculate the pre-exponential factor and activation energy had not been measured accurately enough. Further, as Stoll had remarked, damage during cooling was not included. Convective losses from the skin were not included either, nor were changes to the thermal physical properties of skin, such as found with steam blebs or separation in burns. They pointed out that Stoll used an initial temperature of 32.5°C, and Henriques and Moritz 37°C. Regardless of what the exact reasons for the differences in the results of Stoll from those of Henriques and Moritz, they were not caused by the differences in modes of heat transfer used (Henriques and Moritz had heated the skin by conduction, Stoll had used radiation). They also expressed doubt as to whether data from low intensity, long duration tests could be used in high intensity, short duration tests of concern here.

Later work in which Henriques had tried to extend his criteria to dermal damage was discussed [31]. Mehta and Wong pointed out that the skin was not completely opaque as was assumed in that work. Henriques used only a single layer model of the skin. It did not seem correct to predict dermal damage based on only this epidermal information, as it was well known clinically that two burns can have the same surface appearance, but different damage to deeper layers. Henriques' new correlation was also

based on data which was later found to be incorrect.

Work by Chen [32] was also dismissed. Chen stated that the severity of a burn was dependant on the amount of thermal energy entering into the system above a certain temperature. His correlation was empirical and only applicable to second degree burns in pigs.

Mehta and Wong modelled the skin as a finite solid with different layers, each having different properties. The bioheat transfer equation, discussed earlier, was used to calculate temperatures at depth in the skin. They changed the upper time limit in Henriques' integral to include cooling time. Values for the pre-exponential factor and activation energy based on their data and $\Omega = 1.0$ at the basal layer for second degree burns, and $\Omega = 1.0$ at the dermal base for third degree burns, were determined. The values found for the epidermis and dermis were as follows.

- $P = 1.43 \times 10^{72}\ s^{-1}$ epidermis
- $\Delta E/R = 55\ 000\ K$
- $P = 2.86 \times 10^{69}\ s^{-1}$ dermis
- $\Delta E/R = 55\ 000\ K$

Mehta and Wong also explained the assumptions they made and their effects on burn predictions. The energy required for the thermal denaturation of proteins itself was neglected. This was probably not significant relative to the sensible energy required. The evaporation of superficial water into steam for short, intense exposures (as found in the formation of steam blebs in greater than third degree burns) was neglected. The vapourization or decomposition of superficial tissues (such as the carborization of the top layer(s) of skin in extremely high intensity, short duration exposures) was also neglected. The effect of all these assumptions was that burn predictions would be slightly higher than predictions which included these factors. As the thermal protection offered by a fabric was of concern here, slight over-predictions of burns were justified.

1.6.6 Takata

Takata [33] analyzed data from tests performed by the United States Army at Fort

Rucker, where a large number of anaesthetized pigs were exposed directly to JP-4 liquid fuel fires. The values that Takata obtained for the pre-exponential factor and activation energy for predicting dermal damage using Henriques' burn integral were:

- $P = 4.32 \times 10^{64}\ s^{-1}$ $\quad T < 50^{\circ}C$
- $\Delta E/R = 50\ 000\ K$
- $P = 9.39 \times 10^{104}\ s^{-1}$ $\quad 50 \leq T \leq 60^{\circ}C$
- $\Delta E/R = 80\ 000\ K$

No values of the pre-exponential factor or activation energy were given for dermal base temperatures above 60°C, as temperatures above this value were not observed in tests.

1.7 Aerotherm's Critique of Skin Burn Models

In the late 1960's, the Aerotherm Division of the Acurex Corporation built a thermally instrumented mannequin for the United States Military for testing clothing in simulated JP-4 fuel fires (which are similar to flash fires in terms of intensity and duration of exposure). During the process of developing a computer code to be used to analyze the information from the mannequin tests, possibly the most detailed evaluation of the above skin burn models and thermal physical properties was made [34,35]. This evaluation included comparisons of the different values of the pre-exponential factor and activation energy used in the burn integral for calculating epidermal and dermal burns. The comparisons were done using existing epidermal burn damage data and information from deep burn tests. Stoll's values were found to be the best for the epidermis, and Takata's for the dermis.

A ten node finite difference computer code was used to solve for temperatures in the skin. The skin was assumed to be opaque, as the amount of energy absorbed by the skin for threshold injury (i.e. loss of epidermis) generally implies negligible direct transmission through the skin. Therefore the absorbed radiant energy term was only used for the surface node in the finite difference equations. The density and specific heat were taken as constant throughout the skin, and as the same values as those of water.

The thermal conductivity was varied at each node, from 40% of water at the surface to that of water at depth. The epidermis, dermis, and subcutaneous layers were assumed to be 100 μm, 2 mm, and 1 cm thick, respectively. Boiling was assumed to occur whenever tissue reached the boiling point of water, 100°C, and 2256 kJ/kg, the latent heat of vapourization of water, was absorbed in this process. Blood flow was not included in this model, because of the short durations of exposure here, remembering that Hardy had stated that it took at least 20 s for the body's circulation to respond to any increase in temperature. Variations in thermal properties were thought to have essentially no effect upon the amount of heating to the skin, because skin surface temperatures were relatively low as compared to fabric temperatures. A forced convection surface boundary condition after the exposure (using a convection heat transfer coefficient of 1.0 Btuh/ft^2·°F (3.15 W/m^2·°C)) was used in the solution of the appropriate differential equation.

1.8 Fabric and Clothing Tests

Much research has been undertaken in testing the flammability of various fabrics or pieces of clothing, and the thermal protection that these offer. Early research was concerned with the flammability of ordinary fabrics or clothing, specifically observing flame patterns of burning fabrics, and measuring rates of burning. As fire resistant clothing was developed, it was necessary to test the protection that these pieces of clothing provided the skin. Eventually, tests were developed using information from the skin burn research outlined above.

1.8.1 Skin Simulants

As actual living human skin cannot be used for tests involving high heat fluxes or temperatures, skin simulants, materials which have thermal physical properties similar to skin, have been used. The fabric, or piece of clothing, is then placed over this simulant and subjected to a simulated accident. As the skin simulant has similar thermal

physical properties to skin, the heat transfer in this simulant should be close to that in actual skin.

It can be shown [36] that for a semi-infinite solid with constant initial temperature and thermal physical properties subjected to a constant heat flux on its surface, the temperature difference at any point in time and space is given by

$$T(x,t) - T_i = \frac{q_o}{k}\left[2\sqrt{\frac{\alpha t}{\pi}}\, e^{-\frac{x^2}{4\alpha t}} - x\, erfc\left(\frac{x}{2\sqrt{\alpha t}}\right)\right] = \frac{2\, q_o \sqrt{t}}{\sqrt{k\rho c}}\, ierfc\left(\frac{x}{2\sqrt{\alpha t}}\right) \tag{1.7}$$

where erfc is the complementary error function and ierfc is the integral of the complimentary error function.

For small values of x, such as in the skin, the second term in the brackets approaches zero, producing Equation (1.6), which was introduced earlier.

$$T(x,t) - T_i = \frac{2\, q_o \sqrt{t}}{\sqrt{k\rho c\ \pi}} \tag{1.6}$$

Therefore it is important that the thermal inertia, $k\rho c$, or the thermal absorptivity [37], $(k\rho c)^{0.5}$, of the simulant be close to that of skin. Some materials which have values similar to skin are pyrex glass [38], and colorceran [2]. Mehta and Wong [9,10] developed a copper-air rod type skin simulant.

1.8.2 Thermal Protective Performance Test

W.P. Behnke [39] from E.I. DU PONT DE NEMOURS AND COMPANY devised a test for measuring the performance of fabrics to high heat flux, short duration exposures, such as in flash fires and JP-4 fuel fires caused by carrier deck crashes of planes.

In the original Thermal Protective Performance (TPP) test, nine quartz tubes

powered by a variable voltage supply were used to supply the desired level of radiant energy. A pair of Meker burners supplied the appropriate amount of convective energy. A water cooled shutter was used to time the exposure. The test fabric itself was mounted over a blackened 40 mm copper disk mounted in an insulating block, which served as a heat flux sensor. When this test is now used for fabric which must withstand mainly convective and conductive exposures, the quartz tubes are not used (although as can be seen by the closed form solutions, as long as the radiation does not penetrate the fabric, it is simply the total amount of flux which is important, rather than the form of the flux).

The TPP rating of a fabric is the amount of energy which can be supplied to the fabric until second degree burns of the underlying skin would occur. This rating is found by exposing the fabric to a constant 2 $cal/cm^2 \cdot s$ (83.732 kW/m^2) heat flux from the burners and recording the readings from the heat flux sensor. The temperature-time history based on the readings of the sensor can be input into Henriques' burn integral, and the time until second degree burns would occur to the skin can be found. As the TPP rating is the energy (in cal/cm^2) that can be transferred to the fabric before such burns occur, the rating is simply found by multiplying the 2 $cal/cm^2 \cdot s$ heat flux from the burners by the time to second degree burns.

It is important in any test to approximate the hazard as closely as possible. The heat flux used here is typical of flash fires. This is very important in testing fabrics as it has been found [39] that almost all textile fibres will transfer approximately the same amount of heat until they reach a critical temperature. The amount of heat transferred will depend upon the fabric construction, not the fibre type. Above this temperature the thermal behaviour of the fibres becomes important to the heat transfer through a fabric. The mounting of the fabric specimen in the TPP test can also be changed to model such situations as a tight-fitting single layer, or multiple, loose-fitting layers of fabric.

The TPP test provides a basis of comparing competing fabrics. One variation of the TPP test is the basis for ASTM Standard D 4108-87 (Standard Test Method for the Thermal Protective Performance of Materials For Clothing by Open Flame Method) [40]. It is also cited in National Standard of Canada CAN/CGSB-155.1-M88 (Firefighters' Protective Clothing for Protection Against Heat and Flame) [41].

Despite these attempts to model accidents, there are questions as to the applicability of these test results in appraising protective garments. For example, the mechanical integrity of the fabric is not tested either during or after the exposure in the TPP test. It has been suggested [42] that while this test is a useful research and development tool for protective fabrics for JP-4 fuel fires and similar accidents, it has also been used to rate fabrics for many entirely different accidents which it does not accurately simulate.

1.8.3 Mannequin testing

In order to test protective clothing under more realistic conditions, non-instrumented and instrumented mannequins have been used. By using mannequins, the performance of the entire garment subject to simulated accidents can be evaluated, rather than just the performance of the fabric which makes up the garment. Factors such as the location of closures, finishes, and fit of the garment can then be studied.

1.8.3.1 Early Mannequin Research

In the 1940's non-instrumented mannequins [43] were used to observe the garment burning behaviour (e.g. the rate and pattern of flame spread), self-extinguishment process, and the garment area consumed in burning of shirts for forensic purposes. Garments were also tested on wire frame body forms. In 1962, Stoll conducted tests for the United States Navy using leather-covered mannequins equipped with temperature detector paper and melting point indicators. This was the first of many instrumented mannequins, some of which are briefly discussed below.

1.8.3.2 Thermo-man®

Thermo-man® was first developed by the Aerotherm Division of the Acurex Corporation for the United States Military for testing flight suits in JP-4 fuel fires [44].

It was later purchased by E.I. DU PONT DE NEMOURS AND COMPANY, who altered its data acquisition system and registered the trade name Thermo-man®. There are now Thermo-men at the company's facilities in Wilmington, Delaware and Geneva, Switzerland. Propane torches are used to simulate accident scenarios, and a data acquisition system takes information from sensors located over the surface of the mannequin and converts these sets of data into burn predictions for the portion of the body around that sensor. From this information, the percentages of body surface area which receive second and third degree burns can be determined.

1.8.3.3 Minnesota Woman

Mannequins have also been used to test the performance of clothing during simulated domestic accidents. One of these mannequins, the University of Minnesota's Minnesota Woman, was the first female instrumented mannequin [38]. Previously women's clothing had been tested using male mannequins. This was thought to result in different garment burning behaviour and predicted injuries from tests where the same garments were burned on anatomically different women's forms. One example of work done using this mannequin was a study of the flammability hazards of women's nightgowns [45].

1.8.3.4 Mannequin Testing at the University of Alberta

"Harry" is a male, size 40 regular, thermally instrumented mannequin which is used to test flame-resistant clothing in simulated flash fire conditions [2]. Twelve propane diffusion flames are used to simulate flash fire conditions. The information from 110 skin simulant sensors is used to compute the percentages of the body which would experience second and third degree burns using a finite difference computer code.

1.9 Overview of this Study

In this thesis a finite element model of the heat transfer in human skin will be described. From this model, skin temperatures and times to second and third degree burns can be obtained for simulated flash fire conditions. As with the Thermo-man® and present University of Alberta mannequin systems, first degree burns, which are relatively mild compared with second and third degree burns, will be ignored. A flash fire is quite different from many other exposures studied in the literature, such as medical uses of lasers, skin under normal temperature distributions, and long duration, low heat flux exposures. Therefore this heat transfer model will be different from those used in these other cases. Many of the thermal physical properties used in the model are difficult to measure, or vary widely depending on the exposure. The surface boundary condition after the exposure is difficult to define exactly, and may have an effect on skin damage. The heat transfer model developed here will be used to decide how important these variations and this boundary condition are, and if the heat transfer model must be modified to account for these factors. A comparison will then be made between the heat transfer model developed here and other models proposed in the literature. Recommendations for further research will also be made.

CHAPTER 2
DEVELOPMENT OF THE FINITE ELEMENT MODEL

In this chapter the development of a finite element model of the skin will be outlined. The advantages of using the finite element method for problems involving heat transfer in the skin will be discussed, along with some examples of where it has been used in the past in this area. A computer program based on this model was developed to predict skin temperatures and times to second and third degree burn under flash fire conditions. This program was tested by comparing its results with those of closed form solutions for classical boundary condition problems. The computer program, test results, and some of the problems encountered in using the finite element method to model this particular heat transfer problem will be discussed.

2.1 The Finite Element Method

While the finite element method has been used extensively in areas of engineering such as acoustics and structural design in the past, it is only in the last twenty years that this method has begun to be used in problems involving heat transfer in human skin. The same advantages which have led to its use in traditional fields also make it an attractive method for approaching biomechanical engineering problems.

Some of these advantages are as follows. The complex geometry of the skin, and thermal physical properties which vary with location, time, and temperature can be modelled. Variable element sizes can be used to handle the steep temperature gradients in the outer portions of the skin. Energy sources or sinks inside the skin, such as the blood perfusion term in Pennes' bioheat transfer equation can be included in models.

There are many examples of use of the finite element method in biomechanical engineering. Gustafson and his colleagues at the University of Minnesota [46] used a finite element program in conjunction with the Minnesota Woman mannequin (discussed in Section 1.8.3.3) to predict skin burns. Diller and Hayes [47] developed an axisymmetric model of a composite man with distributed internal heat generation in a convective, subfreezing environment. Diller and Hayes [48] also modelled the burn process resulting from the application of a hot, circular source to the skin surface. Sekins, Emery, Lehmann, and MacDougall [49] used a two dimensional finite element

model to represent a human thigh undergoing microwave diathermy (a medical heat treatment which increases the blood flow). Osman and Afify [50,51] developed three dimensional models of normal and malignant woman's breasts. These models were used to study the effect of cancerous tumours on the temperature distribution in the breast in order to aid in the use of infrared thermography to detect and treat breast cancer.

2.2 Derivation of Finite Element Matrix Equation

As mentioned earlier in Section 1.5, the Pennes' bioheat transfer equation can be used to determine temperatures in the skin. Here the skin will be assumed to be opaque, so as to simplify the analysis of the problem. As the emissivity of human skin is 0.94 [24], this should result in the opaque model predicting only slightly higher surface temperatures, and slightly lower temperatures at depth (and therefore burn damage) than with actual diathermanous skin. For a clothed person, very little radiation would penetrate through the clothing to the skin, and this assumption will have even less of an effect. The energy lost due to evaporation of moisture in the skin, and carborization of the skin at very high exposures will also be neglected, such as in Mehta and Wong's work [9,10]. This will result in temperature and burn predictions which are slightly higher than in actual skin. Since the object of this study is to predict second and third degree burns, evaporation of moisture or carborization of skin may occur after second and/or third degree damage has already been sustained, and therefore would not be of interest here. The slightly higher burn predictions which result from these two assumptions should also be at least partially compensated for by the slightly lower burn predictions made by assuming opaque skin.

Heat transfer was assumed to be one-dimensional. The Pennes' bioheat transfer equation for blood perfused skin is:

$$\rho c \frac{\partial T}{\partial t} = k \frac{\partial^2 T}{\partial x^2} - G(\rho c)_b (T - T_c) \tag{2.1}$$

To model the exposure to a flash fire, the following initial and boundary conditions were

used:

$$T(x,t=0) = T_i(x) \tag{2.2}$$

where $T_i(x)$ is some initial temperature gradient in the skin.

$$T(x=L,\ t) = T_c \quad , t > 0 \tag{2.3}$$

$$k\left(\frac{\partial T}{\partial x}\right) + q(t) = 0 \quad (x=0,\ t) \tag{2.4}$$

where q(t) is the heat flux incident on the surface of the skin from the flash fire as a function of time.

Galerkin's weighted residual method was used to formulate a finite element matrix equation to solve this differential equation, subject to the given initial and boundary conditions. This and other weighted residual methods are alternatives to variational methods, which are also commonly used to derive finite element matrix equations. Weighted residual methods, unlike variational methods, do not rely on forming functionals, but instead use the differential equation directly to form a matrix equation. Weighted residual methods can also be used to solve more general problems than the variational methods, which cannot handle first derivatives, dissipation terms, and non-linearities. The derivation of the finite element equation is described in detail in Appendix 1, and is based on [52].

Three one dimensional temperature interpolation polynomials were considered: linear, quadratic, and cubic Hermitian. While all of the temperature interpolation polynomials for these elements are presented in Hermitian form, the cubic Hermitian element will be referred to as the "Hermitian" element for the remainder of this report.

The linear temperature element, shown in Figure 2.1(a), has the following interpolation polynomials.

$$
\begin{aligned}
T(x) &= \left(1 - \frac{x}{l}\right) T_a + \left(\frac{x}{l}\right) T_b \\
&= \left\lfloor \left(1 - \frac{x}{l}\right) \frac{x}{l} \right\rfloor \left\langle \begin{matrix} T_a \\ T_b \end{matrix} \right\rangle \\
&= \langle f_L \rangle^T \langle T_e \rangle
\end{aligned}
\tag{2.5}
$$

The quadratic temperature element is shown in Figure 2.1(b). Its temperature interpolation polynomials are

$$
\begin{aligned}
T(x) &= \left(1 - 3\left(\frac{x}{l}\right) + 2\left(\frac{x^2}{l^2}\right)\right) T_a \\
&\quad + \left(4\left(\frac{x}{l}\right) - 4\left(\frac{x^2}{l^2}\right)\right) T_b \\
&\quad + \left(-\frac{x}{l} + 2\left(\frac{x^2}{l^2}\right)\right) T_d \\
&= \left\lfloor f_{q1} \;\; f_{q2} \;\; f_{q3} \right\rfloor \left\langle \begin{matrix} T_a \\ T_b \\ T_d \end{matrix} \right\rangle \\
T(x) &= \langle f_q \rangle^T \langle T_e \rangle
\end{aligned}
\tag{2.6}
$$

The Hermitian temperature element, shown in Figure 2.1(c), has the following temperature interpolation polynomials:

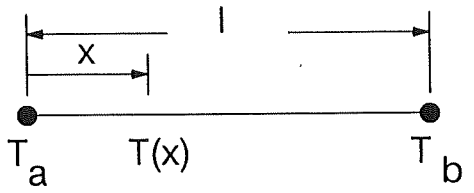

Figure 2.1(a) Linear Temperature Element

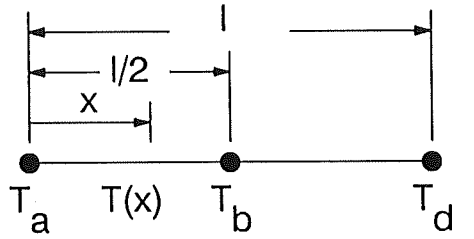

Figure 2.1(b) Quadratic Temperature Element

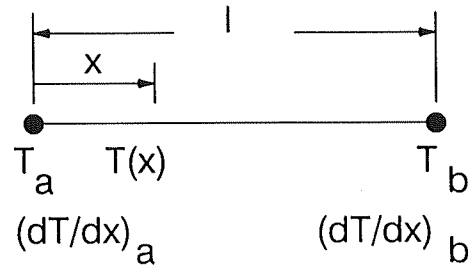

Figure 2.1(c) Hermitian Temperature Element

$$
\begin{aligned}
T(x) &= \left(2\left(\frac{x^3}{l^3}\right) - 3\left(\frac{x^2}{l^2}\right) + 1 \right) T_a \\
&+ \left(\frac{x^3}{l^3} - 2\left(\frac{x^2}{l^2}\right) + \frac{x}{l} \right) l \left(\frac{\partial T}{\partial x}\right)_a \\
&+ \left(-2\left(\frac{x^3}{l^3}\right) + 3\left(\frac{x^2}{l^2}\right) \right) T_b \\
&+ \left(\frac{x^3}{l^3} - \left(\frac{x^2}{l^2}\right) \right) l \left(\frac{\partial T}{\partial x}\right)_b \\
&= \lfloor\, f_{h1} \;\; f_{h2} \;\; f_{h3} \;\; f_{h4} \,\rfloor \left\langle \begin{matrix} T_a \\ \left(\frac{\partial T}{\partial x}\right)_a \\ T_b \\ \left(\frac{\partial T}{\partial x}\right)_b \end{matrix} \right\rangle \\
T(x) &= \langle f_h \rangle^T \langle T_e \rangle
\end{aligned}
\tag{2.7}
$$

As shown in Appendix 1, the finite element matrix equation for the differential equation is

$$
\begin{aligned}
&\left([B] + \frac{\Delta t}{2} \left([A] - [k] + [M] \right) \right) \langle T^{(j+1)} \rangle \\
&\quad = \left([B] + \frac{\Delta t}{2} \left(-[A] + [k] - [M] \right) \right) \langle T^{(j+1)} \rangle \\
&\quad + \frac{\Delta t}{2} \left(\langle BC^{(j)} \rangle + \langle BC^{(j+1)} \rangle \right)
\end{aligned}
\tag{2.8}
$$

or

$$
[LHS] \; \langle T_e \rangle = \langle RHS \rangle \tag{2.9}
$$

As the nodes and elements in the skin were numbered in order from the surface to the base of the subcutaneous region, [LHS] is a banded matrix with a bandwidth of four. Therefore a banded matrix solver was used to solve Equation (2.9) at each time step. This decreases the computation time considerably over the time that a Gaussian

elimination matrix solver would take to solve Equation (2.9).

2.3 Finite Element Computer Program

A computer program based on the above finite element derivation was written to solve for the nodal temperatures and fluxes. The program was written in Microsoft® QuickBASIC™ 4.5 for use on a 80386 based personal computer with a 33 MHz clock. This computer also contained a 80387 math coprocessor. A flow chart for the program is shown in Figure 2.2.

The program operation is as follows. In the initial stages of the program, shown in Figure 2.2(a), variable declarations are made and parameter values are read (e.g. number of elements, heat flux incident on skin, etc.). Vectors of material properties for each element, depths from the skin surface for each node, and initial nodal temperatures and fluxes are formed. A nodal connectivity matrix which relates the node and element numbers, and a vector of elapsed time for each time step are also formed.

The program then marches forward in given time increments. At each time step the [LHS] matrix and the information used to calculate the $<RHS>$ vector are formed for each element, and then assembled to form the global [LHS] matrix and $<RHS>$ vector using the information in the nodal connectivity matrix. The [LHS] matrix and the $<RHS>$ vector are then constrained by applying the boundary conditions at the skin surface and base of the subcutaneous layer. This constrained [LHS] matrix is then converted into a banded matrix, and the matrix equation is solved for nodal temperatures and fluxes. These steps are shown in Figure 2.2(b).

From the temperatures at the basal layer and the base of the dermis, the values of Henriques' burn damage rate (Equation 1.3) are now calculated. These damage rates are then integrated over time using the trapezoidal rule to give cumulative Henriques' burn integral values for the basal layer and the dermal base to this time step. These values are then compared to the values of 1.0 at these depths to give second and third degree burns, so that the times to each of these burns can be presented. The temperatures and cumulative damage at these two nodes are printed to a datafile. These

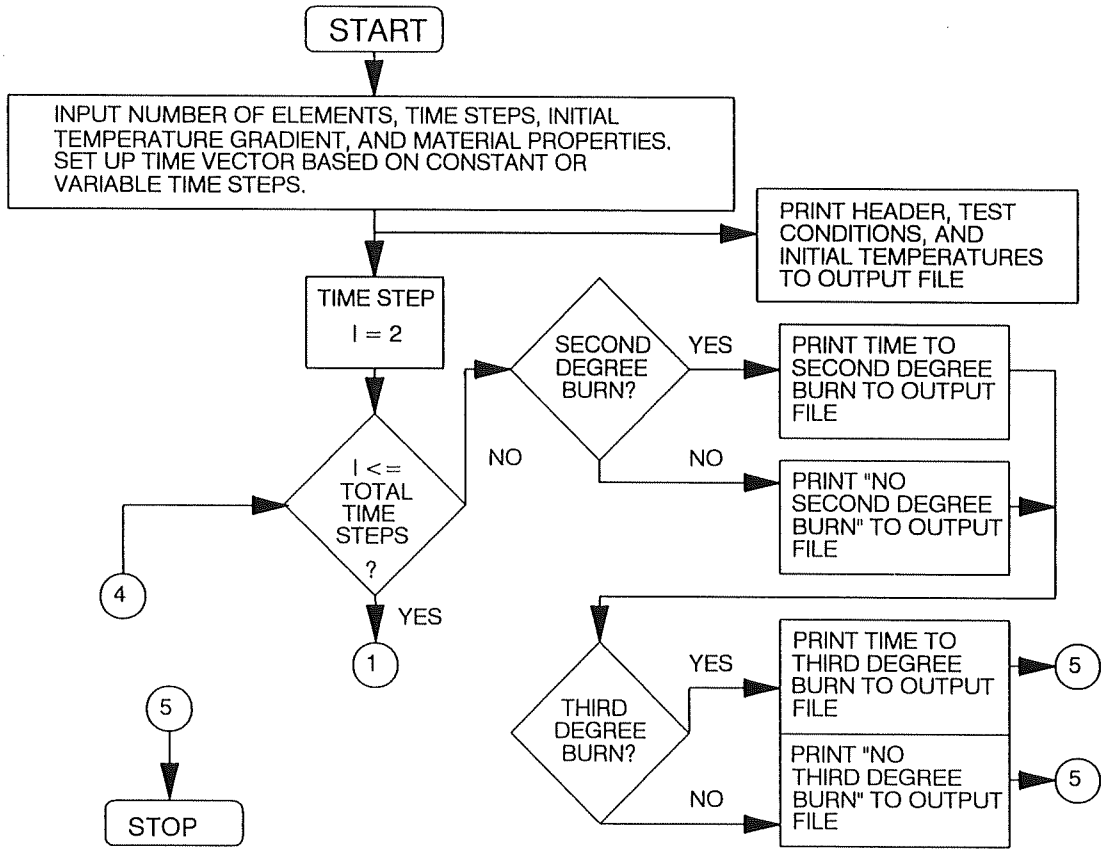

Figure 2.2(a) Flow Diagram of Finite Element Computer Program - Initial Stages

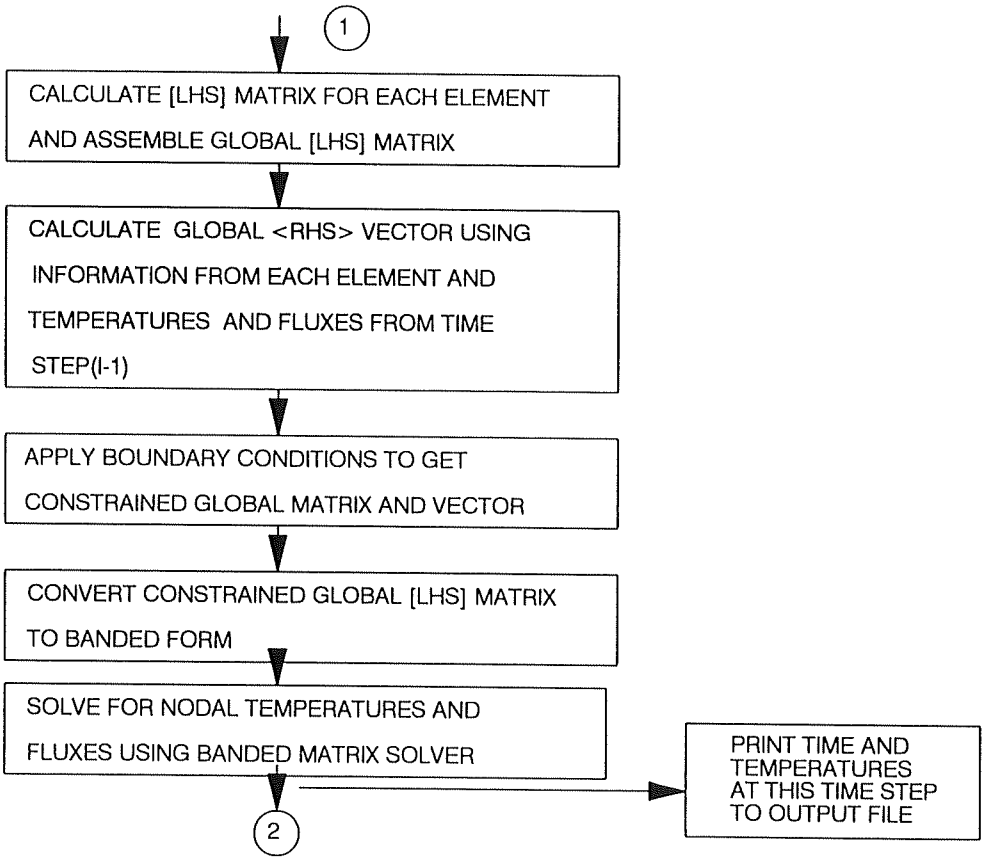

Figure 2.2(b) Flow Diagram of Finite Element Computer Program - Skin Temperature Module

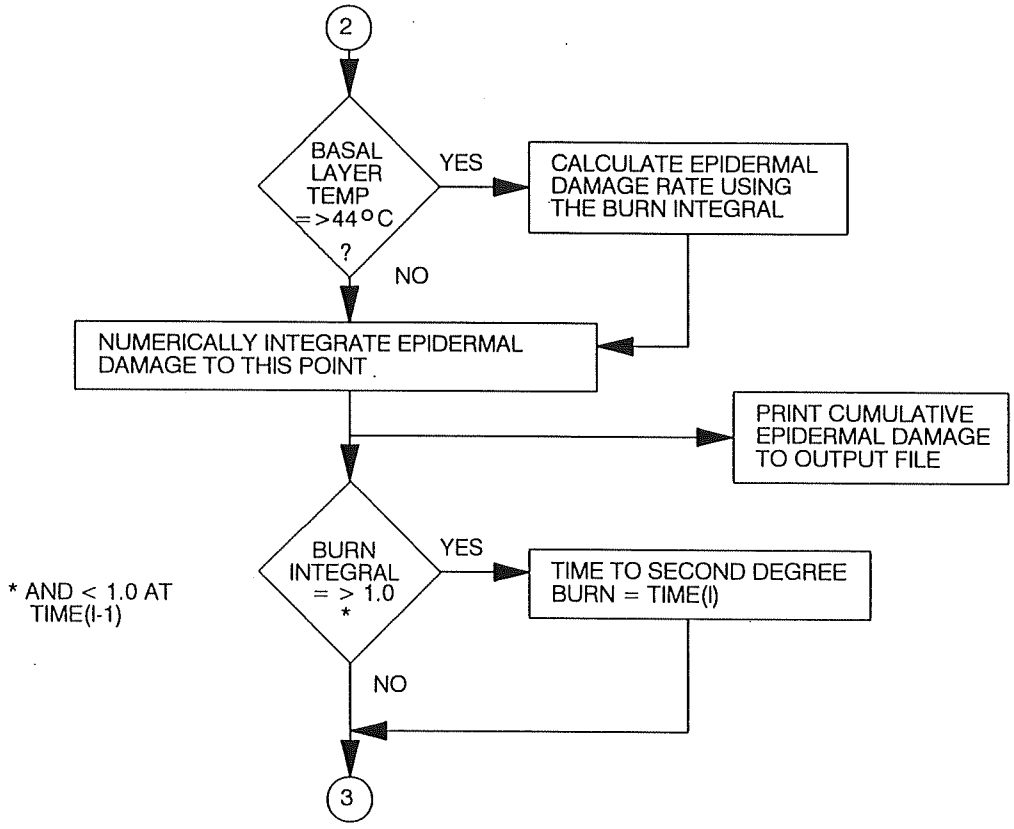

Figure 2.2(c) Flow Diagram of Finite Element Computer Program - Epidermal Burn Module

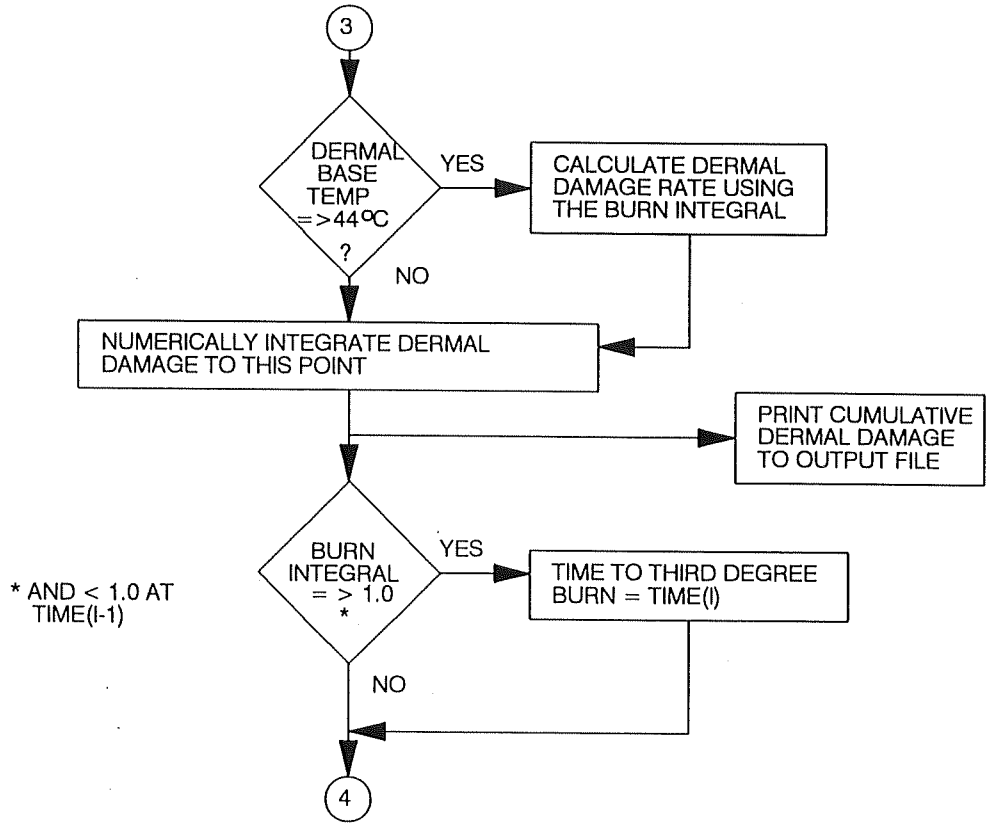

Figure 2.2(d) Flow Diagram of Finite Element Computer Program - Dermal Burn Module

procedures for calculating epidermal and dermal damage are shown in Figures 2.2(c) and (d), respectively.

The program continues calculating temperatures for the entire time of interest. Flash fires are short, typically 5 s or less, but skin temperatures can take 60 s or longer to cool below critical values. Therefore temperatures and burns were calculated for 60 or 120 s depending on the heat flux. The program then prints the times to second and third degree burn to the datafile, as shown in Figure 2.2(a). A sample partial datafile generated by the program is shown in Appendix 2.

2.4 Comparison of Finite Element Solutions with Closed Form Solutions for Classical Boundary Condition Problems

In a similar manner to that described above, finite element solutions to three classical problems with closed form solutions were derived in order to test the computer code. The finite element solutions were extremely close to closed form solutions for constant surface temperature and convection boundary conditions, which will not be shown here. The comparison of the finite element solution with the closed form solution for a constant incident heat flux boundary condition will be shown, as it is similar to the situation of interest, and is instructive in showing some of the difficulties inherent in modelling the heat transfer in this problem.

2.4.1 Constant heat flux boundary condition

A simple model of skin subjected to flash fire conditions is an inert semi-infinite solid, initially at constant temperature, subjected to a constant heat flux at its surface for a period of time, t_{ex}, after which the surface is insulated. The differential equation and initial and boundary conditions are as follows.

$$\rho c \frac{\partial T}{\partial t} = k \frac{\partial^2 T}{\partial x^2} \tag{2.10}$$

$$T(x,t=0) = T_i \tag{2.11}$$

$$T(x=L,t) = T_i \tag{2.12}$$

$$k \frac{\partial T}{\partial x} + q(t) = 0 \quad (x = 0\ ,\ t > 0) \tag{2.13}$$

where the heat flux, q(t), is given by

$$\begin{aligned} q(t) &= q_o \quad 0 < t \leq t_{ex} \\ &= 0 \quad t > t_{ex} \end{aligned} \tag{2.14}$$

and shown in Figure 2.3.

The closed form solution is given in [53] as

$$T(x,t) = T_i + \frac{2q_o}{\sqrt{k\rho c}} \left(\sqrt{t}\ ierfc\left(\frac{x}{2\sqrt{\alpha t}}\right) - \sqrt{t - t_{ex}}\ ierfc\left(\frac{x}{2\sqrt{\alpha(t - t_{ex})}}\right) S(t) \right) \tag{2.15}$$

where S(t), the unit step function is given by

$$\begin{aligned} S(t) &= 0 \quad t \leq t_{ex} \\ &= 1 \quad t > t_{ex} \end{aligned} \tag{2.16}$$

A comparison of basal layer temperatures predicted by the finite element model and the closed form solution is shown in Figure 2.4 for an incident heat flux of 83.2 kw/m^2 for 3 s, conditions typical of a flash fire. Both the finite element model and closed form solution used one skin layer with the thermal physical properties that were measured by Perkins [54], and used by Hardee and Lee in their single layer skin model [53].

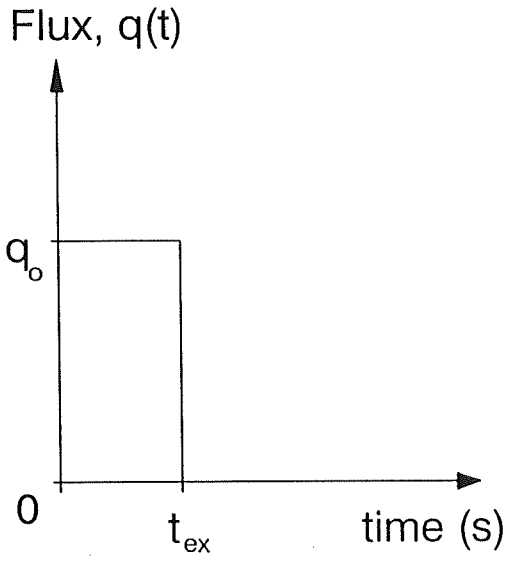

Figure 2.3 Imposed Step Heat Flux Function

There are several difficulties to overcome when using the finite element method to solve this problem. The step heat flux presents numerical problems when it is "turned on" at t = 0, and "turned off" at t = 3 s. Equation (2.8),

$$\left([B] + \frac{\Delta t}{2} \left([A] - [k] + [M] \right) \right) \langle T^{(j+1)} \rangle = \left([B] + \frac{\Delta t}{2} \left(-[A] + [k] - [M] \right) \right) \langle T^{(j+1)} \rangle + \frac{\Delta t}{2} \left(\langle BC^{(j)} \rangle + \langle BC^{(j+1)} \rangle \right) \tag{2.8}$$

includes the boundary condition vectors on the right hand side of the equation which contain the heat flux at the time step being calculated and the previous time step. During the exposure both of these boundary condition vectors will be the same. Immediately after the exposure, one boundary condition vector will contain the flux term, the other vector will be zero. As the fluxes considered here are relatively large, this sudden

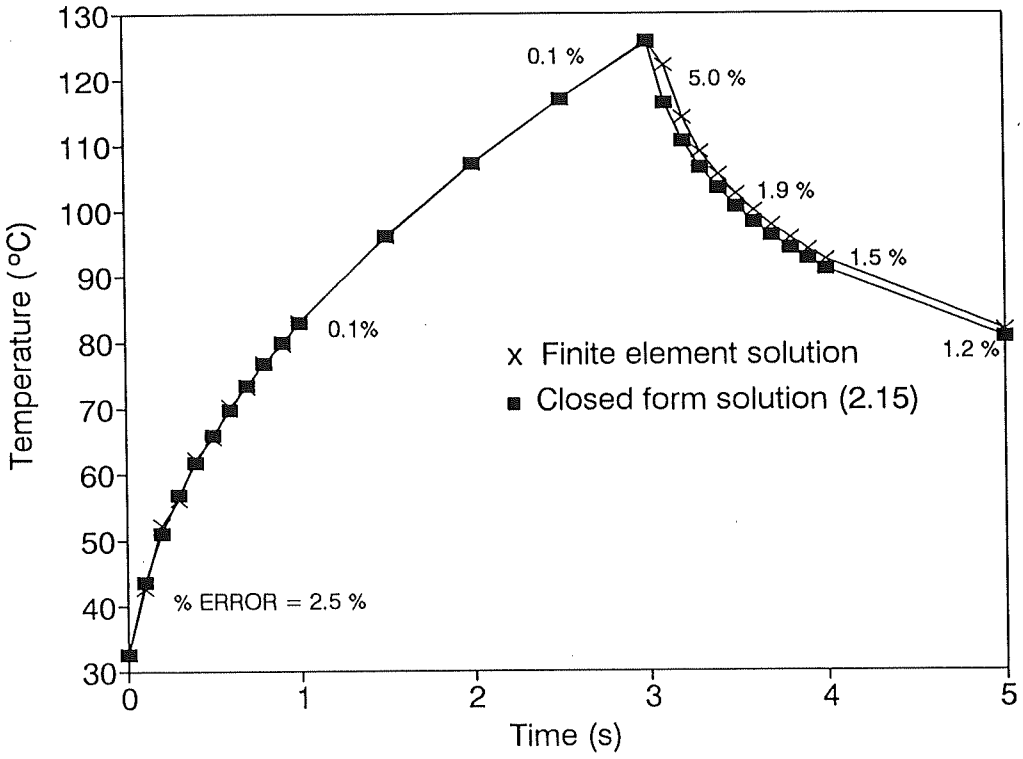

Figure 2.4 Comparison of Basal Layer Temperatures Determined Using Finite Element Model with Closed Form Solution (3 s exposure of 83.2 kW/m^2, 5 Hermitian elements, time steps of 0.01 s)

change will make the finite element solution much less accurate immediately after the exposure ends than just before it ends. Figure 2.4 illustrates that while the finite element solution is close to the closed form solution, its accuracy decreases substantially immediately after the exposure. Its accuracy begins to increase, but it takes some time before the same level of accuracy as during the exposure is achieved.

Another problem is numerical oscillations in time and space. As discussed in Appendix 1, the Crank-Nicholson method was used in the program to solve ordinary differential equations in time. Myers [55] comments that while any numerical oscillations in this technique are always stable, a finite element solution using this technique is more sensitive to these oscillations than a finite difference solution using the same technique. Stability limits are a function of the Courant number [56],

$$r = \alpha \frac{\Delta t}{l^2} \tag{2.17}$$

Therefore, if the critical grid size for stability is halved, the time step must be one quarter of its original value. With the small grid sizes used in modelling the skin, one can easily see that the time steps must be very small to avoid oscillations. Using fewer elements will allow larger time steps to be used, as well as saving on computation time.

Using the Hermitian polynomials, one would also expect that fewer elements would be required than if the lower order linear or quadratic interpolation polynomials were used. These three polynomials were tested using a time step of 0.01 s. Figure 2.5 compares the basal layer temperatures, and Figure 2.6 compares the dermal base temperatures for the first 5 s of interest calculated from the closed form solution and the following finite element schemes.

- 18 linear elements
- 9 quadratic elements
- 5 Hermitian elements.

As the burn damage rate is highly sensitive to temperature, it is important to predict these temperatures as accurately as possible. The 5 Hermitian element scheme and the 9 quadratic element scheme predict temperatures very close to the closed form

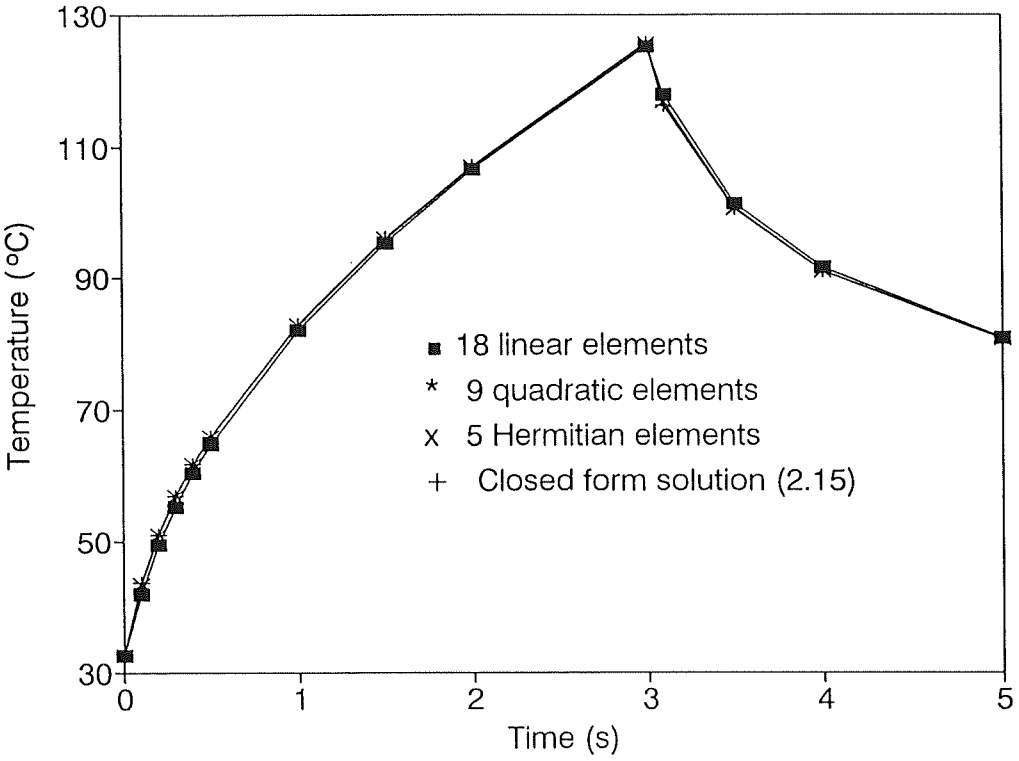

Figure 2.5 Comparison of Basal Layer Temperatures Predicted Using Closed Form Solution and Various Finite Element Schemes (exposure of 83.2 kW/m^2 for 3 s, time steps of 0.01 s for finite element solution)

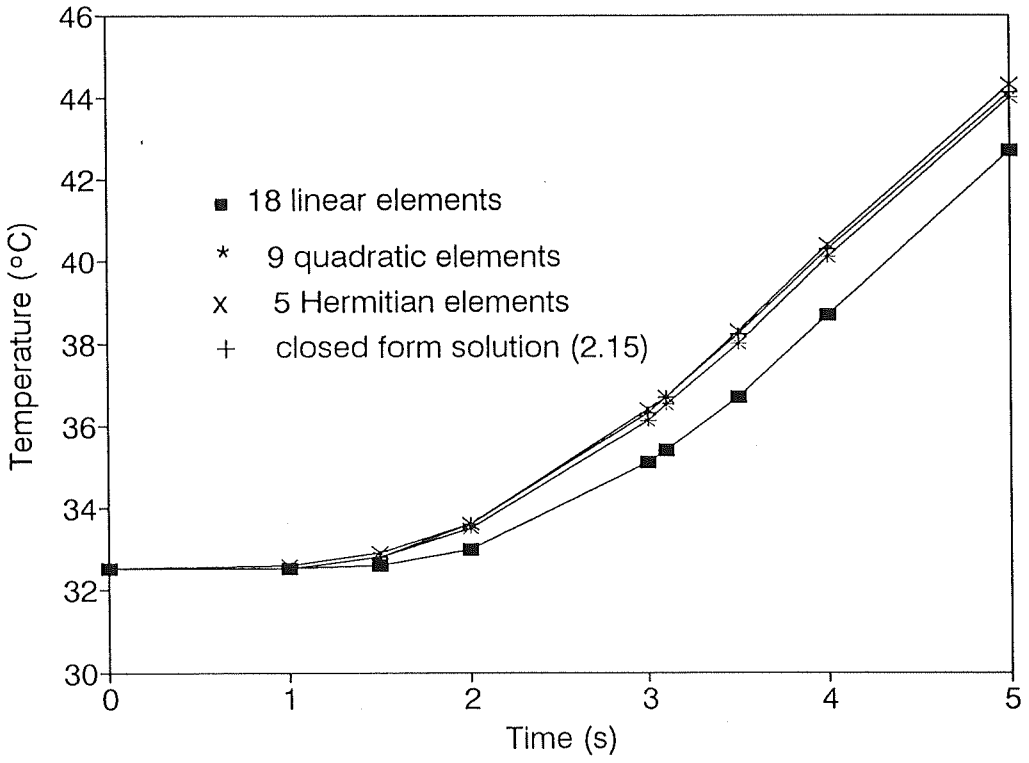

Figure 2.6 Comparison of Dermal Base Temperatures Predicted Using Closed Form Solution and Various Finite Element Schemes (Exposure of 83.2 kW/m^2 for 3 s, time steps of 0.01 s used for finite element solutions)

solution. Their temperature predictions were much closer to the closed form solution than the 18 linear element scheme. This difference is very apparent when looking at the dermal base temperature comparison in Figure 2.6. As the 5 Hermitian element scheme had fewer unknowns (10) than the 9 quadratic element scheme (18), it was used for the remainder of the tests.

A variable time step scheme was used to help reduce or eliminate oscillations and to aid in handling the step heat flux function. This will be discussed in relation to the variable property model in the next chapter.

2.5 Testing of the Burn Integral Routine

The burn integral portion of the computer program was tested to ensure that it would calculate accurate values of the burn integral at the basal layer and the base of the dermis.

First the values of the burn damage rate were calculated for temperatures from 44 to 58°C for the basal layer and the base of the dermis using the pre-exponential factors and activation energies of Henriques and Moritz [19], Stoll [25], Mehta and Wong [9], and Takata [33]. These values were then compared with those in Figures 1 and 2 of Morse, et al. [35]. The values were found to be very close to those in the Figures. Henriques' burn integral for a constant temperature, and hence a constant burn damage rate, can easily be integrated by hand. The results from this hand calculation for several temperatures were found to be the same as those from the computer program.

Henriques and Moritz [18] used the closed form solution for a prescribed temperature boundary condition and the burn integral to calculate the times expected to first and second degree burns using their measured values of thermal conductivity and diffusivity. These calculated values were then compared with the times to first and second degree burns which they measured.

The closed form solution for a constant temperature boundary condition was used to generate temperature-time histories for various surface temperatures above 50°C Henriques and Moritz also used surface temperatures below 50°C, but as these

exposures, unlike flash fires, required many hundreds or thousands of seconds to produce burns, they were not included in the comparison. The burn module of the program was then used to determine the burn damage rate at each time increment, and hence the times to first and second degree burns. These times are compared to those calculated and measured by Henriques and Moritz in Table 2.1 below.

Table 2.1 Comparison of Times to First and Second Degree Burns Due to an Imposed Surface Temperature Determined Using the Burn Integral Computer Module with those of Henriques and Moritz [18]

Surface Temperature (°C)	Time to First Degree Burn (s) (Ω = 0.53)			Time to Second Degree Burn (s) (Ω = 1.0)		
	Prog	H/M_c	H/M_m	Prog	H/M_c	H/M_m
50	140	165	130	250	325	300
52	50	52	44	80	91	90
54	16	19	18	25	31	35
56	7	8.1	8.3	10	13	16
60	1.9	2.3	2.6	2.6	3	5
65	0.7	0.7	1.0*	0.9	1.0	2*
70	0.4	0.4	no burn	0.5	0.5	1*

Notes:

- Prog denotes Burn Integral Program
- H/M denotes Henriques and Moritz [18]
  - c denotes calculated results
  - m denotes measured results
  - * denotes uncertain results

As can be seen from Table 2.1, the computer program's predictions of times to first and second degree burns were of the same order of magnitude as those measured, but were not very close at some surface temperatures. The values from the program were also different from those calculated by Henriques and Moritz even though the same closed form solution was used to calculate the basal layer temperatures. Stoll [24] had noted that the times to second degree burn that she observed were close to those predicted by Henriques' burn integral, but that the value of Ω from her results for second degree burns was different from the value of 1.0 in Henriques' criterion. Henriques assumed that the basal layer temperature was the same as the surface temperature in order to simplify the integration necessary to predict the value of Ω. If this is done, the burn integral then takes the form

$$\Omega = P\ t\ \exp\left(-\frac{\Delta E}{R\ T}\right) \tag{2.18}$$

For each surface temperature, the times Henriques and Moritz measured to first and second degree burn were substituted into Equation (2.18) along with their values of the pre-exponential factor and the activation energy. The resulting values of Ω for a few of the temperatures are shown in Table 2.2, below.

Table 2.2 Comparison of the Value of Henriques' Burn Integral Calculated from Henriques and Moritz's Measured Data with Their Criteria for First and Second Degree Burn for Various Surface Temperatures

Surface Temperature (°C)	First Degree Burn (Ω = 0.53)		Second Degree Burn (Ω = 1.0)	
	Time to burn (s)	Ω	Time to burn (s)	Ω
50	130	0.65	300	1.49
52	44	0.91	90	1.86
54	18	1.53	35	3.0
56	8.3	2.83	16	5.5

For temperatures higher than those in the Table, the differences between the expected and calculated values of Ω were even larger. The values of the burn damage rate, $d\Omega/dt$, for a constant temperature, shown in Figure 1 of Morse, et al. [35], were also integrated over time in a similar way, giving the same values of Ω shown above.

It can be seen that none of the values of Ω calculated using the same equation which Henriques and Moritz used to fit their data were the same as those expected, and that the difference increases with temperature. One possible reason for the large differences is the exponential term in the Henriques burn integral. The ratio of activation energy to universal gas constant is of the order 10^4, the temperatures 10^2. Hence the argument of the exponential term will be of the order 10^{-2}. The value of this term will therefore be extremely small. Today, this term can be calculated quickly with computers, whereas in Henriques and Mortiz's time, tables or manual calculating machines were required. Perhaps it is in this calculation that the differences lie.

All of these calculations were for surface temperatures above 50°C. It should be noted again that Stoll and Takata used two sets of values for the activation energy and pre-exponential factor--one set below 50°C, one set at or above 50°C. The results discussed here, as well as the findings of the other investigators indicate that the values of the pre-exponential factor of Stoll should be used for calculating epidermal burn damage. As mentioned in Section 1.7, Morse, et al. [34,35] also found that Takata's values should be used for calculating dermal burn damage. These two sets of data were therefore used for the remainder of the work. The effects of using the pre-exponential factors and activation energies from various investigators on burn predictions made by the multiple layer, variable property finite element model will be further discussed in Section 4.2.

2.6 Summary

A finite element computer program for calculating temperatures and times to second and third degree burns for skin subjected to a high intensity, short duration step change heat flux has been described. Temperature computations were found to be very close to closed form solutions for three classical boundary condition problems. The burn prediction module was tested using analytical and experimental results from the literature. Burn predictions were close to some analytical results, but differed with other analytical and experimental results. These differences were explained in terms of the differences in computational technology between the present and the time period in which the work in question was done.

CHAPTER 3
EFFECTS OF THERMAL PHYSICAL PROPERTIES AND SURFACE BOUNDARY CONDITION

The constant property and initial temperature program was now revised to handle variable thermal physical properties for each element, and an initial temperature gradient. A literature search was first conducted to determine the ranges of values for the relevant thermal physical properties. Numerical tests were then performed using the new finite element program to determine the effects that changes to these properties would have on predicted skin temperatures and burns. The boundary condition on the surface of the skin after the exposure may also affect the predicted temperatures and burns, and thus the effect of changing this boundary condition was also investigated. This chapter describes the results of these sensitivity studies.

3.1 Skin Thermal Physical Property Literature Search

Unlike many engineering applications, the relevant properties of skin cannot be easily found using common handbooks. For example, the value of Young's Modulus for steel varies little from its common value of 200 GPa, as the structure of steel varies little from batch to batch. On the other hand, skin structure varies widely depending on age, race, and sex. It also varies on an individual by location and time. Hence, many of the thermal physical properties of skin will vary considerably. Many of these properties are also difficult to measure exactly. Values for excised skin differ from those of living skin due to the loss of blood flow and moisture. Excised skin has a tendency to distort once removed from the body, where it is normally held taut by tension. Many values are sensitive to temperature increases and the effects which occur during tissue burns. For example, Henriques and Moritz [15] found that the edema fluid which builds up in burned tissue alters the values of density and specific heat of skin.

The purpose of this literature search was to define the range over which these parameters will vary and to note the specific conditions under which the measurements were made. These sets of data were used in the skin model to investigate the effects of varying each parameter, and if possible to identify which values should be used when predicting burns from flash fires.

3.2 Variable Property Finite Element Program

In this model, the properties were assumed to vary for each layer, but were held constant over each individual layer. An initial temperature gradient was also used.

3.2.1 Time Steps and Number of Elements Required

As a result of the work done in determining the time steps and grid spacings necessary with the constant property program (Section 2.4), variable time steps were used for this model.

The size of time steps necessary was first determined. For this study, the properties used in the University of Alberta [2] finite difference program to analyze data from mannequin tests were used. These are listed in Table 3.1 below.

Results using time steps of 1.0, 0.1, 0.02, and 0.01 s were compared for a 3 s exposure of 83.2 kW/m^2. Figure 3.1 shows a comparison of the basal layer temperatures predicted by the variable property model using these different time steps for the first 5 s after the exposure begins. There is little difference between the results using a time step of 0.02 s or 0.01 s, certainly not enough to justify using the smaller 0.01 s time step, and hence requiring twice as many time steps and calculations. Therefore a 0.02 s time step was selected for the first portion of time, where most of the skin damage occurs, and larger time increments were used for the later time periods. These other time step sizes were selected after the number of elements required was determined.

Table 3.1 Thermal Physical Properties Used in Testing the Variable Property, Multiple Layer Finite Element Skin Model

Property	Epidermis	Dermis	Sub- cutaneous	Blood
Thickness (m)	80×10^{-6}	0.00208	0.010	-
Thermal Conductivity, k (W/m · °C)	0.255	0.523	0.167	-
Specific Heat, c (J/kg · °C)	3598	3222	2760	-
Density, ρ (kg/m^3)	1200	1200	1000	-
Volumetric Heat Capacity, ρc (J/m^3 · °C) x 10^{-6}	4.32	3.87	2.76	3.99
Blood Perfusion Rate, G (m^3/s/m^3 tissue)	0	0.00125	0.00125	-

A variable time step scheme of steps of 0.02 s for the first 10 s, and 1.0 s for the remaining 110 s was used to compare predicted temperatures and burns for heat fluxes of 41.6, 83.2, and 166.4 kW/m^2 using 5,7, and 10 elements to model the skin. The 5 element scheme uses 1 element for the epidermis, and 2 for each of the dermis, and subcutaneous region. The 7 element scheme uses 1 element for the epidermis, 2 for the dermis, and 4 for the subcutaneous region. The 10 element scheme uses 2 elements for the epidermis, and 4 for each of the dermis and subcutaneous region. A comparison of the basal layer temperatures predicted by the 5, 7, and 10 element schemes is found in Figure 3.2, while a comparison of predicted burns using the 5 and 10 element schemes is found in Table 3.2.

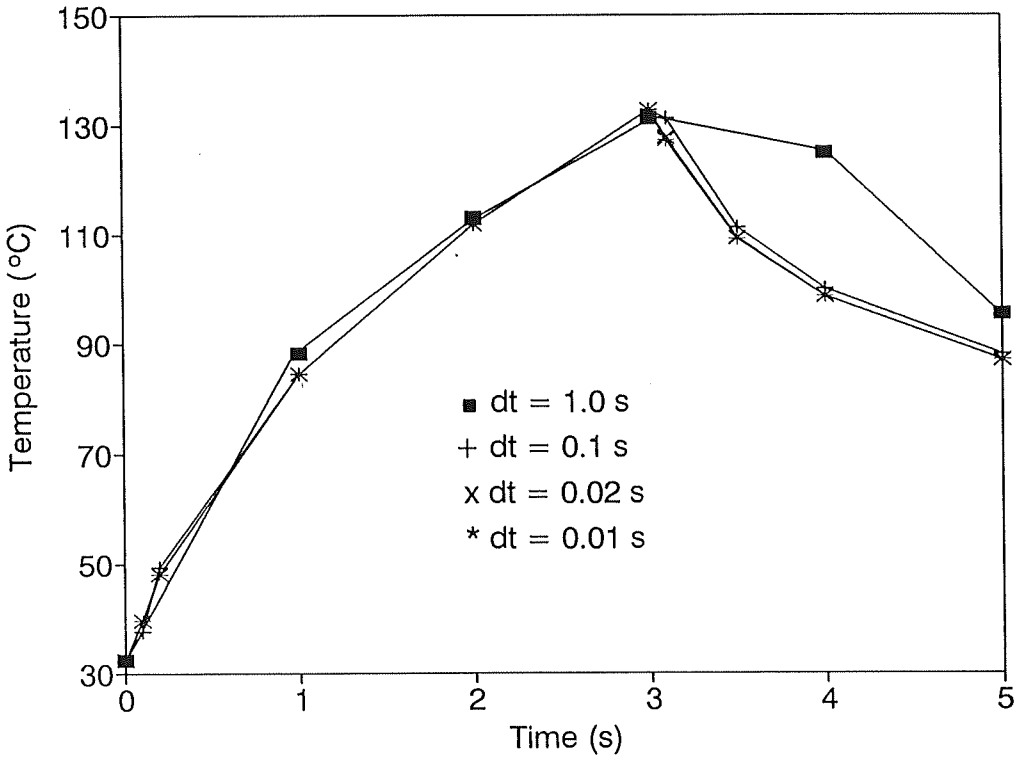

Figure 3.1 Comparison of Basal Layer Temperatures Determined Using the Variable Property Finite Element Program and Four Different Time Steps (Exposure of 83.2 kW/m^2 for 3 s)

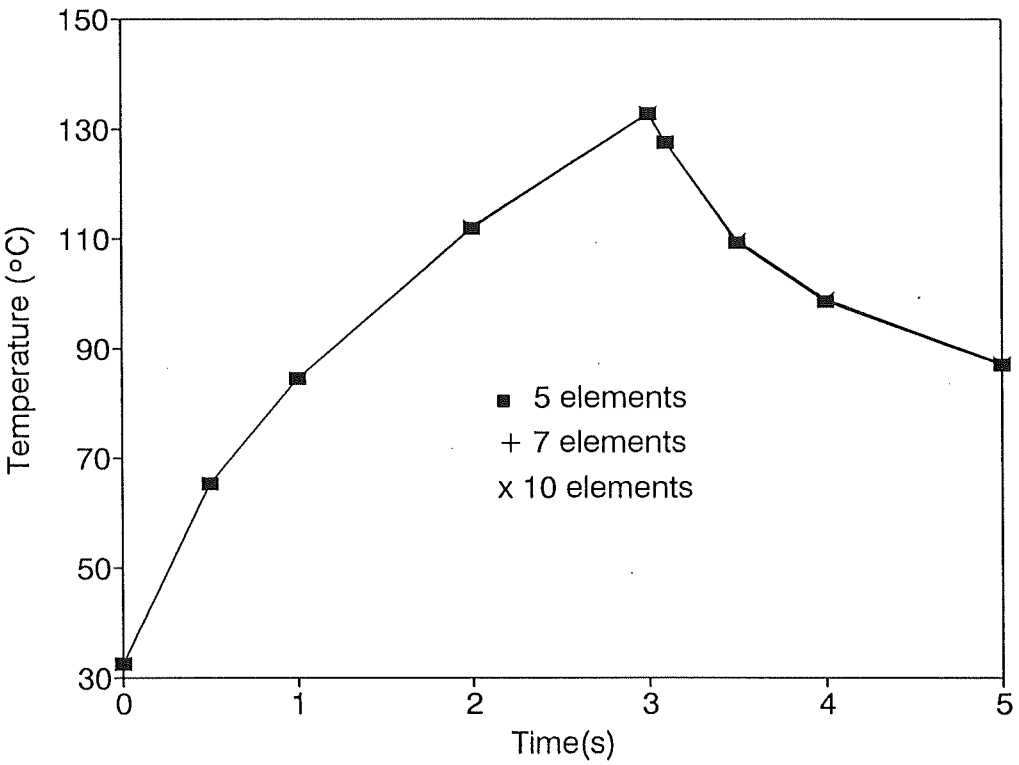

Figure 3.2 Comparison of Basal Layer Temperatures Determined Using 5,7, and 10 Hermitian Elements (Exposure of 83.2 kW/m^2 for 3 s)

Table 3.2 Comparison of times to Second and Third Degree Burn Determined Using 5 and 10 Finite Element Models

Heat Flux (kW/m^2)	Time to 2° Burn (s)		Time to 3° Burn (s)	
	5 element scheme	10 element scheme	5 element scheme	10 element scheme
41.6	1.30	1.18	no burn	no burn
83.2	0.54	0.46	no burn	no burn
166.4	0.24	0.20	7.4	7.2

The 5 element scheme was selected. As shown in Figure 3.2, the differences in predicted temperatures using the various schemes were very small. At 166.4 kW/m^2 the maximum temperature difference was 1.5°C (0.4% difference). Of course, very small temperature differences can result in larger differences in the burn integral value, and hence the time to second or third degree burn. Comparing the times to second and third degree burns in Table 3.2, there is little difference between the results using the 5 element scheme and those using the 10 element scheme, certainly not enough to justify doubling the number of calculations necessary, and hence the computing time. Results using the 7 element scheme were not substantially different from results using the 5 element scheme.

It has already been shown that the temperatures found using time steps of 0.02 s were fairly accurate when compared with those using even smaller time steps of 0.01 s. However it is not practical to use such small time steps throughout the entire 60 or 120 s of interest. Therefore a variable time step scheme will be utilized.

Table 3.3 shows the temperatures calculated using time steps of 0.02 s until a time of 10 s, and those using time steps of 0.02 s until 5 s, and then 0.1 s from 5 s to 10 s. Neither the temperatures or values of the Henriques' burn integral are very

different. It can also be shown that time steps of 1.0 s can be used after 10 s without significant loss of accuracy.

Table 3.3 Comparison of Temperatures and Dermal Damage Determined Using Two Time Step Schemes From 5-10 s After the Beginning of a 83.2 kW/m^2 Exposure

Time(s)	Basal Layer Temperatures (°C)		Dermal Base Temperatures (°C)	
	ΔT = 0.02 s	ΔT = 0.1 s	ΔT = 0.02 s	ΔT = 0.1 s
5.0	86.9	86.9	39.6	39.6
5.1	86.1	86.4	39.9	39.8
6.0	80.0	80.3	42.9	42.7
10	67.1	67.2	50.8	50.7
Dermal Burn Damage Integral Values:				
Ω_D = 0.772 (ΔT = 0.02 s)		Ω_D = 0.771 (ΔT = 0.1 s)		

Therefore the following time steps and grid sizes were selected. 5 Hermitian elements were used, 1 for the epidermis, and 2 for each of the dermis and subcutaneous. Time steps of 0.02 s were be used for the first 5 s after exposure begins, followed by 0.1 s steps for the next 5 s, and 1.0 s steps for the remainder to the time period of interest, usually 60 or 120 s.

3.3 Variable Property Sensitivity Study

The variable property finite element program was now used to perform a sensitivity study of the skin thermal physical properties. Heat fluxes of 83.2, 41.6, and 24 kW/m^2 were used as test cases. These correspond to a typical exposure of a flash fire on nude skin (83.2 kW/m^2), while the two smaller heat fluxes might represent the heat

flux incident on skin covered with a cloth from such a fire. For each property studied, a summary of the finding of the literature search will first be presented, followed by the results of the sensitivity study.

3.3.1 Skin thickness

There are several major difficulties peculiar to measuring skin thicknesses. It is difficult to determine where the boundary between the dermis and subcutaneous tissues lies. The boundary between the epidermis and the dermis itself is hard to define as it is not flat, but instead is where the papillae and corresponding rete ridges meet. As mentioned earlier, tissue will shrink when excised.

Earlier measurements were done with excised skin. Two of these studies were done by Southwood [57] and Whitton and Everall [58]. Investigators found that epidermal and dermal thicknesses vary due to age, sex, and location on the body. Southwood commented that epidermal thickness was inversely proportional to hair density on an individual. For example, the areas with no body hair, the soles and the palms, have the thickest epidermal regions.

Newer, non invasive, in vivo methods have also recently been used, such as pulsed ultrasound and radiography. The results using these do not indicate thicknesses which are very different from those values found earlier, and do show the same general trends as to the difference in layer thicknesses between young males and females.

Generally, the thickness of the epidermis ranges from about 20 to 1400 μm [57,58]. If the palms and soles are disregarded, the mean epidermal thicknesses of most regions of the body is between 20 and 80 μm. Most skin burn models use a value between 75 and 120 μm for the thickness of the epidermis. The majority of these use 80 μm which was used by Henriques and Moritz in their porcine experiments [15], as well as Stoll [25], who found it to be the depth of the basal layer for the volar surface of the forearm. The thickness of the dermis ranges from 450 to 2600 μm [57]. Past skin models have used a value between 800 and 2000 μm, with the majority using the 2000 μm value. Past skin models have used subcutaneous layer thicknesses from 0.3 to

1.0 cm.

Due to the wide variation in thicknesses throughout the body, and from person to person, the effects of variations in the thicknesses of skin on the temperature and burn predictions from the model will not be investigated. The following values, consistent with other investigators, will be used here:

- epidermis 80 μm
- dermis 2 mm
- subcutaneous 1 cm

3.3.2 Temperature gradients in the skin

As mentioned earlier, the skin helps to regulate the body's core temperature. In order to keep biochemical reactions proceeding at required rates, the core temperature of the body must be maintained within a small range around 37°C. Depending what the environmental conditions are, the surface temperature of exposed skin can vary. Under normal ambient conditions, it is about 32.5°C to 34°C. Thus a temperature gradient exists in the skin at any given time. Some skin models have used constant initial skin temperatures of, for example, 32.5°C [24], 34°C [48], or 37°C [16]. A linear initial temperature gradient is used by other models, such as the present University of Alberta finite difference model. Others use a higher order initial temperature distribution.

Pennes [8] used a radiometer to measure surface temperatures and thermocouples to measure temperatures at depth in resting subjects. He found that at room temperatures of 26°C to 28°C rectal temperatures were higher than brachial arterial temperatures, which were in turn higher than deep forearm temperatures. The temperature distribution in the forearm was found to be almost parabolic, with a maximum temperature near the geometrical axis of the limb. Temperatures on either side of the geometrical axis were not symmetric, so it was commented that isothermal surfaces inside the forearm could not be represented by concentric cylinders.

When using Hermitian polynomials, not only are the initial nodal temperatures of concern, but so are the initial nodal heat fluxes. Emery and Carson [59] suggest that

these initial heat fluxes be set to zero to begin with, rather than making an initial calculation or guess. This will eliminate the introduction of further transient effects into the solution.

If a linear temperature gradient is used between a surface temperature of 32.5°C and a core temperature (at 12.08 mm) of 37°C, the initial value of $\partial T/\partial x$ will be 372.5°C/m at any node. Therefore the program was run with initial k $\partial T/\partial x$ values of 0, 100, 200, and 400 W/m^2 with an incident heat flux of 83.2 kW/m^2 to see if the choice of these initial heat fluxes had a significant effect on the temperatures and burns predicted by the model. The results of these tests are shown in Table 3.4 below.

Table 3.4 Times to Second and Third Degree Burn Predicted Using the Finite Element Model and Different Initial Nodal Heat Fluxes

Initial k $\partial T/\partial x$ (W/m^2)	Time to 2° burn (s)	Time to 3° burn (s)
0	0.6	no burn
100	0.6	no burn
200	0.6	111
400	0.6	55

There were no differences in the times predicted to second degree burns and some differences in times to third degree burns, and in fact whether third degree burns do occur. However, it should be noted that for a heat flux of 83.2 kW/m^2, the value of Henriques' Burn Integral for the dermal base is just over 1.0 for those cases showing third degree burns, and in the two cases here where no third degree burns were shown to have occurred, the values were 0.95 and 0.99 (for initial heat fluxes of 0 and 100 W/m^2, respectively). Therefore for all practical purposes, there were third degree burns for all four cases. As a result of these tests and Emery and Carson's [59] work, it was decided to set all the initial heat fluxes to zero in the model before the exposure began.

The sensitivities of the temperature and burn predictions to the initial temperatures of the skin were next tested. Three initial temperature distributions were used.

- linear distribution from 32.5°C (surface) to 37°C (subcutaneous base)
- quadratic distribution from 32.5°C (surface) to 37°C (subcutaneous base)
- quadratic distribution from 33.7°C (surface) to 36.1°C (depth of 4 cm)--this distribution is suggested by Figure 16 in Pennes [8]. Note that this required modelling an extra 2.8 cm of tissue. It was first determined that the number of nodes and values of thermal properties (thermal conductivity and volumetric heat capacity) used to model this extra tissue had little or no effect on the basal layer and dermal base temperatures. Therefore properties similar to those of the subcutaneous layer were used for a one element model of this extra depth. The temperature at 4 cm was then held constant as required by the boundary condition at $x = L$, given by Equation (2.3).

The temperature-time histories for the basal layer and dermal base found using the model and these three initial temperature distributions are shown in Figures 3.3 and 3.4. The times to second and third degree burns predicted by the model when the skin is subjected to various heat fluxes are shown in Table 3.5.

The initial temperature distribution had very little effect on the predictions of basal layer temperatures and second degree burns. In Table 3.5 the results for a heat flux of 83.2 kW/m^2 and an initial constant temperature of 37°C throughout the skin are shown in addition to the three gradients already discussed. Here a difference in initial temperature of the basal layer of about 4°C leads to only a difference of 0.1 s in times to second degree burns.

In terms of dermal base temperatures and third degree burns, the initial temperature distribution makes much more of a difference. This is shown in Figure 3.4. This is to be expected as it takes some time for the heat to propagate to this layer and raise temperatures significantly. Therefore for these exposures the initial temperature of the dermis-subcutaneous interface is very important. The linear distribution gives a lower initial dermal base temperature than the other two distributions and therefore third

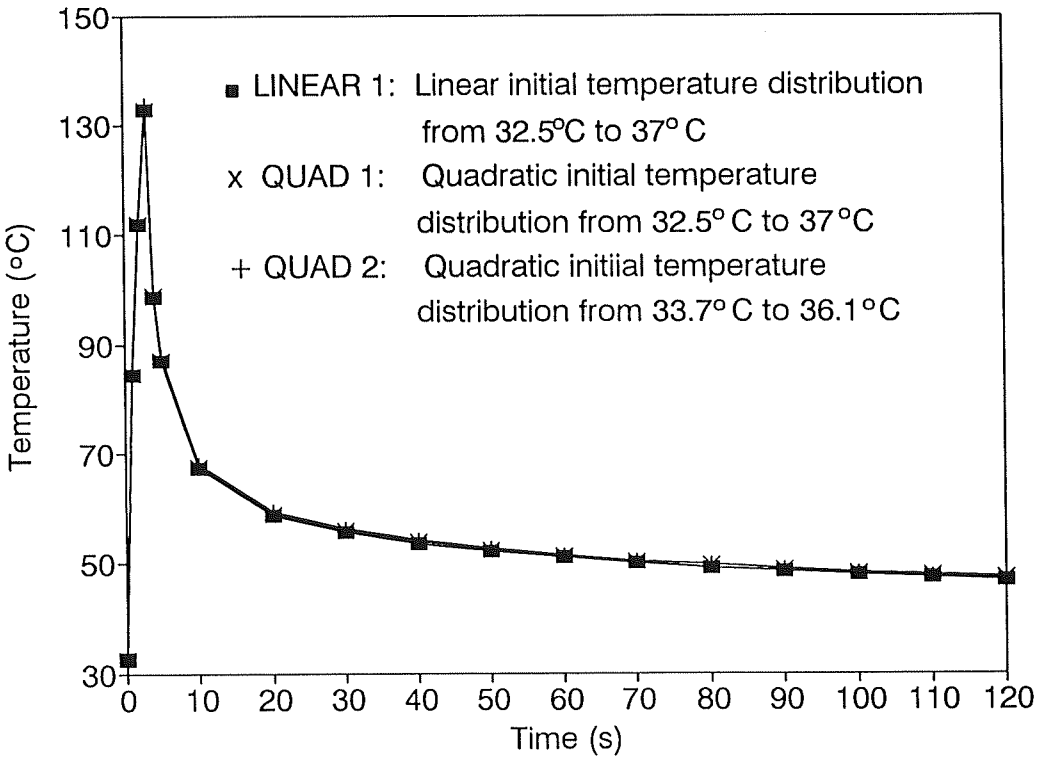

Figure 3.3 Comparison of Basal Layer Temperature-Time Histories Determined Using Three Different Initial Temperature Gradients (Exposure of 83.2 kW/m^2 for 3 s, 5 Hermitian elements used)

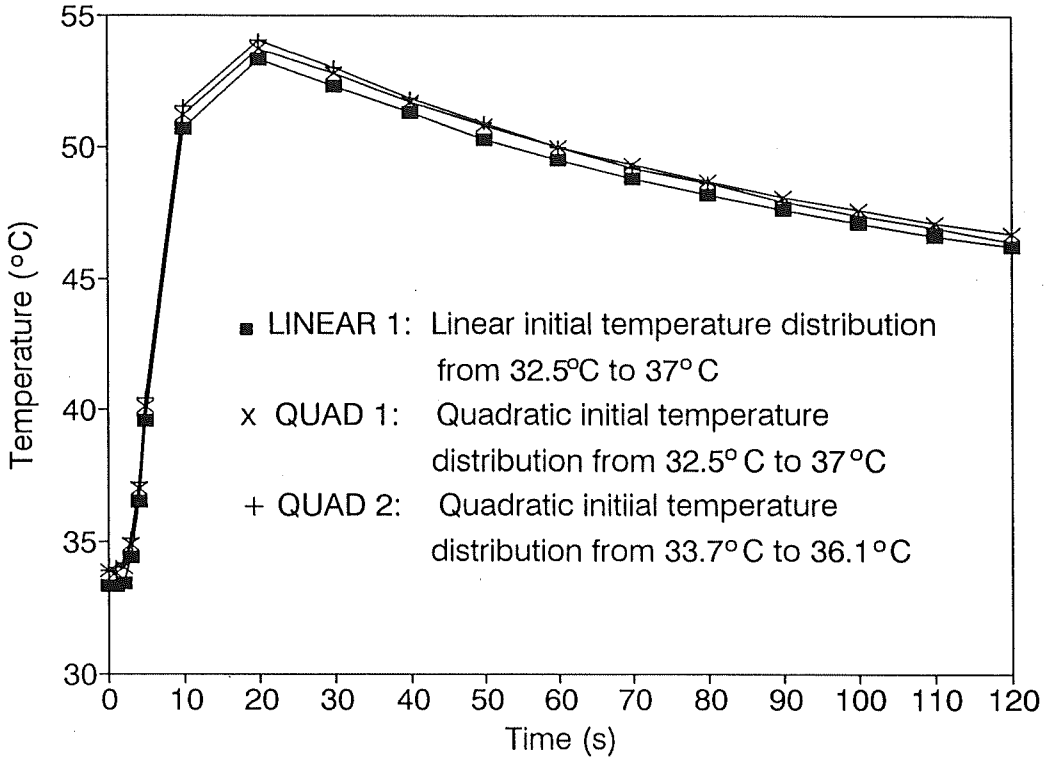

Figure 3.4 Comparison of Dermal Base Temperature-Time Histories Determined Using Three Different Initial Temperature Gradients (Exposure of 83.2 kW/m^2 for 3 s, 5 Hermitian elements used)

degree burns were not predicted for the 83.2 kW/m^2 exposure.

Table 3.5 Times to Second and Third Degree Burns Predicted Using Four Different Initial Temperature Gradients

Heat Flux (kW/m^2)	Time to 2° Burn (s)			
	Linear1	Quad1	Quad2	T=37°C constant
24	2.82	2.78	2.66	no burn
41.6	1.3	1.3	1.24	no burn
83.2	0.50	0.54	0.54	0.44
	Time to 3° Burn (s)			
83.2	no burn	58	36	14

Notes:

- Linear1 = linear temperature distribution from 32.5°C (surface) to 37°C (subcutaneous base)
- Quad1 = quadratic temperature distribution between the above limits
- Quad2 = quadratic temperature distribution from 33.6°C (surface) to 36.1°C (4 cm depth)

As the exact temperature distribution in the body can change due to surface conditions, and as the two quadratic temperature distributions predict temperatures and second and third degree burns very closely, the quadratic distribution from 32.5°C (surface) to 37°C (subcutaneous base) will be used in this program. It has the same

general shape as experimentally observed gradients, and predicts burns and temperatures fairly close to those predicted using a gradient based on Pennes' experimental data. In addition, using this distribution does not require modelling the extra 2.8 cm of tissue required when using Pennes' gradient. Regardless, the temperature gradient appears to play a fairly minor role in predicting second degree burns with these exposures, and a larger role in predicting third degree burns.

3.3.3 Thermal Properties

As with the other reported properties of skin, the thermal properties, namely the volumetric heat capacity and the thermal conductivity, vary widely by investigator, layer, body site, and moisture content. It is difficult to measure properties of living skin, and measurements on excised skin are not entirely satisfactory, as it has been found that the thermal properties are very dependant on blood flow. Bowman, Cravalho, and Woods' survey [60] was used in addition to the literature search of skin burn research and models to determine the ranges of thermal physical properties for this report. In their survey, they commented on experimental techniques, noting that invasive techniques are not valid near the skin surface, and noninvasive techniques are not valid at depth. The burn process itself changes thermal properties. Henriques and Moritz [15] found that edema fluid released after a burn increased the value of the thermal conductivity by two to three times (it was also found that the dermis became swollen due to this fluid, and thus the dermis actually became a slightly better heat barrier). Stoll [24] believed that the product of the thermal conductivity and volumetric heat capacity, $k\rho c$, the thermal inertia, increased with radiation heat flux incident on the skin (although some [34] believed that this effect was merely due to the blackened skin tested not being completely opaque as was assumed, but instead that some energy was transmitted to the skin).

3.3.3.1 Volumetric Heat Capacity

The volumetric heat capacity of the skin is generally assumed to be close to that

of water. As water content is different in the different skin layers, the volumetric heat capacity will be different for the various layers. The ranges of values for the different layers of skin are:

- epidermis 2.8 to 4.4 x 10^6 J/m^3 · °C
- dermis 2.6 to 4.2 x 10^6 J/m^3 · °C
- subcutaneous 1.8 to 3.1 x 10^6 J/m^3 · °C

The model was tested at the three test cases, 24, 41.6, and 83.2 kW/m^2 using first the low values in the above ranges for all the layers, and then the high values in the above ranges for all three skin layers. The times to second and third degree burns for the different heat fluxes and volumetric heat capacities are listed in Table 3.6 below.

Table 3.6 Times to Second and Third Degree Burn Predicted Using the Lowest and Highest Published Values of Volumetric Heat Capacity of the Different Skin Layers

Heat Flux (kW/m^2)	Time to 2° Burn (s)		Time to 3° burn (s)	
	Low	High	Low	High
24	1.98	2.94	no burn	no burn
41.6	0.92	1.36	no burn	no burn
83.2	0.36	0.56	7	no burn

There is some variation in times to second and third degree burn. If the volumetric heat capacity is split into its two components, the density and the specific heat, much of the variation in the volumetric heat capacity values is due to the variation in densities reported for the individual layers. Henriques and Moritz [15] used a density of 800 kg/m^3, the only justification being that it was "a most reasonable value".

Stoll [24] pointed out that the density was actually closer to 1100 to 1200 kg/m^3. Most recent skin models use values of 1100 to 1200 kg/m^3 for the epidermis, 1200 kg/m^3 for the dermis, and 1000 kg/m^3 for the subcutaneous regions.

The densities of the various layers were now set equal to the values in the University of Alberta finite difference program, namely 1200 kg/m^3 for the epidermis and dermis, and 1000 kg/m^3 for the subcutaneous region, which, as noted above, are consistent with other investigators. The specific heat was then varied between its lowest and highest values from the literature search for each layer, while keeping the specific heat of the other layers constant. The ranges of specific heats tested for the individual layers were as follows:

- epidermis 3578 to 3600 J/kg · °C
- dermis 3200 to 3400 J/kg · °C
- subcutaneous 2288 to 3060 J/kg · °C

The times to second and third degree burns are shown in Table 3.7 for the various tests.

There was practically no effect on second degree burn predictions by varying specific heat values. Basal layer temperatures varied no more than 2.4 °C. There is an effect on third degree burn predictions, but once again in those cases where one value of specific heat predicted third degree burns, while the other did not, the model barely predicted third degree burns or barely did not. For example, for the two cases where third degree burns were predicted with one specific heat value and not with the other, the burn integral values for the non third degree burn cases were 0.958 and 0.864. The University of Alberta values for density and specific heat, and hence volumetric heat capacity were therefore continued to be used in the model, as any change from these would have had minimal effect.

Table 3.7 Times to Second and Third Degree Burn Predicted Using the Lowest and Highest Published Values of Specific Heat for Each Skin Layer

Heat Flux (kW/m^2)	Time to 2° burn (s)		Time to 3° burn (s)	
Epidermis	c = 3578 J/kg·°C	c = 3600 J/kg·°C	c = 3578 J/kg·°C	c = 3600 J/kg·°C
83.2	0.52	0.52	26	26
Dermis	c = 3200 J/kg·°C	c = 3400 J/kg·°C	c = 3200 J/kg·°C	c = 3400 J/kg·°C
41.6	1.30	1.34	no burn	no burn
83.2	0.54	0.54	28	no burn
Sub-cutaneous	c = 2288 J/kg·°C	c = 3060 J/kg·°C	c = 2288 J/kg·°C	c = 3060 J/kg·°C
41.6	1.34	1.34	no burn	no burn
83.2	0.54	0.54	28	no burn

3.3.3.2 Thermal Conductivity

The thermal conductivity of the skin varies greatly. There is also some confusion as to the role of blood perfusion in the thermal conductivity. Some investigators use a separate blood perfusion source term in addition to thermal conductivity in the Pennes' bioheat transfer equation. Others prefer to think of the thermal conductivity as an "effective conductivity", which incorporates the effect of convection heat transfer in blood perfused skin. The values of the thermal conductivity reported vary greatly for

excised and living skin because of blood flow, with the value for living skin continuing to increase substantially with increased blood flow [60]. It has been noted, however, that it takes up to 20 s for the body to react to heating by increasing blood flow [28]. As flash fires are of very short duration with high heat fluxes, skin damage will likely occur before the blood flow can increase. Another source of uncertainty in thermal conductivity values was discussed by some investigators (e.g. [34]), who noted that the equation which is used to calculate the thermal inertia or absorptivity,

$$\Delta T = \frac{2q_o\sqrt{t}}{\sqrt{\pi k \rho c}} \tag{3.1}$$

and hence the thermal conductivity (if the volumetric heat capacity is known or estimated), is based on assumptions which may not be justified. These include assuming uniform temperatures throughout the skin, and that properties do not vary with temperature, time, or depth.

The range of published thermal conductivity values [60] is as follows:

- epidermis 0.21 to 0.26 W/m·°C
- dermis 0.37 to 0.52 W/m·°C
- subcutaneous 0.16 to 0.21 W/m·°C
- single layer models
    - in vivo 0.48 to 2.8 W/m·°C
    - in vitro 0.45 to 0.6 W/m·°C
- epidermis/dermis 0.188 to 0.335 W/m·°C
- water 0.620 W/m·°C
- fat (in vitro) 0.094 to 0.37 W/m·°C

The sensitivity of temperature and burn predictions to variations in thermal conductivity values was first tested by using the lowest and highest reported values for each layer, while keeping the values for the other layers constant. The results of these tests are shown in Table 3.8 below.

Table 3.8 Times to Second and Third Degree Burn Predicted Using the Lowest and Highest Published Values of Thermal Conductivity for Each Skin Layer

Heat Flux (kW/m^2)	Time to 2° burn (s)		Time to 3° burn (s)	
Epidermis	k = 0.21 W/m·°C	k = 0.26 W/m·°C	k = 0.21 W/m·°C	k = 0.26 W/m·°C
24	2.80	2.78	no burn	no burn
41.6	1.30	1.30	no burn	no burn
83.2	0.54	0.54	58	55
Dermis	k = 0.37 W/m·°C	k = 0.53 W/m·°C	k = 0.37 W/m·°C	k = 0.53 W/m·°C
24	2.28	2.78	no burn	no burn
41.6	1.08	1.30	no burn	no burn
83.2	0.46	0.54	no burn	55
Sub-cutaneous	k = 0.167 W/m·°C	k = 0.21 W/m·°C	k = 0.167 W/m·°C	k = 0.21 W/m·°C
24	2.78	2.78	no burn	no burn
41.6	1.30	1.30	no burn	no burn
83.2	0.54	0.54	55	no burn

Again there was practically no effect on times to second degree burn, although it should be noted that the variation in dermal thermal conductivities caused up to a 16°C difference in basal layer temperatures calculated by the model. Clearly the largest

difference in burn predictions and temperatures is caused by the largest variation in thermal conductivity, that is, in the dermis. The effect of varying the thermal conductivity on third degree burns was again larger than for second degree burns, although the same comments about the 83.2 kW/m^2 heat flux barely producing or not producing third degree burns are again appropriate here.

A single layer, variable property model was then used to test the sensitivity of temperature and burn predictions to the in vivo (0.48 to 2.8 W/m · °C) and in vitro (0.4 to 0.6 W/m · °C) ranges of thermal conductivity of the entire skin. The times to second and third degree burn predicted over these ranges are shown in Table 3.9 below.

Table 3.9 Times to Second and Third Degree Burn Predicted Using the Lowest and Highest Common Values of In Vivo and In Vitro Thermal Conductivity

Heat Flux (kW/m^2)	Time to 2° burn (s)		Time to 3° burn (s)	
In Vivo	k = 0.48 W/m · °C	k = 2.8 W/m · °C	k = 0.48 W/m · °C	k = 2.8 W/m · °C
24	2.72	no burn	no burn	no burn
41.6	1.24	no burn	no burn	no burn
83.2	0.50	1.34	no burn	no burn
In Vitro	k = 0.45 W/m · °C	k = 0.6 W/m · °C	k = 0.45 W/m · °C	k = 0.6 W/m · °C
24	2.62	3.20	no burn	no burn
41.6	1.20	1.40	no burn	no burn
83.2	0.48	0.54	no burn	no burn

There were large differences between the results over the range of in vivo thermal conductivities. This was expected because of the large range of thermal conductivity values observed under different conditions. The differences in second degree burn predictions over the range of in vitro thermal conductivities increased as the heat flux decreased and the thermal properties become more important in predicting times to second degree burn (as damage did not occur almost instantaneously, as with the higher heat fluxes). The maximum temperature differences over the range of in vitro thermal conductivities are shown in Table 3.10.

Table 3.10 Maximum Basal Layer and Dermal Base Temperature Differences Over the Published Range of In Vitro Thermal Conductivities

Heat Flux (kW/m^2)	Maximum Basal Layer Temperature Difference (°C)	Maximum Dermal Base Temperature Difference (°C)
24	3.6	0.7
41.6	6.3	1.4
83.2	12.6	2.6

The perfusion term was included in the model which tested sensitivity over the range of in vitro thermal conductivities. The temperature differences shown in Table 3.10 are roughly proportional to the heat flux to the skin. Recalling the closed form solution for the inert skin model (Equation (2.15)), the temperature difference is expected to be proportional to the heat flux. This may be an indication that the perfusion term does not have any effect on the solution. The results of the test of the effect of the perfusion term will be presented later in this work.

One other attempt to understand the role of the perfusion term was made. Tanasawa and Katsuda [61] found that the thermal conductivity for skin with normal blood flow was 0.476 W/m·°C, while that of skin with compromised flow was

0.36 W/m·°C. Lomholt [62] found the thermal conductivity of excised skin to be 0.21 W/m·°C. The thermal conductivity value for skin with normal blood flow was used in the model with the perfusion term set to zero. The temperatures and skin burn predictions were then compared with those found using the compromised flow and excised skin thermal conductivity values, and the normal value of the perfusion term. It was thought that if the temperatures and burn times predicted using the two approaches were found to be equal, then the perfusion term might be responsible for the differences in thermal conductivity values between excised and living, perfused skin. The times to second degree burn found from these tests are shown in Table 3.11 below.

Table 3.11 Times to Second Degree Burn Predicted Using Different Thermal Conductivity Values With and Without Perfusion

Heat Flux (kW/m^2)	Times to 2° Burn (s)		
	k = 0.21 W/m·°C with perfusion	k = 0.36 W/m·°C with perfusion	k = 0.476 W/m·°C no perfusion
24	1.72	2.30	2.70
41.6	0.86	1.08	1.24
83.2	0.40	0.44	0.50

As shown in Table 3.11, no correlation could be found between the predictions made using the different approaches. Temperature differences up to 40°C were found at the basal layer. Therefore, the perfusion term was not responsible for the differences in the thermal conductivity values of the skin in different states.

Thus far, thermal properties have been varied independent of each other. Hardee and Lee [53] give three sets of thermal conductivity and volumetric heat capacity data from three different investigators for a single layer model of skin without blood

perfusion. These sets of data are as follows:

- Perkins [59] $k = 0.764$ W/m·°C
  $\rho c = 3.55 \times 10^6$ J/m³·°C
- Mitchell [63] $k = 0.591$ W/m·°C
  $\rho c = 4.19 \times 10^6$ J/m³·°C
- Stoll [64] $k = 0.628$ W/m·°C
  $\rho c = 3.68 \times 10^6$ J/m³·°C

Perkins' data were obtained from flash burns caused by high intensity carbon arc sources. Mitchell assumed the skin had the same thermal properties as water. Stoll's data were based on tests described in Section 1.6.3.

The single layer, constant property finite element model was used to compare results found using each of these sets of data. There were no third degree burns from the heat fluxes used. The times to second degree burns predicted using each set of data are shown in Table 3.12, below.

Table 3.12 Comparison of Times to Second Degree Burn Predicted Using the Single Layer, Constant Property Finite Element Model, and Thermal Properties from Perkins [54], Mitchell [63], and Stoll [64]

Heat Flux (kW/m^2)	Time to Second Degree Burn (s)		
	Perkins	Mitchell	Stoll
24	3.04	3.16	2.90
41.6	1.36	1.40	1.30
83.2	0.50	0.54	0.50

The differences in times to second degree burns using the various properties were small. The maximum basal layer temperature difference between the predictions was 4.3°C for an incident heat flux of 83.2 kW/m^2. It would appear that varying the properties over these ranges has minimal effect on burn predictions.

3.3.4 Blood Perfusion

If a source term is included to account for convection heat transfer by blood, the following published ranges of thermal properties for blood can be used:

- perfusion rate 0.00024 to 0.00125 m^3/s/m^3 tissue
- volumetric heat capacity 3.63 to 3.99 x 10^6 W/m^3 · °C

The volumetric heat capacity of blood was held constant, and the perfusion rate was given values of 0, 0.00125, and 0.0025 m^3/s/m^3 tissue. The times to second and third degree burns for various incident heat fluxes and blood perfusion rates are given in Table 3.13.

There was no difference in times to second degree burns, and little difference in times to third degree burns. It would be expected that there would be no difference in times to second degree burns as there is no blood flow in the epidermis. The fact that third degree times were slightly different would also be expected, as the important temperature is that at the dermis-subcutaneous interface. As there is blood flow carrying energy away from the dermis and subcutaneous, it would be expected that this would have an effect on the dermal base temperature. Third degree burns also take longer to occur, allowing the blood an opportunity to carry away some of the energy before damage is sustained. Basal layer temperatures using the three blood flow rates were about the same during early times and were about 3.2°C different at 120 s. Dermal base temperatures were about 1.7°C different at 120 s.

Table 3.13 Times to Second and Third Degree Burns Predicted Using Various Blood Perfusion Rates and Heat Fluxes

Heat Flux (kW/m^2)	Time to 2° Burn		
	G = 0.0 $m^3/s/m^3$	G = 0.00125 $m^3/s/m^3$	G = 0.0025 $m^3/s/m^3$
21.7	5.3	no burn	no burn
22	3.28	3.30	3.30
24	2.78	2.78	2.78
41.6	1.30	1.30	1.30
83.2	0.54	0.54	0.54
10.4*	9.4	9.4	9.4
	Time to 3° burn (s)		
83.2	31	55	no burn
10.4*	34	35	35

* the 10.4 kW/m^2 heat flux was kept constant over the entire 120 s time period; the other heat fluxes were only applied for 3 s

Besides the 24, 41.6, and 83.2 kW/m^2 levels normally tested, three other heat fluxes were used here. During clothed mannequin tests it usually takes about 20 s for second degree burns to occur. In this model, the surface of the skin is insulated after the exposure ends. In the mannequin test, or an actual accident, the skin continues to receive heat from the garment on top of the skin, be it through conduction (garment touching the skin), or convection and radiation (garment not touching the skin). Therefore smaller heat fluxes, such as those expected to reach the skin through cloth

covering the surface were also used to test the model. As this heat flux decreased, the blood perfusion eventually did have an effect in determining whether or not there were second degree burns. However, as mentioned earlier this would be for the case where the skin surface was insulated after the exposure. A more realistic boundary condition might be the lower heat flux kept constant throughout the entire time of interest. Here a heat flux of 10.4 kW/m^2 was placed on the skin for the entire 120 s of interest. With this heat flux there was practically no difference in burn time predictions with and without perfusion.

There has been some question as to what the perfusion term represents and whether it should be included in this skin model. In longer duration exposures of low heat fluxes, the perfusion term is often included because of the ability of the body to react to heat. However, as Lipkin and Hardy [28] point out, it takes about 20 s for the skin to react by increasing the blood flow. In flash fire exposures, second degree damage, and even much of third degree damage can already take place by the time this increase in blood flow occurs. During some accidents, such as a jet crash, one could argue that the body has some time to prepare for exposure. In the case of flash fires, it is more likely that the body would not have time to prepare for the exposure. As well, it has been shown here that the perfusion term has little effect on burn predictions, especially second degree predictions, under conditions where the skin is insulated after exposure, and also when a constant heat flux is applied over a longer period of time. Therefore it is recommended that blood perfusion be ignored in any further model of this accident.

3.4 Sensitivity Study of Surface Boundary Condition After Exposure

It was mentioned earlier that determining the skin surface boundary condition after the flash fire exposure is difficult. As the skin surface temperatures are quite high (up to 160°C), radiation may be important when modelling nude burns. Convection may also aid in cooling the skin. However, if radiation is to be incorporated into this model, it will make the solution more difficult by introducing a non-linear term into first row

of the left hand side "stiffness" matrix. Myers [55] discusses this problem and suggests that any finite element model be set up so that the first set of equations, which contain the non-linear term, be solved with a non-linear equation routine. The remainder of the equations would then be solved with a linear algebraic equation routine. The only other alternative is to linearize the non-linear radiation term if the surface temperature and the wall temperature used to calculate the radiation heat transfer are close together. Here the skin surface and wall temperatures are very different, and that simplification might not be justified. Therefore it is desirable to see if this boundary condition has a large effect on burn predictions. If it does, this boundary condition could be incorporated into a revised model in the future.

The convection and radiation heat transfer from the surface was estimated based on the maximum surface temperature for each of the three heat fluxes tested, 24, 41.6, and 83.2 kW/m^2. These values were then used as the surface heat flux loss term after exposure had ceased. The three values were calculated (see Appendix 3) to be about 600, 1050, 2470 W/m^2, respectively. Times to second degree burns will be unaffected, as for all three heat fluxes, second degree burns occur before the exposure ends.

There was a large effect on temperatures. The temperature-time histories for the insulated, and the radiation and convection heat transfer boundary conditions after exposure are shown in Figure 3.5. It is easy to see that this is an unrealistic test as both convection and radiation heat losses at any point in time are based on a difference between the surface temperature and some surrounding temperature. As this surface temperature is already decreasing after the exposure and even more so with these heat losses, the radiation and convection heat loss will continue to decrease as time goes on, not stay constant as is assumed here. With the insulated boundary condition, a temperature gradient is eventually set up between the higher surface temperature and the lower core temperature. With the radiation and convection boundary condition, a "reverse gradient" appears with the surface temperature being less than some temperature at depth, and the temperature then decreasing again to that at the core.

To provide a more realistic situation, a convection heat transfer coefficient of 6.0 $W/m^2 \cdot {}^\circ C$ based on the estimates shown in Appendix 3 was input into the program,

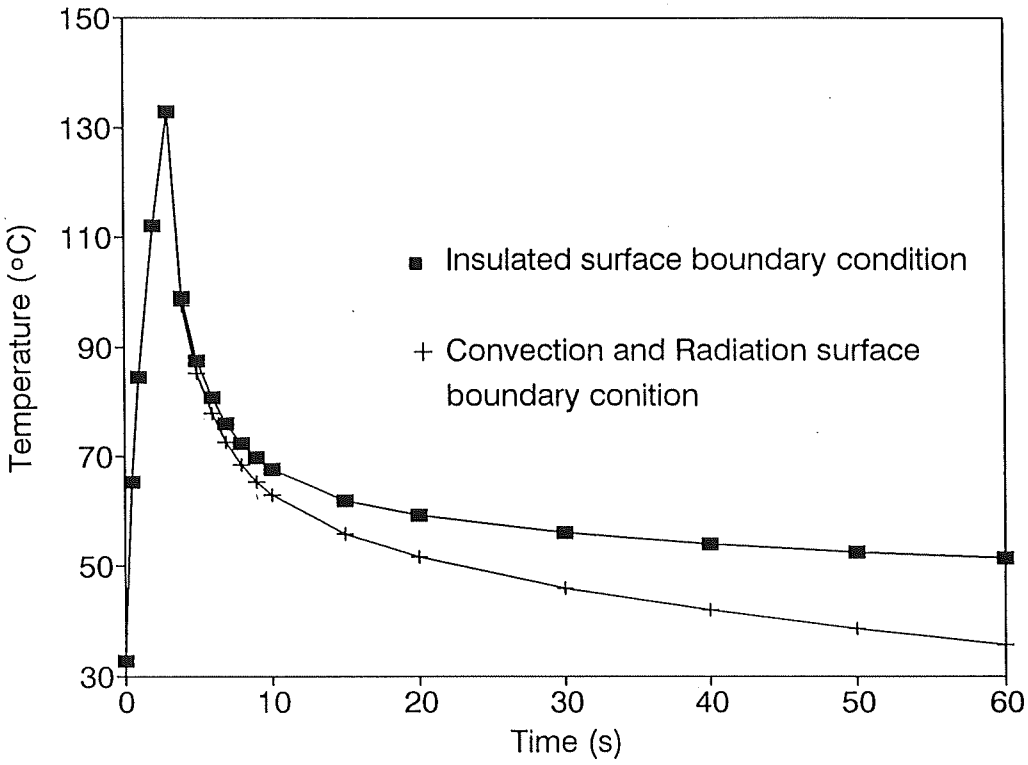

Figure 3.5 Comparison of Basal Layer Temperatures Determined Using Insulated, and Convection and Radiation Surface Boundary Conditions After Exposure (Exposure of 83.2 kW/m^2 for 3 s, 5 Hermitian elements used)

just as when the classical boundary condition of Section 2.4 was evaluated. Convection alone was then considered throughout the entire time period right from the beginning of the exposure. The times to second and third degree burn calculated are as shown in Table 3.14.

Table 3.14 Times for Second and Third Degree Burns Predicted When Convection Heat Loss Is or Is Not Included in the Skin Model

Heat Flux (kW/m^2)	Time to 2° Burn (s)		Time to 3° Burn (s)	
	Convection	No Convection	Convection	No Convection
24	2.82	2.78	no burn	no burn
41.6	1.30	1.30	no burn	no burn
83.2	0.54	0.54	no burn	55

Clearly there is very little effect on second degree burns, especially with the higher heat fluxes, as this convection heat loss is much less than the incident heat flux when damage occurs very early in the exposure. There is increased effect on third degree burns, as these take longer to occur. If radiation was also included (which accounts for about twice the heat loss as with convection at the higher heat fluxes) there would be an even larger effect.

For nude burns, the boundary condition has practically no effect on the second degree burns. It appears to have some effect on third degree burns. In terms of a clothed person or mannequin, the boundary condition would be different from that examined here, and may or may not play an important role in temperature and skin burn predictions.

3.5 Summary of the Effects of Variable Skin Properties and Boundary Condition

Variable skin properties were found to have little or no effect on predicting second degree burns in the ranges of heat fluxes and exposure times expected during flash fires. Some effect on third degree burns was noticed, although it should also be noted that one of the heat fluxes examined here (83.2 kW/m^2) barely produced, or barely did not produce third degree burns.

An initial quadratic temperature gradient between 32.5°C (surface) and 37°C (subcutaneous base) was found to be better for predicting temperatures and burns than an initial linear temperature gradient between the same two temperatures. The subcutaneous base node was constrained at 37°C throughout the time of interest. The nodal heat fluxes were set to zero, as varying these initial heat fluxes had little effect on temperature or burn predictions.

The variation in volumetric heat capacity values was mainly caused by the differences in skin density values. If the density is maintained at its presently accepted value for each layer, the reported variations in specific heats, and hence volumetric heat capacities of the layers have little effect.

Because of their large variations, the thermal conductivity values for single layer models cause considerable variation in temperature and burn predictions. An attempt to correlate thermal conductivity values for living and excised skin using the blood perfusion term was unsuccessful. The ranges for the individual layers were fairly small, and for the most part had little effect on skin burn predictions. The dermal values varied the most and hence had the greatest effect. Again, although this variation affected third degree burn predictions, the test case used here barely predicted or barely did not predict third degree burns. Three different sets of thermal conductivities and volumetric heat capacities for a single layer model of the skin were used in the single layer, constant property finite element model without a perfusion term. Temperatures and skin burn predictions were practically the same for all sets of data.

Blood perfusion was varied from 0, to its normal rate, to double its normal rate. Little or no effect was seen on second degree burn predictions or basal layer

temperatures. Third degree burn predictions and dermal base temperatures were slightly affected. As it takes about 20 s for the body to respond to thermal trauma by increasing blood flow, and in flash fires most damage is done or well under way by this time, it is recommended to disregard the blood perfusion term in future models.

A convection and radiation surface boundary condition can have a large effect on temperatures later in time. This will not affect second degree burns, but may affect third degree burn predictions. However, as the boundary condition for the nude burn studied here is expected to be much different from that for a clothed mannequin or person, this result may not be applicable to a similar model of clothed skin.

CHAPTER 4
COMPARISON OF SKIN BURN MODELS

A finite element model to predict the temperatures and burns in the skin subject to typical flash fire exposures was developed. The effects of changes in skin thermal physical properties and the surface boundary condition on burn and temperature predictions were tested. As a result of these tests, some portions of the model were revised. Temperature and burn predictions made by this revised version were compared with those made by other models over the range of high intensity, short duration exposures typical of flash fires. The models were also compared with experimental results from lower intensity, continuous exposures.

4.1 Comparison of Temperature-Time Histories

Temperature-time histories predicted by the variable property, multiple layer finite element program, and a constant property, single layer closed form solution were compared with experimental results. The closed form solution, given earlier as Equation (2.15), is

$$T(x,t) = T_i + \frac{2q_o}{\sqrt{k\rho c}} \left[\sqrt{t_{ex}}\ ierfc\left(\frac{x}{2\sqrt{\alpha t}}\right) - \sqrt{t - t_{ex}}\ ierfc\left(\frac{x}{2\sqrt{\alpha(t - t_{ex})}}\right) S(t) \right] \tag{4.1}$$

For the constant property, single layer model, the entire skin was assumed to be at an initially uniform temperature of 32.5°C. The values of thermal conductivity and volumetric heat capacity recommended by Hardee and Lee [53] (from Perkins [54]) for a single layer model were used, namely, k = 0.764 W/m·°C and $\rho c = 3.35 \times 10^6$ J/m³·°C.

The experimental results for this comparison were those reported by Stoll [26]. As mentioned in Section 1.6.3, Stoll determined the exposure times and temperatures for pain and blister thresholds using blackened skin irradiated with heat fluxes between 4.186

and 16.744 kW/m^2 (0.1 to 0.4 cal/cm^2·s). From these measured skin surface temperatures, the temperatures at the basal layer were calculated, as discussed in [65].

The temperature-time histories for the basal layer and the surface are shown in Figures 4.1 and 4.2, respectively. Both are a result of an incident heat flux of 4.2 kW/m^2 for 34 s (the time to blistering or second degree burn according to Stoll for this heat flux). The agreement between the finite element solution and the values which Stoll presented was good, except for the initial portion of the exposure. There the temperatures predicted by the closed form solution were much closer to Stoll's values. Later in the exposure, the temperatures predicted by the closed form solution were considerably different that those measured by Stoll.

The finite element surface temperatures were higher than those measured and calculated by Stoll. The finite element solution assumes the skin to be opaque (i.e. emissivity, $\epsilon = 1.0$), whereas actual skin is somewhat diathermanous. Stoll [24] used an emissivity of 0.94 for India ink-blackened skin to account for this in her basal layer temperature calculations. If some radiation does penetrate the skin, the temperature of the surface will be less than that predicted by an opaque model, such as the finite element model. This is evident in Figure 4.2. This reasoning was also used by Morse, et al. [34] to explain away the apparent increase in thermal inertia ($k\rho c$) with incident heat flux which Stoll found [24].

Stoll calculated the basal layer temperatures from the surface temperatures. The finite element basal layer temperatures were also higher than these calculated temperatures, as shown in Figure 4.1. Using the same reasoning as previously, the opaque finite element model should predict lower temperatures than Stoll's diathermanous model. The fact that the opposite was true here perhaps indicates that the finite element model calculates basal layer temperatures more accurately than the method which Stoll utilized. After exposure, for the insulated boundary condition used in the finite element and closed form solutions, one would also expect that basal layer temperatures would continue to be equal to or less than surface temperatures. Stoll's calculated basal layer temperatures were actually higher than the surface temperatures. This would indicate that a different boundary condition after the exposure was used in Stoll's calculations

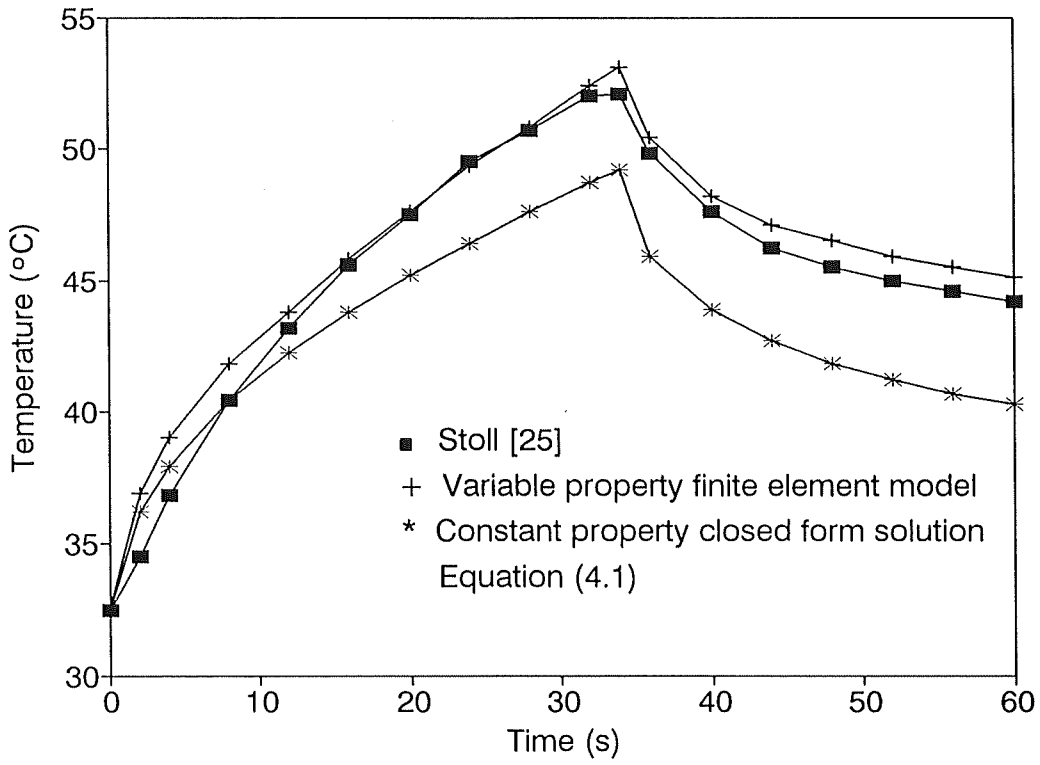

Figure 4.1 Basal Layer Temperature-Time Histories Determined Using Finite Element and Closed Form Solutions and Reported by Stoll [25] (Exposure of 4.2 kW/m^2 for 34 s)

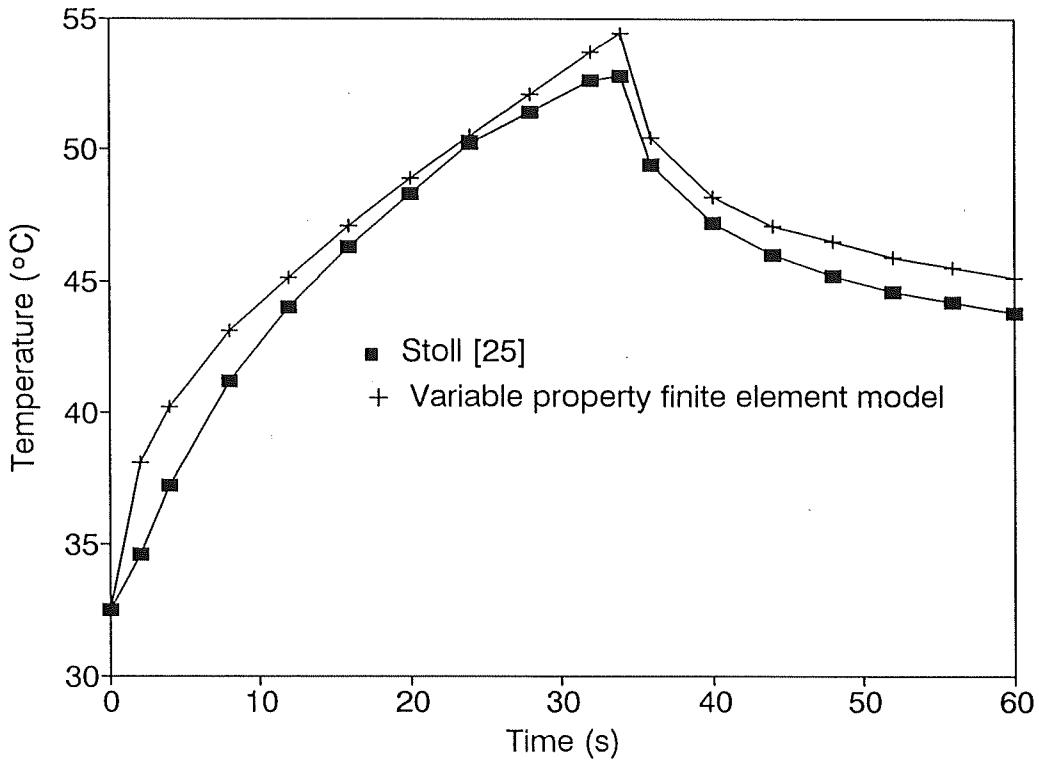

Figure 4.2 Surface Temperature-Time Histories Determined Using Finite Element Solution and Measured by Stoll [25] (Exposure of 4.2 kW/m^2 for 34 s)

than the insulated condition used in the finite element model and the closed form solution. For instance, a rapid cooling of the skin surface would produce this type of temperature gradient, and would of course be in the best interests of the experimental subjects. Regardless of the fact that the surface and basal layer temperatures are higher for the finite element model than those measured and calculated by Stoll, there was still good agreement between the two temperature-time histories. The agreement between temperatures predicted by the closed form solution and those measured by Stoll was not as good. This would indicate that the variable property, finite element model predicts temperatures better than the single layer, constant property closed form solution, at least for these lower intensity, continuous exposures.

4.2 Comparison of Burn Predictions

The predictions of times to second and third degree burns made by the two models were compared with each other, and with Stoll's experimental results in the case of second degree burns. These comparisons were made for high intensity, short duration exposures typical of flash fires, and for the lower intensity, continuous exposures used by Stoll. The thermal physical properties for the single layer, closed form solution were also varied between those given above, and the other two sets of properties mentioned by Hardee and Lee [53]

- Mitchell [63] $k = 0.591$ W/m$\cdot$°C
  $\rho c = 4.19 \times 10^6$ J/m$^3\cdot$°C
- Stoll [64] $k = 0.628$ W/m$\cdot$°C
  $\rho c = 3.68 \times 10^6$ J/m$^3\cdot$°C

4.2.1 Second Degree Burns

The times to second and third degree burn are compared in Tables 4.1 and 4.2, respectively. The times to second degree burn are also shown in Figure 4.3.

Table 4.1 Times to Second Degree Burn Calculated by Finite Element and Closed Form Solution Models, and Observed by Stoll

Heat Flux kW/m^2	Time to 2° Burn (s)				
	Finite Element	Closed Form Solution			Stoll Observed
		Perkins	Mitchell	Stoll	
3 second exposures					
24.0	2.78	3.70	no burn	3.00	-
41.6	1.30	1.40	1.50	1.40	-
83.2	0.54	0.50	0.60	0.50	-
166.4	0.24	0.20	0.30	0.20	-
Continuous exposures					
4.2	35	47	47	45	33.8
6.2	21	26	25	24	20.8
8.3	14	17	16	15	13.4
12.5	7.2	9.0	9.0	8.0	7.8
16.6	4.7	6.0	6.0	6.0	5.6

For the high intensity, short duration (3 s) exposures the times to second degree burn predicted by all the models were practically the same. The differences were highest for the lower intensity, continuous exposures. The predicted burn times using the closed form solution with Stoll's properties were the closest to those predicted by the variable property, multiple layer finite element model.

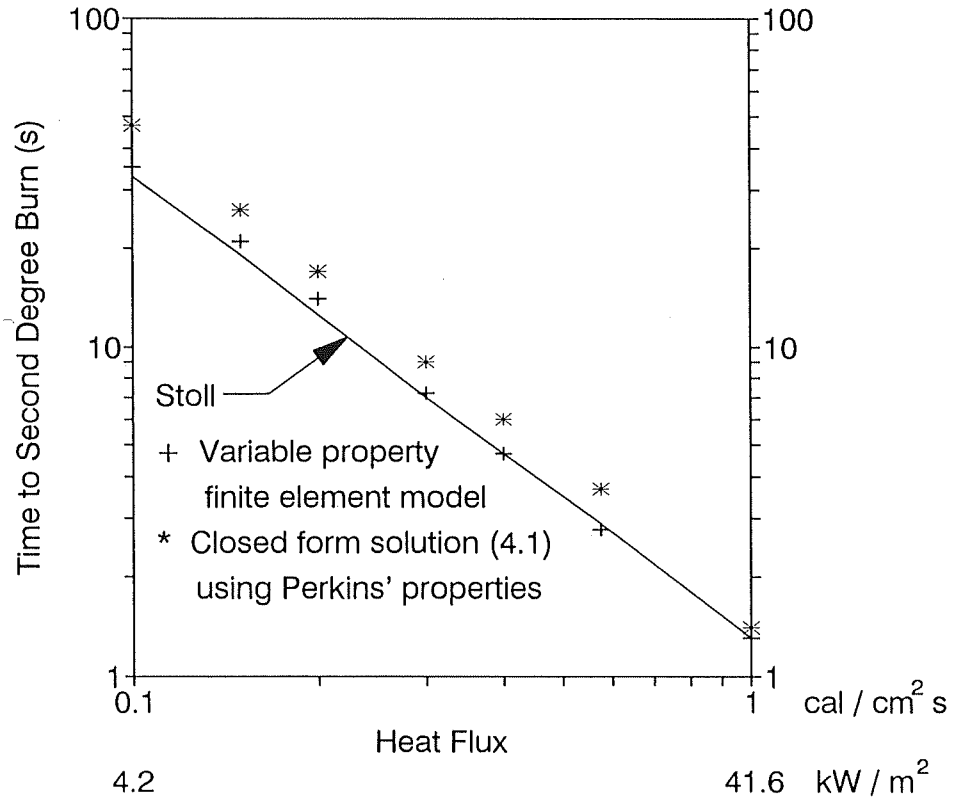

Figure 4.3 Times to Second Degree Burn as Predicted by Finite Element and Closed Form Solutions, and Observed by Stoll [26]

The line in Figure 4.3 labelled "Stoll" was reproduced from Figure 11 in [26] and was based on observed times to second degree burn for incident heat fluxes from 4.186 to 16.744 kW/m^2 (0.1 to 0.4 cal/cm^2 • s), and theoretically predicted times for heat fluxes from 16.744 to 41.86 kW/m^2 (0.4 to 1.0 cal/cm^2 • s). The finite element and closed form solution predictions (with Perkins' properties, as recommended by Hardee and Lee) were compared with this set of data. The finite element predictions were very close to the times observed by Stoll. The closed form solution predictions were closer than those of the finite element program at higher heat fluxes, but were not as close at lower heat fluxes. As shown in Table 4.1, there was little difference in predicted times to second degree burns using the different sets of properties in the closed form solution. Predictions made using the model with Stoll's property values were closest to the finite element predictions and observed data (which of course is expected, as these properties were calculated based on this experimental data), but here predictions made by the model using Mitchell's data were slightly closer to the finite element predictions than those using Perkins' data. This was the opposite to the case with the higher heat flux and shorter duration exposures. Perkins' value of thermal conductivity is higher (0.764 versus 0.591 W/m • °C), while his value of thermal capacity is lower (3.35 x 10^6 versus 4.19 x 10^6 J/m^3 • °C). Therefore for the lower intensity exposures, the thermal conductivity is the more important parameter, whereas with the higher intensity exposures, the volumetric heat capacity is the more important parameter.

4.2.2 Third Degree Burns

The times to third degree burns predicted by the variable property, multiple layer finite element model, and the constant property, single layer closed form solutions are shown in Table 4.2 below.

Table 4.2 Times to Third Degree Burn Calculated by the Finite Element Model and Closed Form Solutions

Heat Flux (kW/m^2)	Time to 3° Burn (s)				
	Finite Element		Closed Form Solution		
	With Blood	No Blood	Perkins	Mitchell	Stoll
3 s exposures					
83.2	55	33	no burn	no burn	no burn
166.4	7.3	7.2	6	11	8
Continuous exposures					
4.2	79	76	120	no burn	no burn
6.2	53	53	74	86	77
8.3	41	41	53	63	56
12.5	30	29	34	42	37
16.6	24	24	26	33	29

No experimental observations were included here, as Stoll only observed times to second degree burns. However the same lower heat flux levels that she used were also used here in order to make comparisons for these exposures as well as the high intensity, 3 s exposures. No data are shown for heat fluxes of 24 and 41.6 kW/m^2 as no third degree burns were predicted by any of the models as a result of 3 s exposures to these heat fluxes.

The effect of including the blood perfusion term in the finite element model, discussed in the previous chapter, was also reexamined here. The addition of the blood

perfusion term in the finite element model nearly doubled the time to third degree burn for the 83.2 kW/m^2 exposure. However, it made little difference when the heat flux was doubled to 166.4 kW/m^2. It also made little or no difference for the longer duration, lower heat flux cases Stoll investigated. It would appear that the perfusion term will only make a difference if the incident heat flux is not so high as to almost immediately cause third degree burns, and only when the heat flux is removed from the skin. The fact that the blood perfusion rate can increase substantially after 20 s was not included in the finite element model, but it may make a difference in what would be observed in an actual burn, especially in lower intensity, longer duration exposures.

The predictions made by the closed form solutions were different than those made by the finite element model, just as with second degree burns. Of the three closed form solutions, the predictions made using Perkins' property values were the closest to those of the finite element model. The differences between the closed form and finite element predictions increased once again as the heat fluxes decreased. It cannot be said that the finite element predictions are more accurate than the closed form solution predictions, as no experimental data were used to compare the two models. However, based on the results for second degree burns, and intuition, it would again make sense that a multiple layer model of the skin using different properties for each layer would make more accurate predictions of deeper burns than a single layer model of the skin. As well, the closed form solution uses a constant initial temperature gradient of 32.5°C, whereas the finite element model uses a quadratic initial temperature gradient. As noted previously in Section 3.3.2 this difference in initial dermal base temperatures (32.5°C for the closed form solution and 33.9°C for the finite element solution) can make a large difference in predicted times to third degree burns, or whether third degree burns will in fact be predicted.

One final note of caution in interpreting burn prediction times. Both the closed form solution and finite element model computer programs used variable time step schemes to calculate temperatures and numerically integrate Henriques' burn integral. Both programs used smaller time steps during the first portion of the time span and larger time steps later on. This may have an effect on longer duration exposures, where the

time steps close to the critical value 1.0 for the burn integral at the basal layer and dermal base will be larger than for the short duration exposures. However, in these lower intensity, longer duration cases, the temperature-time histories do not increase or decrease as sharply as with the higher incident heat fluxes, so this should have minimal effect on the results obtained.

4.3 Pre-Exponential Factor and Activation Energy in Henriques' Burn Integral

As mentioned in the review of skin burn research in Section 1.6, different investigators found different values for the pre-exponential factor and activation energy in the burn damage rate equation,

$$\frac{d\Omega}{dt} = P \exp\left(\frac{-\Delta E}{RT}\right) \qquad (4.2)$$

The effects of varying the pre-exponential factor, P, and the activation energy, ΔE, on the predicted times to second and third degree burns were tested over the range of exposures typical of flash fires.

4.3.1 Second Degree Burns

The different published values of the pre-exponential factor and the activation energy for the basal layer and second degree burns are as follows.

- Stoll [25]
  - $P = 2.185 \times 10^{124}\ s^{-1}$ $44 \leq T < 50^{\circ}C$
  - $\Delta E/R = 93\ 534.9\ K$
  - $P = 1.823 \times 10^{51}\ s^{-1}$ $T \geq 50^{\circ}C$
  - $\Delta E/R = 39\ 109.8\ K$
- Henriques and Moritz [19]
  - $P = 3.1 \times 10^{98}\ s^{-1}$
  - $\Delta E/R = 75\ 000\ K$

- Mehta and Wong [9,10]
  - P = 1.43×10^{72} s^{-1}
  - $\Delta E/R$ = 55 000 K

Up until this point in the study, the values from Stoll were used in all the models, as suggested by Morse, et al. [35] (Section 1.7). The values for the pre-exponential factor suggested by Henriques and Moritz, and Mehta and Wong were also used in tests here. A comparison between the times to second degree burn predicted using the different values is shown in Table 4.3, below.

Table 4.3 Comparison of Times to Second Degree Burn Predicted Using the Different Values of the Pre-Exponential Factor and Activation Energy Found in the Literature

Heat Flux (kW/m^2)	Time to 2° Burn (s)		
	Stoll [25]	Henriques / Moritz [19]	Mehta / Wong [9,10]
24	2.78	2.64	2.72
41.6	1.30	1.16	1.22
83.2	0.54	0.46	0.48
166.4	0.24	0.22	0.22

Little differences in times to second degree burn resulted from changing the values of the pre-exponential factor and activation energy value for this range of heat fluxes. Therefore if values other than those of Stoll were used, this should have little effect on burn predictions. Stoll's values will however continue to be used in the finite element model, as suggested by Morse, et al [35], and discussed in Section 2.5.

4.3.2 Third Degree Burns

The different published values of the pre-exponential factor and the activation energy for the dermal base, and third degree burns are as follows.

- Takata [33]
  - $P = 4.32 \times 10^{64}\ s^{-1}$ $\quad 44 \leq T < 50^{\circ}C$
  - $\Delta E/R = 50\ 000\ K$
  - $P = 9.39 \times 10^{104}\ s^{-1}$ $\quad 50 \leq T \leq 60^{\circ}C$
  - $\Delta E/R = 80\ 000\ K$
- Mehta and Wong [9,10]
  - $P = 2.86 \times 10^{69}\ s^{-1}$
  - $\Delta E/R = 55\ 000\ K$

Up until this point in the study, Takata's values were used in all of the models. Takata's second set of values are only strictly valid for dermal base temperatures from 50 to 60°C. However, the finite element program will continue to use these values for dermal base temperatures greater than 60°C due to the absence of data above this temperature.

A comparison of the times to third degree burn using the different values of the pre-exponential factor, and the activation energy is shown in Table 4.4.

Table 4.4 Comparison of Times to Third Degree Burn Predicted Using the Different Values of the Pre-Exponential Factor and Activation Energy Found in the Literature

Heat Flux (kW/m^2)	Time to 3° Burn (s)	
	Takata [33]	Mehta / Wong [9,10]
83.2	55	none
166.4	12	7.3

The effect of changing the values here is much larger than with the second degree burn times. As the times to third degree burn are much longer, this would be expected. It is often difficult to distinguish between deep second degree, and third degree burns. Therefore, it would be more difficult to get accurate values for the pre-exponential factor and activation energy in third degree burn experiments than in first and second degree burn experiments. Due to all the uncertainties surrounding third degree burn predictions, and Aerotherm's [35] test results using the two sets of data, Takata's values will continue to be used in the program. Using these values results in predictions of shorter times to third degree burns over the heat fluxes studied than if Mehta and Wong's values were used, so using Takata's values will result in more conservative estimates of the protection offered by fabric or clothing.

4.4 Selection of Models for Flash Fire Burn Predictions

In deciding upon a model to predict skin burns in flash fire conditions, the end user must be kept in mind. A highly accurate model, but which takes large amounts of computational time may be suitable for individual research into the effects of skin properties. However, when the model is coupled to a mannequin data acquisition system, such a model may not be suitable. In this situation, many research associates are involved in running experiments, and close to real time results are desirable. The highly accurate model may be too slow, unless a substantially quicker and more expensive computer is used. One end user may be mainly concerned with the surface area of the body suffering second degree burns or worse, whereas another may be concerned with a breakdown of second and third degree burns. All of these requirements must be looked at in the context of the accident studied here, flash fires.

Based on all of the results to date, a closed form solution will predict the time to second degree burns from a typical flash fire exposure slightly less accurately than a finite element model, but quicker. As long as the heat fluxes incident on the skin do not become too small, then the difference between second degree burn predictions using the

closed form solution and the finite element solution should not be very large. Fairly high heat fluxes (e.g. 15 to 83.2 kW/m^2) are expected even through most clothing, so this should not be a problem. A compiled version of the finite element program described here takes 22.2 s to run on a 80386 based personal computer with a 33 MHz clock and math coprocessor. A compiled version of a program which uses the closed form solution takes 4.2 s to obtain the same results, over five times quicker. No attempt was made to optimize the finite element program (e.g. saving matrices, rather than calculating them at each time step), so this time difference could be reduced substantially. This difference in speed is not important if only one skin location is examined, but may make a difference in calculating results serially from many skin locations, such as with the University of Alberta mannequin tests where data from 110 sensors are analyzed. It was also noted that for typical flash fire exposures, the variations in thermal physical properties do not have a significant difference on times to second degree burns.

If information on the amounts of, or times to second and third degree burns is required, the finite element model is the better choice. The differences between the temperature and burn predictions made by the finite element model and the closed form solution were larger for third degree burns than for second degree burns. However, recalling the results of the previous sections and chapters, the effects of varying thermal physical properties, initial temperature gradients, perfusion rates, and constants in Henriques' burn integral were much greater for third degree burns than for second degree burns. As well, the exact surface boundary condition after exposure ceases is uncertain, and may affect burn predictions further. As a result further study may have to be done, before deciding whether the model described here is appropriate for predicting third degree burns in a mannequin test system.

One other point must be raised when comparing the models for use in a mannequin test system. This report has looked at a short duration, high intensity step heat flux incident on the surface of the skin, which is an idealized picture of a flash fire on nude skin. If the skin is now covered with cloth, it may take some time for the heat flux to propagate through the clothing and a smaller, time varying heat flux will be incident on the skin. Therefore the surface boundary condition will be different from

that studied here, both during the flash fire and afterwards. The closed form solution for a time varying heat flux incident on the face of an inert, semi-infinite solid at initially constant temperature is given in [36] as

$$T(x,t) = T_o + \frac{1}{\sqrt{\pi k \rho c}} \int_o^t q(t - \tau) \exp\left(-\frac{x^2}{4\alpha t}\right) \frac{d\tau}{\tau^{1/2}} \qquad (4.3)$$

If the heat flux is known as a function of time, Equation (4.3) can be integrated to give the solution. The finite element solution would simply have to be revised so that rather than the heat flux having a constant step heat flux value, it would be represented by a vector with heat fluxes at each time step. One topic for future study could be how the closed form solution for a given heat flux-time history compares with a finite element solution for the same history. Another useful comparison would be how well the heat flux incident through fabric onto the skin can be modelled as a step change. Holcombe and Hoschke [42] indicate that in TPP tests, the heat flux-time history of the sensor beneath the garment is not of the rectangular step form. The whole question of what boundary condition exists for the clothed mannequin after exposure ceases should also be a topic of future study.

CHAPTER 5
CONCLUSIONS AND RECOMMENDATIONS

5.1 Conclusions

From this research in modelling the heat transfer in skin subjected to a flash fire, the following conclusions can be made:

- Hermitian temperature elements model the heat transfer in skin more economically than linear or quadratic elements. Here 5 Hermitian elements (1 for the epidermis, and 2 each for the dermis and subcutaneous tissue) provided the same or better accuracy than 9 quadratic or 18 linear elements.

- The initial temperature gradient had minimal effect on second degree burn predictions, but a larger effect on third degree burn predictions. An initial quadratic gradient was preferable to a linear gradient.

- Variations in thermal physical properties over the ranges used in multiple layer skin models had minimal effects on second degree burn predictions, but larger effects on third degree burn predictions.

- The blood perfusion term can be neglected in predicting second degree burns due to flash fires.

- The convection and radiation surface boundary condition used after the exposure has no effect on second degree burn predictions, as these burns occur before the exposure ends. It may have an effect in predicting slower developing third degree burns.

- Variations in the pre-exponential factor and activation energy in Henriques' burn integral have minimal effect on second degree burn predictions, but a larger effect on third degree burn predictions.

- The variable property, multiple layer finite element model developed here is more accurate in making temperature and burn predictions than the constant property, single layer closed form solution for a step heat flux. However, if only second degree burn predictions must be made in close to real time serially from data for a large number of mannequin sensors, the closed form solution is preferable. Its predictions are only slightly different from the finite element predictions, but it requires a fraction of the computing time.

5.2 Recommendations

The following recommendations for future research are made as a result of this study.

- The skin surface boundary condition after exposure of covered skin should be determined more accurately. From mannequin test results, the heat flux-time history incident on the skin should be known. This history can be input into the finite element model, and the results can be compared to the closed form solution for a time-varying incident heat flux, and to step change heat flux finite element and closed form solutions. The exact nature of this boundary condition should be studied. In other words the relative contributions of conduction, convection, and radiation should be determined.

- A finite element model of covered skin should be constructed. This would require modelling the heat and mass transfer through fabric. This model could be tested using TPP test results.

- From this finite element model of covered skin, a model of a clothed person or mannequin should be developed. Depending on geometric effects, and the heat transfer inside the skin, a two or three dimensional model may be required. Here the surface boundary condition on the clothed person after the exposure may be

important, and should be studied. These results could be compared to mannequin test results.

REFERENCES

1. Smith, Greg, Alberta Occupational Health and Safety, personal communication, December, 1991

2. Dale, J.D., Crown, E.M., Ackerman, M.Y., Leung, E., and Rigakis, K.B., "Instrumented Mannequin Evaluation of Thermal Protective Clothing", Performance of Protective Clothing: Fourth Volume, ASTM STP 1133, James P. McBriarty and Norman W. Henry, eds., American Society for Testing and Materials, Philadelphia, 1992

3. Diller, K.R., "Analysis of Skin Burns", in Heat Transfer in Medicine and Biology, A. Shitzer and R.C. Eberhart, eds., Plenum Press, New York, 1985, pp. 85-134

4. Gardner, W.D., and Osburn, W.A., "The Integumentary System", Chapter Three in Anatomy of the Human Body, W.B. Saunders Co., Philadelphia, 1978

5. Anthony, C.P., and Thibodeau, G.A., Textbook of Anatomy and Physiology, 10th ed., The C.V. Mosby Co., St. Louis, 1979, pp. 70-73, 290-294, 530-533

6. Krizek, T.J., Robson, M.C., and Wray, R.C., Jr., "Care of the Burned Patient", in The Management of Trauma, 2nd ed., W.F. Ballinger, R.B. Rutherford, and G.D. Zuidema, eds., W.B. Saunders Co., Philadelphia, 1973, pp. 650-718

7. Pillsbury, D.M., A Manual of Dermatology, W.B. Saunders Co., Philadelphia, 1971

8. Pennes, H.H., "Analysis of Tissue and Arterial Blood Temperatures in Resting Human Forearm", Journal of Applied Physiology, Vol. 1, 1948, pp. 93-122

9. Mehta, A.K, and Wong, F., Measurement of Flammability and Burn Potential of Fabrics, Summary Report from Fuels Research Laboratory, Massachusetts Institute of Technology, Cambridge, Massachusetts, 1972

10. Mehta, A.K, and Wong, F., Measurement of Flammability and Burn Potential of Fabrics, Full Report from Fuels Research Laboratory, Massachusetts Institute of Technology, Cambridge, Massachusetts, 1973

11. Hodson, D.A., Eason, G., Barbenel, J.C., "Modelling Transient Heat Transfer Through the Skin and Superficial Tissues - I:Surface Insulation", Transaction of the ASME, Journal of Biomechanical Engineering, Vol. 108, 1986, pp. 183-188

12. "Physiological Principles, Comfort, and Health", Chapter 8 in ASHRAE Handbook of Fundamentals, American Society of Heating, Refrigerating, and Air Conditioning Engineers, Inc., Atlanta, 1989

13. Weinbaum, S., and Jiji, L.M., "A New Simplified Bioheat Equation for the Effect of Blood Flow on Local Average Tissue Temperature", Transactions of the ASME, Journal of Biomechanical Engineering, Vol. 107, 1985, pp. 131-139

14. Charny, C.K., Weinbaum, S., and Levin, R.L., "An Evaluation of the Weinbaum-Jiji Bioheat Equation for Normal and Hyperthermic Conditions", Transactions of the ASME, Journal of Biomechanical Engineering, Vol., 112, 1990, pp. 80-87

15. Henriques, F.C., Jr. and Moritz, A.R., "Studies of Thermal Injuries I. The Conduction of Heat to and Through Skin and The Temperatures Attained Therein. A Theoretical and an Experimental Investigation", The American Journal of Pathology, Vol. 23, 1947, pp. 531-549

16. Henriques, F.C., Jr. and Moritz, A.R., "Studies of Thermal Injuries II. The Relative Importance of Time and Surface Temperature in the Causation of Cutaneous Burns", The American Journal of Pathology, Vol. 23, 1947, pp. 695-720

17. Moritz, A.R., "Studies of Thermal Injuries III. The Pathology and Pathogenesis of Cutaneous Burns. An Experimental Study", The American Journal of Pathology, Vol. 23, 1947, pp. 915-941

18. Moritz, A.R., Henriques, F.C., Jr., Dutra, F.R., and Weisiger, J.R., "Studies of Thermal Injuries IV. An Exploration of the Casulty-Producing Attributes of Conflagrations, Local and Systemic Effects of General Cutaneous Exposure to Excessive Circumambient (Air) and Circumradiant Heat of Various Duration and Intensity", Archives of Pathology, Vol. 43, 1947, pp. 466-488

19. Henriques, F.C., Jr., "Studies of Thermal Injuries V. The Predictability and the Significance of Thermally Induced Rate Processes Leading to Irreversible Epidermal Injury", Archives of Pathology, Vol. 43, 1947, pp. 489-502

20. Buettner, K., "Conflagration Heat", Chapter XIII-A in German Aviation Medicine, World War II, pp. 1167-1187

21. Buettner, K., "Effects of Extreme Heat and Cold on Human Skin I. Analysis of Temperature Changes Caused by Different Kinds of Heat Application", Journal of Applied Physiology, Vol. 3, 1951, pp.691-702

22. Buettner, K., "Effects of Extreme Heat and Cold on Human Skin II. Surface Temperature, Pain and Heat Conductivity in Experiments with Radiant Heat", Journal of Applied Physiology, Vol. 3, 1951, pp.703-713

23. Buettner, K., "Effects of Extreme Heat and Cold on Human Skin III. Numerical Analysis and Pilot Experiments on Penetrating Flash Radiation Effects", Journal of Applied Physiology, Vol. 5, 1952, pp.207-220

24. Stoll, A.M., and Greene, L.C., "Relationship Between Pain and Tissue Damage Due to Thermal Radiation", Journal of Applied Physiology, Vol. 14, 1959, pp. 373-382

25. Weaver, J.A., and Stoll, A.M., "Mathematical Model of Skin Exposed to Thermal Radiation", Aerospace Medicine, Vol. 40, 1969, pp. 24-30

26. Stoll, A.M., and Chianta, M.A., "Heat Transfer Through Fabrics as Related to Thermal Injury", Transactions of the New York Academy of Sciences, Vol. 33, 1971, pp. 649-669

27. Stoll, A.M., and Chianta, M.A., "Burn Production and Prevention in Convective and Radiant Heat Transfer", Aerospace Medicine, Vol. 39, 1968, pp. 1097-1100

28. Lipkin, M, and Hardy, J.D., "Measurement of Some Thermal Properties of Human Tissues", Journal of Applied Physiology, Vol. 7, 1954, pp. 212-217

29. Hardy, J.D., Wolff, H.G., and Goodell, H., "Studies on Pain: Discrimination of Differences in Intensity of a Pain Stimulus as a Basis of a Scale of Pain Intensity", Journal of Clinical Investigation, Vol. 26, 1947, pp. 1152-1158

30. Hardy, J.D., "Thresholds of Pain and Reflex Contraction as Related to Noxious Stimulation", Journal of Applied Physiology, Vol. 5, 1953, pp. 725-739

31. Henriques, F.C., Jr., and Maxwell, R.A., The Applicability of the Skin Damage Integral to the Prediction of Flash Burn Injury Thresholds, Including Those Caused by Atomic Detonation, Technical Operations, Inc., TOI 54-19, 1956

32. Chen, N.Y., and Jensen, W., Skin Simulants with Depth Magnification, Technical Report No. 5, Fuels Research Laboratory, Massachusetts Institute of Technology, Cambridge, Massachusetts, March, 1957

33. Takata, A.N., Rouse, J., and Stanley, T., Thermal Analysis Program, I.I.T. Research Institute Report IITRI-J6286, Chicago, 1973

34. Morse, H.L., Thompson, J.G., and Clark, K.J., Analysis of the Thermal Response of Protective Fabrics, Acurex Corporation, Aerotherm Division Report AFML-TR-73-17, 1973

35. Morse, H.L., Tickner, G., Brown, R., Burn Damage and Burn Depth Criteria, Acurex Corporation, Aerotherm Division Report TN-75-26, 1975

36. Carslaw, H.S., and Jaeger, J.C., Conduction of Heat in Solids, 2nd ed., Oxford University Press, London, 1959

37. Harmathy, T.Z., "Viewpoint: $k\rho c$ or $\sqrt{(k\rho c)}$ - Thermal Inertia or Thermal Absorptivity?", Fire Technology, Vol. 21, 1985, pp. 146-149

38. Norton, M.J.T., Kadoph, S.J., Johnson, R.F., and Jordan, K.A., "Design, Construction, and Use of Minnesota Woman, A Thermally Instrumented Mannequin", Textile Research Journal, Vol. 55, 1985, pp. 5-12

39. Behnke, W.P., "Predicting Flash Fire Protection of Clothing From Laboratory Tests Using Second-Degree Burn to Rate Performance", Fire and Materials, Vol. 8, 1984, pp. 57-63

40. Standard Test Method for Thermal Protective Performance of Materials for Clothing By Open-Flame Method, ASTM Standard D 4108-87, American Society for Testing and Materials, Philadelphia, 1987

41. Firefighters' Protective Clothing for Protection Against Heat and Flame, National Standard of Canada CAN/CGSB-155.1-M88, Canadian General Standards Board, Ottawa

42. Holcombe, B.V., and Hoschke, B.N., "Do Test Methods Yield Meaningful Performance Specifications?", Performance of Protective Clothing: First Volume ASTM STP 900, R.L. Barker and G.C. Coletta, eds., American Society for Testing and Materials, Philadelphia, 1986, pp. 327-339

43. Hasselbrack, S.A., InVitro Mannequin Simulation of InVivo Clothing Fire Accidents, PhD. Thesis, University of Minnesota, 1977

44. Elkins, W. and Thompson, J.G., Instrumented Thermal Mannikin, Acurex Corporation, Aerotherm Division Report AD-781 176, 1973

45. Norton, M.J.T., Johnson, R.F., and Jordan, K.A., "Assessment of Flammability Hazard and Its Relationship to Price for Women's Nightgowns", Textile Research Journal, Vol. 54, 1984, pp. 748-760

46. Gustafson, R.J., Jordan, K.A., Hasselbrack, S.A., Kadoph, S.J., and Johnson, R.F., Estimating Thermal Injury from Clothing Burns on A Mannequin - Finite Element Model, presented at the 1978 Annual Meeting, North Central Region, American Society of Agricultural Engineers (Paper Number NCR-78-4005), 1978

47. Hayes, L.J., and Diller, K.R., A Finite Element Model for the Exposure of A Composite Man with Distributed Heat Generation to a Convective, Subfreezing Environment, ASME Paper 81-WA/HT-52, 1981

48. Diller, K.R., and Hayes, L.J., "A Finite Element Model of Burn Injury in Blood-Perfused Skin", Transactions of the ASME, Journal of Biomechanical Engineering, Vol. 105, 1983, pp. 300-307

49. Sekins, K.M., Emery, A.F., Lehmann, J.F., and MacDougall, J.A., "Determination of Perfusion Field During Local Hyperthermia with the Aid of Finite Element Thermal Models", Transactions of the ASME, Journal of Biomechanical Engineering, Vol. 104, 1982, pp. 272-279

50. Osman, M.M., and Afify, E.M., "Thermal Modelling of the Normal Woman's Breast", Transactions of the ASME, Journal of Biomechanical Engineering, Vol. 106, 1984, pp. 123-130

51. Osman, M.M., and Afify, E.M., "Thermal Modelling of the Malignant Woman's Breast", Transactions of the ASME, Journal of Biomechanical Engineering, Vol. 110, 1988, pp. 269-276

52. Craggs, A., University of Alberta, private communication, 1990

53. Hardee, H.C., and Lee, D.O., "A Simple Conduction Model for Skin Burns Resulting from Exposure to Chemical Fireballs", Fire Research, Vol. 1, 1977/78, pp. 199-205

54. Perkins, J.B., Pearse, H.E., and Kingsley, H.D., Studies of Flash Burns: The Relation of Time and Intensity of Applied Thermal Energy to the Severity of Burn, University of Rochester Report UR-317, 1952

55. Myers, G.E., Analytical Methods in Conduction Heat Transfer, McGraw-Hill Book Company, New York, 1971

56. Allaire, P.E., Basics of the Finite Element Method: Solid Mechanics, Heat Transfer, and Fluid Mechanics, Wm C. Brown Publishers, Dublique, Iowa, 1985

57. Southwood, W.F.W., "The Thickness of the Skin", Plastic and Reconstructive Surgery, Vol. 15, 1955, pp. 423

58. Whitton, J.T., and Everall, J.D., "The Thickness of the Epidermis", British Journal of Dermatology, Vol. 89, 1973, pp. 467-476

59. Emery, A.F., and Carson, W.W., "An Evaluation of the Use of the Finite-Element Method in the Computation of Temperature", Transactions of the ASME, Journal of Heat Transfer, Vol. 93, 1971, pp. 136-145

60. Bowman, H.F., Cravalho, E.G., and Woods, M., "Theory, Measurement, and Application of Thermal Properties of Biomaterials", Annual Review of Biophysics and Bioengineering, Vol. 4, 1975, pp. 43-80

61. Tanasawa, I., and Katsuda, T., Seisan Kenkyu, Vol. 24, 1972, pp. 440-443 (Reported in [60])

62. Lomholt, S., Strahlentherapie, Vol. 35, 1930, pp. 324 (Reported in [60])

63. Mitchell, H.H., A General Approach to the Problem of Estimating Personnel Damage on Atom Bombed Targets, Rand Report RM-1149, 1953

64. Stoll, A.M., "Heat Transfer in Biotechnology", in Advances in Heat Transfer, Vol. 4, J.P. Hartnett and T.F. Irvine, Jr., eds., Academic Press, New York, 1967, pp. 65-141

65. Weaver, J.A., Calculation of Time-Temperature Histories and Prediction of Injury to Skin Exposed to Thermal Radiation, Report NADC-MR-6623, U.S. Naval Air Development Center, Johnsville, Maryland, 1967

66. Wu, Ray-Shing, Cheng, K.C., Craggs, A., "Convective Instability in Porous Media with Maximum Density and Throughflow Effects by Finite-Difference and Finite-Element Methods", Numerical Heat Transfer, Vol. 2, 1979, pp. 303-318

67. Holman, J.P., Heat Transfer, 6th ed., McGraw-Hill Book Company, New York, 1986

APPENDICES

APPENDIX 1: DERIVATION OF FINITE ELEMENT MATRIX EQUATION

The differential equation for heat transfer in the skin under flash fire conditions is the Pennes' bioheat transfer equation,

$$\rho c \frac{\partial T}{\partial t} = k \frac{\partial^2 T}{\partial x^2} - G(\rho c)_b (T - T_c) \qquad \text{(A1.1)}$$

with the following initial and boundary conditions:

$$T(x,t=0) = T_i(x) \qquad \text{(A1.2)}$$

where $T_i(x)$ is some initial temperature gradient in the skin.

$$T(x=L,t) = T_c \quad (t>0) \qquad \text{(A1.3)}$$

$$k \left(\frac{\partial T}{\partial x}\right) + q(t) = 0 \quad (x=0,t) \qquad \text{(A1.4)}$$

where q(t) is the incident heat flux on the skin, given by

$$\begin{aligned} q(t) &= q_o \quad 0 \le t_{ex} \\ &= 0 \quad t > t_{ex} \end{aligned} \qquad \text{(A1.5)}$$

The Hermitian temperature element was used here. All the terms in Equation (A1.1) are brought to the left hand side, and the Hermitian temperature interpolation polynomials are substituted for the temperature and its derivatives. Noting that

$$T = \langle f \rangle^T \langle T_e \rangle \qquad \text{(A1.6)}$$

$$\frac{\partial T}{\partial x} = \langle f' \rangle^T \langle T_e \rangle \qquad \text{(A1.7)}$$

$$\frac{\partial^2 T}{\partial x^2} = \langle f'' \rangle^T \langle T_e \rangle \tag{A1.8}$$

$$\frac{\partial T}{\partial t} = \langle f \rangle^T \langle \dot{T}_e \rangle \tag{A1.9}$$

where $\langle f' \rangle^T$ and $\langle f'' \rangle^T$ are the row vectors of the first and second derivatives of the interpolation polynomials with respect to x, Equation (A1.1) now becomes

$$(\rho c) \langle f \rangle^T \langle \dot{T}_e \rangle - k \langle f'' \rangle^T \langle T_e \rangle + G(\rho c)_b (\langle f \rangle^T \langle T_e \rangle - T_c) = R(x) \tag{A1.10}$$

where the right hand side of Equation (A1.10) is equal to a residual, R(x), which is a function of x.

Galerkin's equation is

$$\int_0^l \langle f \rangle R(x) dx = 0 \tag{A1.11}$$

Substituting Equation (A1.10) into Equation (A1.11) for R(x) gives

$$\int_0^l \Big[(\rho c) \langle f \rangle \langle f \rangle^T \langle \dot{T}_e \rangle - k \langle f \rangle \langle f'' \rangle^T \langle T_e \rangle + G(\rho c)_b \left(\langle f \rangle \langle f \rangle^T \langle T_e \rangle - \langle f \rangle T_c \right) \Big] dx = 0 \tag{A1.12}$$

Rearranging terms, Equation (A1.12) becomes

$$\left(\int_0^l (\rho c) \langle f \rangle \langle f \rangle^T dx \right) \langle \dot{T}_e \rangle - \left(\int_0^l k \langle f \rangle \langle f'' \rangle^T dx \right) \langle T_e \rangle + \left(\int_0^l G(\rho c)_b \langle f \rangle \langle f \rangle^T dx \right) \langle T_e \rangle - \left(G(\rho c)_b \langle f \rangle dx \right) T_c = 0 \tag{A1.13}$$

Integrating the second term on the left hand side by parts gives

$$-\int_0^l k \langle f \rangle \langle f'' \rangle^T \langle T_e \rangle dx = -k \langle f \rangle \langle f' \rangle^T \langle T_e \rangle \Big]_0^l + \int_0^l k \langle f' \rangle \langle f' \rangle^T \langle T_e \rangle dx \tag{A1.14}$$

As temperatures and fluxes must be continuous across element boundaries, and remembering that

$$T = \langle f \rangle^T \langle T_e \rangle$$

$$k \frac{\partial T}{\partial x} = k \langle f' \rangle^T \langle T_e \rangle$$

the first term on the right hand side of Equation (A1.14) will cancel out at all of the interior element interfaces. Therefore only values of this term at the exterior nodes (i.e. x = 0 (surface), and x = L (base of the subcutaneous layer)) of the skin will be of concern.

At x = 0, the first term on the right hand side of Equation (A1.14) becomes:

$$-k \langle f \rangle \langle f' \rangle^T \langle T_e \rangle \Big]_{x=0} = -k \langle f \rangle \left(\frac{\partial T}{\partial x} (x=0) \right)$$

Applying the boundary condition given by Equation (A1.4), this term becomes

$$\langle f \rangle \; q(t) \Big]_{x=0} \tag{A1.15}$$

At x = L, the first term on the right hand side of Equation (A1.14) cannot be simplified further using the boundary condition given by Equation (A1.3). Therefore this term remains as

$$-k \langle f \rangle \langle f' \rangle^T \langle T_e \rangle \Big]_{x=L} \tag{A1.16}$$

Equations (A1.15) and (A1.16) are substituted into Equation (A1.14), and the resulting equation is substituted into Equation (A1.13). Sorting like terms gives

$$\begin{aligned} \left(\int_0^l k \langle f' \rangle \langle f' \rangle^T dx - k \langle f \rangle \langle f' \rangle^T \Big]_{x=L} + \int_0^l G(\rho c)_b \langle f \rangle \langle f \rangle^T dx \right) \langle T_e \rangle \\ + \left(\int_0^l (\rho c) \langle f \rangle \langle f \rangle^T dx \right) \langle \dot{T}_e \rangle \\ - \langle f \rangle \Big]_{x=0} (q(t)) - \int_0^l G(\rho c)_b \langle f \rangle \, dx \; T_c = 0 \end{aligned} \tag{A1.17}$$

or

$$\Big([A] - [k] + [M]\Big) \langle T_e \rangle + [B] \langle \dot{T}_e \rangle - \langle BC \rangle = 0 \tag{A1.18}$$

where

$$[A] = \int_0^l k \langle f' \rangle \langle f' \rangle^T dx$$

$$= \frac{k}{30\ l} \begin{vmatrix} 36 & 3l & -36 & 3l \\ 3l & 4l^2 & -3l & -l^2 \\ -36 & -3l & 36 & -3l \\ 3l & -l^2 & -3l & 4l^2 \end{vmatrix} \qquad \text{(A1.19)}$$

(Note that the values of this and the other integrals are tabulated in [66].)

$$[k] = k \langle f \rangle \langle f' \rangle^T \Big]_{x=L}$$

$$= \begin{vmatrix} . & . & . & . & . & . \\ . & . & . & . & . & . \\ . & . & 0 & 0 & 0 & 0 \\ . & . & 0 & 0 & 0 & 0 \\ . & . & 0 & 0 & 0 & k \\ . & . & 0 & 0 & 0 & 0 \end{vmatrix} \qquad \text{(A1.20)}$$

$$[M] = \int_0^l G(\rho c)_b \langle f \rangle \langle f \rangle^T dx$$

$$= \frac{G(\rho c)_b\ l}{420} \begin{vmatrix} 156 & 22l & 54 & -13l \\ 22l & 4l^2 & 13l & -3l^2 \\ 54 & 13l & 156 & -22l \\ -13l & -3l^2 & -22l & 4l^2 \end{vmatrix} \qquad \text{(A1.21)}$$

$$[B] = \int_0^l (\rho c) \langle f \rangle \langle f \rangle^T dx$$

$$= \frac{(\rho c)\, l}{420} \begin{vmatrix} 156 & 22l & 54 & -13l \\ 22l & 4l^2 & 13l & -3l^2 \\ 54 & 13l & 156 & -22l \\ -13l & -3l^2 & -22l & 4l^2 \end{vmatrix} \qquad \text{(A1.22)}$$

$$\langle BC \rangle = \langle f \rangle \Big]_{x=0} q(t) + \int_0^l G(\rho c)_b \langle f \rangle \, dx \; T_c$$

$$= \begin{Vmatrix} q(t) + G(\rho c)_b \, T_c(l/2) \\ G(\rho c)_b \, T_c \, (l^2/12) \\ G(\rho c)_b \, T_c \, (l/2) \\ -G(\rho c)_b \, T_c \, (l^2/12) \end{Vmatrix} \qquad \text{(A1.23)}$$

It should be noted that the above matrices are used if the temperature response vector is

$$\begin{Vmatrix} T_1 \\ \left(\frac{\partial T}{\partial x}\right)_1 \\ T_2 \\ \left(\frac{\partial T}{\partial x}\right)_2 \end{Vmatrix} \qquad \text{(A1.24)}$$

This response vector can be used if there are constant material properties throughout the skin. In this case the requirement that fluxes be continuous across element boundaries reduces to the temperature gradients being continuous at element boundaries, as

$$k_1\left(\frac{\partial T}{\partial x}\right)_1 = k_2\left(\frac{\partial T}{\partial x}\right)_2$$

$$k_1 = k_2$$

$$\left(\frac{\partial T}{\partial x}\right)_1 = \left(\frac{\partial T}{\partial x}\right)_2$$

However, if the thermal conductivity and other properties are not constant for each element, the following temperature response vector must be used in order to ensure compatibility of the fluxes at the element boundaries.

$$\begin{Bmatrix} T_1 \\ k_1\left(\frac{\partial T}{\partial x}\right)_1 \\ T_2 \\ k_2\left(\frac{\partial T}{\partial x}\right)_2 \end{Bmatrix} \qquad \text{(A1.25)}$$

The matrices in Equation (A1.18) then become

$$[A] = \frac{1}{30\ l}\begin{vmatrix} 36k & 3l & -36k & 3l \\ 3l & 4l^2/k & -3l & -l^2/k \\ -36k & -3l & 36k & -3l \\ 3l & -l^2/k & -3l & 4l^2/k \end{vmatrix} \qquad \text{(A1.26)}$$

$$[k] = \begin{vmatrix} . & . & . & . & . & . \\ . & . & . & . & . & . \\ . & . & 0 & 0 & 0 & 0 \\ . & . & 0 & 0 & 0 & 0 \\ . & . & 0 & 0 & 0 & 1 \\ . & . & 0 & 0 & 0 & 0 \end{vmatrix} \tag{A1.27}$$

$$[M] = \frac{G(\rho c)_b \, l}{420 \, k} \begin{vmatrix} 156k & 22l & 54k & -13l \\ 22l & 4l^2/k & 13l & -3l^2/k \\ -54k & 13l & 156k & -22l \\ -13l & -3l^2/k & -22l & 4l^2/k \end{vmatrix} \tag{A1.28}$$

$$[B] = \frac{(\rho c) \, l}{420 \, k} \begin{vmatrix} 156k & 22l & 54k & -13l \\ 22l & 4l^2/k & 13l & -3l^2/k \\ -54k & 13l & 156k & -22l \\ -13l & -3l^2/k & -22l & 4l^2/k \end{vmatrix} \tag{A1.29}$$

$$\langle BC \rangle = \begin{Bmatrix} q(t) + G(\rho c)_b \, T_c \, (l/2) \\ G(\rho c)_b \, T_c \, (l^2/12k) \\ G(\rho c)_b \, T_c \, (l/2) \\ -G(\rho c)_b \, T_c \, (l^2/12k) \end{Bmatrix} \tag{A1.30}$$

The Crank-Nicholson technique is used to solve the resulting equations in time. The Crank-Nicholson equation is

$$\langle T^{(j+1)} \rangle = \langle T^{(j)} \rangle + \frac{\Delta t}{2} \left(\langle \dot{T}^{(j)} \rangle + \langle \dot{T}^{(j+1)} \rangle \right) \tag{A1.31}$$

where (j) and (j+1) represent time steps (j) and (j+1), respectively. Premultiplying Equation (A1.31) by [B], substituting Equation (A1.18) into the resulting equation, and rearranging terms gives

$$\left([B] + \frac{\Delta t}{2} \left([A] - [k] + [M] \right) \right) \langle T^{(j+1)} \rangle$$
$$= \left([B] + \frac{\Delta t}{2} \left(-[A] + [k] - [M] \right) \right) \langle T^{(j+1)} \rangle \qquad \text{(A1.32)}$$
$$+ \frac{\Delta t}{2} \left(\langle BC^{(j)} \rangle + \langle BC^{(j+1)} \rangle \right)$$

or

$$[LHS] \langle T^{(j+1)} \rangle = \langle RHS \rangle \qquad \text{(A1.33)}$$

Details of the computer program which uses this approximate finite element matrix equation are found in Section 2.3.

APPENDIX 2: SAMPLE DATAFILE

The following is a sample datafile generated by the finite element program. Data for all time steps is printed to this file, and it may then be edited by the user. Here, the file has been edited to conserve space.

```
FINITE ELEMENT SOLUTION
USING HERMITIAN TEMPERATURE INTERPOLATION FUNCTION
NUMBER OF ELEMENTS =          5
FLUX (KW/M^2 S) =  83.2
EXPOSURE TIME(S) = 3
TOTAL TIME OBSERVED (S) = 120

TEMPERATURE-TIME AND BURN HISTORY AT DEPTHS

               BASAL LAYER                      DERMAL BASE

TIME (S) TEMPERATURE (C)  BURN INTEGRAL   TEMPERATURE (C)  BURN INTEGRAL
  0.00       32.6             0.000D+00       33.9             0.000D+00
  0.10       39.7             0.000D+00       34.0             0.000D+00
  0.20       48.1             0.130D-03       34.1             0.000D+00
  0.50       65.3             0.704D+00       33.9             0.000D+00
  1.00       84.5             0.557D+03       33.8             0.000D+00
  2.00      111.9             0.217D+07       34.0             0.000D+00
  3.00      132.9             0.569D+09       34.9             0.000D+00
  3.10      127.9             0.769D+09       34.9             0.000D+00
  3.20      121.3             0.807D+09       35.0             0.000D+00
  3.50      109.5             0.820D+09       35.7             0.000D+00
  4.00       98.9             0.822D+09       37.0             0.000D+00
  5.00       87.3             0.822D+09       40.1             0.000D+00
  6.00       80.6             0.822D+09       43.2             0.000D+00
  7.00       75.8             0.822D+09       46.1             0.200D-03
  8.00       72.3             0.822D+09       48.3             0.950D-03
  9.00       69.6             0.822D+09       50.0             0.283D-02
 10.00       67.5             0.822D+09       51.2             0.754D-02
 20.00       59.1             0.822D+09       53.8             0.372D+00
 30.00       55.9             0.822D+09       52.8             0.735D+00
 40.00       54.0             0.822D+09       51.8             0.900D+00
 50.00       52.5             0.822D+09       50.8             0.977D+00
 60.00       51.4             0.822D+09       50.0             0.102D+01
 70.00       50.4             0.822D+09       49.3             0.104D+01
 80.00       49.6             0.822D+09       48.7             0.106D+01
 90.00       48.9             0.822D+09       48.1             0.107D+01
100.00       48.3             0.822D+09       47.6             0.108D+01
110.00       47.8             0.822D+09       47.1             0.109D+01
120.00       47.3             0.822D+09       46.7             0.109D+01
TIME TO SECOND DEGREE BURN (S) =  0.54

TIME TO THIRD DEGREE BURN (S) = 55.00
```

APPENDIX 3: CALCULATION OF RADIATION AND CONVECTION BOUNDARY CONDITION

For a given incident heat flux, the maximum surface temperature of the skin predicted by the variable property finite element model can be used to estimate the radiation and convection boundary condition. The ambient air temperature will be assumed to be 20°C.

A3.1 Natural Convection Heat Loss

The heat loss from free convection is given by

$$q_c = h\ (T_s - T_\infty) \tag{A3.1}$$

The convection heat transfer coefficient will be estimated by assuming the body can be represented by a vertical cylinder. Following the procedure given in Holman [67], the film Rayleigh number, which is the product of the film Grashof and Prandtl numbers,

$$Ra_f = Gr_f\ Pr_f \tag{A3.2}$$

must be determined first to see if the flow is laminar or turbulent. Holman presents simplified equations which can be used to determine the convection heat transfer coefficient for laminar or turbulent natural convection in air.

This Rayleigh number, or Grashof-Prandtl number product, is given by

$$Gr_f\ Pr_f = \frac{g\ \beta\ (T_s - T_\infty)\ L^3}{\nu^2} \tag{A3.3}$$

The film temperature, T_f is taken as the average temperature of the surface and the surroundings. For the 83.2 kW/m^2 heat flux, the maximum surface temperature predicted by the variable property finite element model is 158.0°C. Therefore

$$T_f = \frac{(158 + 20)}{2} = 89°C = 362\ K$$

and β is the inverse of this film temperature.

$$\beta = \frac{1}{T_f} = 0.00276\ K^{-1}$$

The viscosity and Prandtl number for air at this fluid temperature are

$$\nu = 22.0 \times 10^{-6}\ m^2/s$$

$$Pr = 0.695$$

The height of the cylinder, L, will be assumed to be 2 m.

The Rayleigh number, or Grashof-Prandtl number product is

$$Ra_f = Gr_f\, Pr_f = \frac{(9.81)\ (0.00276)\ (89 - 20)\ (2)^3}{(22 \times 10^{-6})^2}$$

$$= 3.54 \times 10^{10}$$

This is turbulent flow ($Ra_f > 10^9$). Holman gives the following equation for the turbulent natural convective heat transfer coefficient for a vertical cylinder in air.

$$h = 1.31\ (\Delta T)^{1/3} \qquad \text{(A3.4)}$$

Therefore

$$h = 1.31\ (158 - 20)^{1/3}$$

$$= 6.8\ W/m^{2\cdot}{}^{\circ}C$$

And the convection heat loss is

$$q_c = 6.8\ (158 - 20) = 934\ W/m^2$$

The convection heat losses for the other two heat fluxes are found in a similar manner. These values are:

- heat flux = 41.6 kW/m^2 q_c = 418 W/m^2
- heat flux = 24.0 kW/m^2 q_c = 236 W/m^2

A3.2 Radiation Heat Loss

It is assumed that the skin surface radiates as a grey body, and is located in a room with walls of uniform temperature which have a surface area much greater than that of the skin. The radiation heat loss can be found using

$$q_r = \sigma\ \epsilon\ (T_s^4 - T_\infty^4) \qquad \text{(A3.5)}$$

For the 83.2 kW/m^2 incident heat flux, assuming $\epsilon = 1.0$,

$$q_r = 5.669\ x\ 10^{-8} \left((158 + 273)^4 - (20 + 273)^4 \right)$$
$$= 1540\ W/m^2$$

The radiation heat losses are calculated similarily for the other two heat fluxes. The values are:

- heat flux = 41.6 kW/m^2 q_r = 628 W/m^2
- heat flux = 24.0 kW/m^2 q_r = 359 W/m^2

A3.3 Total Heat Loss

The total heat loss is simply the sum of the radiation and convection heat losses. For the 83.2 kW/m^2 heat flux,

$$\begin{aligned} q_t &= q_c + q_r \\ &= 934 + 1540 \ W/m^2 \\ &= 2474 \ W/m^2 \end{aligned} \qquad \text{(A3.5)}$$

Similarily for the other two heat fluxes,

- heat flux = 41.6 kW/m^2 q_t = 1046 W/m^2
- heat flux = 24.0 kW/m^2 q_r = 595 W/m^2

These values are substituted into the finite element model to test the role of the boundary conditions after exposure, as described in Section 3.4.